National Aeronautics and Space Administration

Langley Research Center

Hampton, Virginia 23681-2199

Cloud – Aerosol LIDAR and Infrared Pathfinder Satellite Observations (CALIPSO)

Data Users Guide

Frequently Asked Questions (FAQ)

DOI: **https://doi.org/10.5067/CALIOP_IIR_WFC/CALIPSO/CALIPSO_Frequently_Asked_Questions**

Cloud – Aerosol LIDAR and Infrared Pathfinder Satellite Observations

Data Users Guide

Frequently Asked Questions (FAQ)

Primary Authors

Mark Vaughan, Michael Pitts, Charles Trepte, David Winker, Brian Getzewich, Jason Tackett
NASA Langley Research Center
Hampton, Virginia 23681-2199

Jacques Pelon
LATMOS/IPSL, Université Pierre et Marie Curie
75252 Paris Cedex 5 (France)

Anne Garnier, Jayanta Kar, Kam-Pui Lee
Analytical Mechanics Associates (AMA)
21 Enterprise Parkway, Hampton, Virginia 23666

Timothy Murray, Sharon Rodier
ADNET Systems, Inc.
6720B Rockledge Drive, Suite #504, Bethesda, Maryland 20817

Robert Ryan
Coherent Applications, Inc. – Psionic LLC
1100 Exploration Way, Hampton, Virginia 23666

January 30, 2026

The extensive global dataset collected by the Cloud-Aerosol Lidar and Infrared Pathfinder Satellite Observation (CALIPSO) mission continues to deliver new insights into the roles played by clouds and atmospheric aerosols in regulating Earth's weather, climate, and air quality. CALIPSO was launched on 28 April 2006 with three remote sensing instruments aboard: an active lidar instrument (CALIOP, the Cloud Aerosol Lidar with Orthogonal Polarization), a three-channel Imaging Infrared Radiometer (IIR), and a single channel wide field-of-view camera (WFC). Following instrument check-out, the mission acquired its first science data on 12 June 2006. Originally designed for a three-year lifetime, CALIPSO continued operating for an astonishing 17 years, making its final observations on 30 June 2023. During that time CALIPSO provided unprecedented measurements of the vertical structure of the Earth's atmosphere. Until September 2018, CALIPSO flew in the A-Train constellation with CloudSat and MODIS-Aqua, which enabled a wealth of previously unimagined synergies between multiple active and passive space-based sensors. CALIPSO data are publicly available worldwide and have been used in over 5,000 peer reviewed journal papers to advance scientific knowledge of the atmosphere, the hydrosphere, and the cryosphere.

GLOSSARY AND ACRONYM DICTIONARY

Term	Meaning
1kmCLay	CALIOP 1 km cloud layer product
333mMLay	CALIOP 333 m merged layer product (reports clouds and aerosols)
5kmALay	CALIOP 5 km aerosol layer product
5kmAPro	CALIOP 5 km aerosol profile product
5kmCLay	CALIOP 5 km cloud layer product
5kmCPro	CALIOP 5 km cloud profile product
5kmMLay	CALIOP 5 km merged layer product (reports clouds and aerosols)
5kmDiag	CALIOP 5 km merged layer diagnostic product (reports clouds and aerosols)
AERIS	French Data Infrastructure for the Atmosphere

Term	Meaning
AMSL	above mean sea level
AOD	aerosol optical depth
APD	avalanche photo diode
ASDC	Atmospheric Science Data Center
ATBD	algorithm theoretical basis document
AVD	atmospheric volume description
BB	black body
BTD	brightness temperature difference
CAD	cloud-aerosol discrimination
CALIOP	Cloud-Aerosol Lidar with Orthogonal Polarization
CALIPSO	Cloud-Aerosol Lidar and Infrared Pathfinder Satellite Observation
CNES	Centre National d'Études Spatiales
DEM	digital elevation model
ECMWF	European Centre for Medium-Range Weather Forecasts
EOSDIS	Earth Observing System Data and Information System
FAQ	frequently asked question
FCF	feature classification flags
frame	a fundamental data averaging interval used extensively in CALIOP's level 1 and level 2 data processing. A frame consists of 15 consecutive single-shot profiles spanning an along-track distance of ~5 km. 15 shots is the least common multiple of the along-track averaging intervals defined by CALIOP's vertically varying onboard data averaging scheme (Hunt et al., 2009).
GEWEX	Global Energy and Water cycle Experiment
GMAO	Global Modeling and Assimilation Office
granule	continuous data segment in which all measurements were acquired while the lidar was configured for daytime data acquisition only or nighttime data acquisition only; each granule spans approximately one half of a full orbit, with daytime granules being slightly larger/longer than nighttime granules
HDF	Hierarchical Data Format
IAB	integrated attenuated backscatter
ICARE	Cloud Aerosol Water Radiation Interactions
IIR	imaging infrared radiometer
IWP	ice water path
L0	Level 0
L1B	Level 1B
L2	Level 2
L3	Level 3
L3COP	Level 3 Cloud Occurrence Product
L3TAP	Level 3 Tropospheric Aerosol Product
L3SAP	Level 3 Stratospheric Aerosol Product
LEM	low energy mitigation
LRE	lidar receiver electronics

Term	Meaning
LSWG	lidar science working group
MERRA-2	Modern-Era Retrospective analysis for Research and Applications, Version 2
MHz	megahertz
MLS	Microwave Limb Sounder
MODIS	Moderate Resolution Imaging Spectroradiometer
N/A	not applicable
NASA	National Aeronautics and Space Administration
nm	nanometer
ODCOD	ocean-derived column optical depths
PBL	planetary boundary layer
PDAC	payload data acquisition cycle; the shortest amount of time in which an integer number of data records can be acquired by all three instruments
PDF	probability distribution function
PIVB	Payload Instrument Verification Block
PMT	photomultiplier
PSC	polar stratospheric cloud
QA	quality assurance/quality control
QC	quality control/quality assurance
RMS	root mean square
ROI	randomly oriented ice
SAA	South Atlantic Anomaly
SDS	scientific data set
SIBYL	Selective Iterated BoundarY Location
SNR	signal-to-noise ratio
SDS	scientific data set
SV	space view
TOA	top of atmosphere
UTC	Coordinated Universal Time
V5.00	version 5.00 data release
VFM	vertical feature mask
WFC	wide field-of-view camera

GENERAL QUESTIONS

1. What is the difference between CALIPSO and CALIOP?

CALIPSO stands for the Cloud-Aerosol Lidar and Infrared Pathfinder Satellite Observations. This satellite, which launched in April 2006, has three separate instruments on-board: the Infrared Imaging Radiometer (IIR), the Wide Field-of-view Camera (WFC), and the Cloud-Aerosol Lidar with Orthogonal Polarization (CALIOP). CALIPSO is the satellite; CALIOP is one of the instruments aboard the satellite.

2. What file formats do the CALIPSO data products use?

The CALIPSO data products are distributed in Hierarchical Data Format (HDF). Consistent with EOSDIS requirements in force when CALIPSO launched, all but one of the CALIPSO data products use HDF version 4 (HDF4). The sole exception is the Blowing Snow product, developed in collaboration NASA Goddard Space Flight Center, which uses HDF version 5 (HDF5). Both HDF4 and HDF5 contain collections of data structures that report product-specific information in multi-dimension arrays, termed Scientific Data Sets (SDSs) in HDF4 and datasets in HDF5, and contain associated attributes used to make each SDS self-documenting. Related SDSs can be segregated into Vgroups which use a tree-structured format to aggregate collections of similar parameters. Much more information about HDF file structure and usage is provided in the very comprehensive HDF4 Data Users Guide.

3. Which CALIPSO data product level(s) should I use?

Data product levels refer to the amount of processing done to extract different gradations of geophysical information from the raw data. The different data product levels are tailored for different science and engineering research interests. Table 1 shows a condensed version, created 15 August 2025, of a larger table that describes all of the data processing levels defined for the NASA Earth Observing System Data and Information System (EOSDIS). The CALIPSO project produces only a subset of the EOSDIS-defined levels.

Table 1: The subset of EOSDIS data processing levels distributed by the CALIPSO project.

Data Level	Description
Level 0	Reconstructed, unprocessed instrument and payload data at full resolution, with any and all communications artifacts (e.g., synchronization frames, communications headers, duplicate data) removed.
Level 1B	Level 1B (L1B) data are Level 1A (L1A) data that have been processed to instrument units; not all instruments have L1B source data.
Level 2	Derived geophysical variables at the same resolution and location as the L1B source data.
Level 3	Variables mapped on uniform space-time grid scales, usually with some completeness and consistency.

4. What is the naming convention for the CALIPSO data products?

Filenames for all CALIPSO data products are constructed using a series of eight tokens, each of which contains specific information identifying the product type. The general format is

[Mission]_[Sensor]_[Level]_[ProductID]-[MaturityLevel]-[Version].[Instance].[Ext]

with tokens as defined in Table 2. Table 3, Table 4, and Table 5 give filename examples for, respectively, the lidar, IIR, and WFC data products.

Table 2: Interpretation of the components of the CALIPSO filenames

Token	Interpretation
Mission	The name of the mission that acquired the data; for the CALIPSO mission, this will always be 'CAL'
Sensor	The name of the sensor/instrument that acquired the data. There are three possibilities for the CALIPSO mission: LID = CALIOP lidar IIR = imaging infrared radiometer WFC = wide field-of-view camera

Token	Interpretation
Level	EOSDIS data processing level of the product; see Table 1 for CALIPSO processing level definitions
ProductID	Unique identifier for each of the different data products generated within each data processing levels
Maturity	Data processing maturity level indicating that degree to which the product has been validated. For the final CALIPSO data release, the maturity level is set to 'Standard' for all products except the 5 km merged layer products, which are classified as 'Beta'. 'Standard' indicates the highest level of validation. The 5 km merged layer products are designated as 'Beta' products because several of the optical properties reported at 1064 nm have not yet been validated.
Version	Data processing version number
Instance	Specifies the data acquisition date, time, and lighting condition at the start of the granule. The format for this token is yyyy-mm-ddThh:nn:ss.Zx where yyyy specifies the year (2006–2023), mm specifies the month (01–12), and dd specifies the day (01–31). The T character is a constant separator between the date and time fields. For the time fields, hh specifies the hour (00–23), nn specifies the minute (00–59), and ss specifies the second (00–59). The Z character is a constant indicating that time is expressed in UTC. The x character at the end specifies the lighting conditions throughout the granule: D = daytime only, N = nighttime only, and A = all (i.e., both day and night). The x character is not always included. Those files without a day-night indicator (e.g., the lidar level 0 product) can contain a mix of nighttime and daytime data.
Ext	File type extension. Two file types are distributed: HDF4 (Ext = .hdf) and, for the blowing snow product only, HDF5 (Ext = .hdf5).

Table 3: Example filenames for all CALIPSO lidar data products

CALIPSO Lidar Data Product Filenames	
Product	Lidar Level 0 Product
Filename	CAL_LID_L0-Standard-V1-00.yyyy-mm-ddThh-nn-ssZ.hdf
Product	Lidar Level 1B Product
Filename	CAL_LID_L1-Standard-V5-00.yyyy-mm-ddThh-nn-ssZ[N/D].hdf
Product	Lidar Level 2 333 m Merged Layer Product
Filename	CAL_LID_L2_333mMLay-Standard-V5-00.yyyy-mm-ddThh-nn-ssZ[N/D].hdf
Product	Lidar Level 2 1 km Cloud Layer Product
Filename	CAL_LID_L2_01kmCLay-Standard-V5-00.yyyy-mm-ddThh-nn-ssZ[N/D].hdf
Product	Lidar Level 2 5 km Cloud Layer Product
Filename	CAL_LID_L2_05kmCLay-Standard-V5-00.yyyy-mm-ddThh-nn-ssZ[N/D].hdf
Product	Lidar Level 2 5 km Aerosol Layer Product
Filename	CAL_LID_L2_05kmALay-Standard-V5-00.yyyy-mm-ddThh-nn-ssZ[N/D].hdf
Product	Lidar Level 2 5 km Merged Layer Product
Filename	CAL_LID_L2_05kmMLay-Standard-V5-00.yyyy-mm-ddThh-nn-ssZ[N/D].hdf

CALIPSO Lidar Data Product Filenames	
Product	Lidar Level 2 Merged Layer Diagnostic Product
Filename	CAL_LID_L2_MLay_Diagnostic-Beta-V5-00.yyyy-mm-ddThh-nn-ssZ[N/D].hdf
Product	Lidar Level 2 Vertical Feature Mask Product
Filename	CAL_LID_L2_VFM-Standard-V5-00.yyyy-mm-ddThh-nn-ssZ[N/D].hdf
Product	Lidar Level 2 5 km Aerosol Profile Product
Filename	CAL_LID_L2_05kmAPro-Standard-V5-00.yyyy-mm-ddThh-nn-ssZ[N/D].hdf
Product	Lidar Level 2 5 km Cloud Profile Product
Filename	CAL_LID_L2_05kmCPro-Standard-V5-00.yyyy-mm-ddThh-nn-ssZ[N/D].hdf
Product	Lidar Level 2 Polar Stratospheric Cloud Mask - Daily
Filename	CAL_LID_L2_PSCMask-Standard-V3-00.yyyy-mm-ddT00-00-00Z[N/D].hdf
Product	Lidar Level 2 Blowing Snow, Antarctica
Filename	CAL_LID_L2_BlowingSnow_Antarctica-Standard-V2-00.yyyy-mm.hdf5
Product	Lidar Level 2 Blowing Snow, Greenland
Filename	CAL_LID_L2_BlowingSnow_Greenland-Standard-V1-00.yyyy-mm.hdf5
Product	Lidar Level 1.5 Profile Product
Filename	CAL_LID_L15-Standard-V1-01.yyyy-mm-ddThh-nn-ssZ[N/D].hdf
Product	Lidar Level 3 Tropospheric Aerosol All Sky
Filename	CAL_LID_L3_Tropospheric_APro_AllSky-Standard-V5-00.yyyy-mm[N/D].hdf
Product	Lidar Level 3 Tropospheric Aerosol Cloud Free
Filename	CAL_LID_L3_Tropospheric_APro_CloudFree-Standard-V5-00.yyyy-mm[N/D].hdf
Product	Lidar Level 3 Tropospheric Aerosol Cloudy Sky Opaque
Filename	CAL_LID_L3_Tropospheric_APro_CloudySkyOpaque-Standard-V5-00.yyyy-mm[N/D].hdf
Product	Lidar Level 3 Tropospheric Aerosol Cloudy Sky Transparent
Filename	CAL_LID_L3_Tropospheric_APro_CloudySkyTransparent-Standard-V5-00.yyyy-mm[N/D].hdf
Product	Lidar Level 3 Stratospheric Aerosol Product
Filename	CAL_LID_L3_Stratospheric_APro-Standard-V2-00.yyyy-mmN.hdf
Product	Lidar Level 3 Cloud Occurrence Product
Filename	CAL_LID_L3_Cloud_Occurrence-Standard-V2-00.yyyy-mm[N/D/A].hdf
Product	Lidar Level 3 Ice Cloud Product
Filename	CAL_LID_L3_Ice_Cloud-Standard-V2-00.yyyy-mm[N/D/A].hdf
Product	Lidar Level 3 GEWEX Cloud Product
Filename	CAL_LID_L3_GEWEX_Cloud-Standard-V2-00.yyyy-mm[N/D/A].hdf

Table 4: Example filenames for all CALIPSO IIR data products

CALIPSO Imaging Infrared Radiometer (IIR) Data Product Filenames	
Product	IIR Level 1 Calibration
Filename	CAL_IIR_L1_CAL-Standard-V3-00.yyyy-mm-ddThh-nn-ssZ.hdf
Product	IIR Level 1 Calibration Correction
Filename	CAL_IIR_L1_COR-Standard-V3-00.yyyy-mm-ddThh-nn-ssZ.hdf
Product	IIR Level 1 B
Filename	CAL_IIR_L1-Standard-V3-00.yyyy-mm-ddThh-nn-ssZ[N/D].hdf
Product	IIR Level 2 Track
Filename	CAL_IIR_L2_Track-Standard-V5-00.yyyy-mm-ddThh-nn-ssZ[N/D].hdf
Product	IIR Level 2 Swath
Filename	CAL_IIR_L2_Swath-Standard-V5-00.yyyy-mm-ddThh-nn-ssZ[N/D].hdf
Product	IIR Level 3 GEWEX Cloud
Filename	CAL_IIR_L3_GEWEX_Cloud-Standard-V2-00.yyyy-mm[N/D/A].hdf

Table 5: Example filenames for all CALIPSO WFC data products

CALIPSO Wide Field-of-view Camera (WFC) Data Product Filenames	
Product	WFC Level 1 Native Grid Central 5 km Swath
Filename	CAL_WFC_L1_125m-Standard-V4-00. yyyy-mm-ddThh-nn-ssZD.hdf
Product	WFC Level 1 Native 1 km Grid
Filename	CAL_WFC_L1_1Km-Standard-V4-00. yyyy-mm-ddThh-nn-ssZD.hdf
Product	WFC Level 1 IIR Grid
Filename	CAL_WFC_L1_IIR-Standard-V4-00. yyyy-mm-ddThh-nn-ssZD.hdf
Product	WFC Level 1 Calibration
Filename	CAL_WFC_L1_Cal-Standard-V4-00. yyyy-mm-ddThh-nn-ssZ.hdf
Product	WFC Level 1 Assembler - Daily
Filename	CAL_WFC_L1_Asm-Standard-V4-00. yyyy-mm-ddT00-00-00Z.hdf

5. Where can I download CALIPSO data?

As of this writing (30 January 2026), the CALIPSO data products can be downloaded from the following repositories:

- NASA Langley Atmosphere Sciences Data Center (ASDC) via direct download
- NASA Langley ASDC via OpenDAP
- NASA Langley ASDC via LARC_CLOUD

- NASA's Earth Data Search Tool
- AERIS/ICARE Data and Services Centre direct download

CALIOP DATA PRODUCTS

6. What are CALIOP's sampling resolutions?

Onboard the satellite, CALIOP collects profile data at a nominal vertical resolution of 15 m (10 MHz sampling rate) and at a laser pulse repetition rate of 20.16 Hz, which when accounting for the satellite's orbital velocity, translates into a horizontal profile spacing of ~333 m. At the Earth's surface, the diameter of each laser footprint is ~70 m, which lies entirely within the 90 m field-of-view footprint diameter. Due to bandwidth limitations for downlinking the data from the satellite, CALIOP profiles are averaged on-board the satellite in both the horizontal and vertical dimensions.

The goal of the on-board averaging algorithm is to maximize spatial resolution and dynamic range of the signals while simultaneously minimizing the telemetry data volume. By applying an altitude-dependent averaging scheme, the CALIOP telemetry bandwidth was reduced by more than an order of magnitude relative to the raw data, with minimum impact on the information content of the data. Unfortunately, this data compression introduces additional complexity into the telemetry data.

The CALIOP onboard averaging scheme provides the highest resolution in the lower troposphere, where the temporal and spatial variability of clouds and aerosols is the greatest. Coarser resolutions are applied higher in the atmosphere. The degree of averaging varies with altitude, as defined in Table 6 and illustrated in Figure 1.

Table 6: CALIOP's onboard data averaging scheme. Profile data are sampled onboard at 10 MHz (~15 m vertical resolution) then averaged to the spatial resolutions shown below prior to being downlinked. The number of bins given in the Vertical Resolution columns specifies the number of ~15 m bins averaged onboard to create a single vertical sample prior to downlink.

Region	Nominal Altitude Range (km)	Bin Numbers	Horizonal Resolution	532 nm Vertical Resolution	1064 nm Vertical Resolution
5	40.0 – 30.1	1 – 33	15 laser pulses (5 km)	20 bins (300 m)	N/A
4	30.1 – 20.2	34 – 88	5 laser pulses (5/3 km)	12 bins (180 m)	12 bins (180 m)
3	20.2 – 8.3	89 – 288	3 laser pulses (1 km)	4 bins (60 m)	4 bins (60 m)
2	8.3 – -0.5	289 – 578	1 laser pulse (1/3 km)	2 bins (30 m)	4 bins (60 m)
1	-0.5 – -2.0	578 – 583	1 laser pulse (1/3 km)	20 bins (300 m)	20 bins (300 m)

The left panel of Figure 1 illustrates the altitude-dependent averaging applied to 15 consecutive full-resolution lidar profiles (i.e., a nominal 5 km horizontal distance), with annotations to show how the averaging resolutions vary vertically and horizontally as a function of altitude. The five different averaging regimes are shown using five different shades of blue. The vertical lines within each blue band delineate the individual profiles created by horizontally averaging the full resolution data. For example, between 8.2-km and 20.2-km the data is averaged horizontally to a nominal spatial resolution of 1-km; i.e., the data from 3 full resolution (333 m) profiles are averaged to create each 1 km averaged profile segment. Similarly, between 20.2 km and 30.1 km, 5 full resolution (333 m) profiles are averaged to create 3 profiles that each spans a nominal horizontal extent of 5/3 km. Processing in the vertical is done in a similar fashion, as indicated by the thin horizontal black lines shown in the profile on the far right within each altitude regime.

The table in the center of Figure 1 gives the numerical values of the horizontal and vertical averaging for all the altitude regions. The highest resolution data available is in the region between -0.5 km and 8.2 km which is provided at single shot (333 m) resolution horizontally and 30 m resolution vertically.

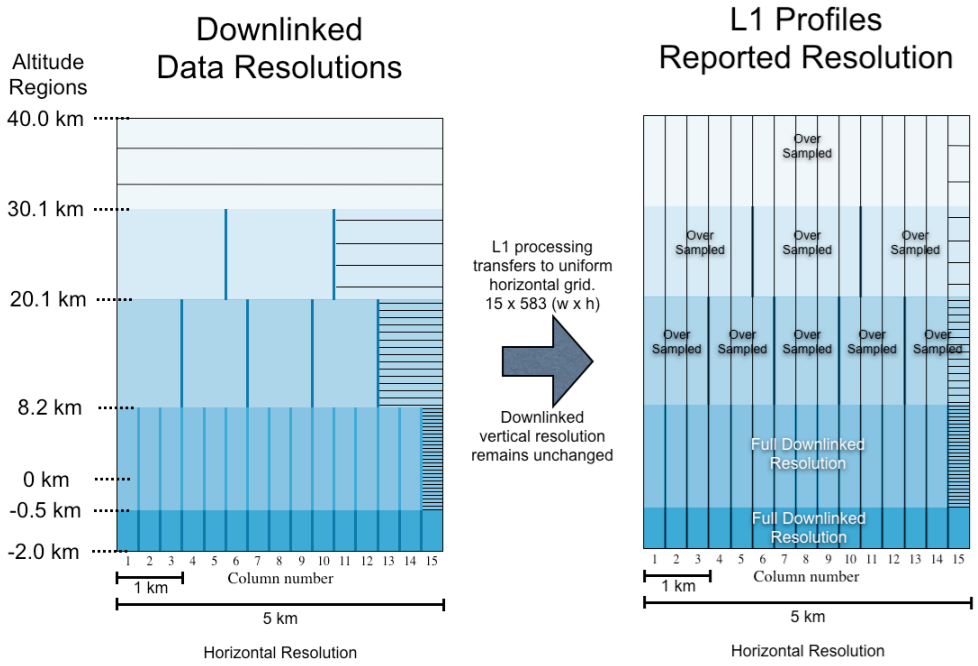

Figure 1: Schematic diagram showing CALIOP data downlink resolutions (left panel) and the organization of the level 1b profile data.

When creating the L1B profile products, the downlinked data is regridded to a uniform horizontal resolution of 333 m. However, in the vertical (i.e. altitude) dimension, the resolution remains identical to that of the downlinked data. Even though the L1B profiles are reported at a uniform horizontal resolution of 333 m, in regions above 8.2 km it is **over sampled**. For example, to create 15 "pseudo-single shot" profiles in the altitude region between 8.2 km to 20.1 km, the downlinked 1 km profiles in this region are **replicated** and grafted onto the top of three consecutive full resolution (single shot) profiles.

7. What information is provided by the CALIOP data products?

This section provides brief introductory overviews of the publicly available CALIOP data products distributed by the CALIPSO project. Significantly more detail is given in the data description documents for each family of products.

a. Lidar Level 0 Data

The raw level 0 binary data downlinked from the satellite is not released to the public. Instead, two publicly available versions are distributed to the community in HDF format. The first of these are the lidar level 0 data files, which translate matched sets of three 90-minute (full orbit) level 0 binary files into single HDF files containing raw lidar profile measurements and health and status data from all three channels: 532 nm parallel, 532 nm perpendicular, and 1064 nm. These data are not calibrated and are averaged on board both horizontally and vertically prior to downlink (see Table 1 and Hunt et al., 2009). Also included in these files are data acquisition times, laser footprint latitudes and longitudes, measurement altitudes, and instrument configuration parameters.

The second level 0 product is the data contained in the CALIOP Payload Instrument Verification Block (PVIB). In CALIPSO's standard payload configuration, software onboard the satellite rescaled the

separate high gain and low gain profile measurements and merged them to create single profiles for each channel. To meet data downlink volume restrictions, these merged and scaled profiles were then averaged both horizontally and vertically prior to being telemetered to Earth (Hostetler et al., 2006). For diagnostic purposes, the CALIPSO payload flight software could also be commanded to deliver PIVB measurements. When configured for PIVB operations, the downlinked data include the single-shot, high vertical resolution (15 m) backscatter profile measurements prior to merging the high and low gain profiles and without applying any spatial averaging. While enormous benefits can be reaped from the full resolution PIVB measurements, capturing this data disrupts the flow of nominal science operations. Furthermore, given the large amount of data involved and the limitations on the size of the on-board data recorder, only a single frame of data (15 consecutive laser pulses) could be down-linked for any PIVB operation. Consequently, PIVB data were obtained only episodically, mostly in the latter half of the mission. PIVB data are not calibrated. Like the level 0 data files, the PIVB files also contain data acquisition times, laser footprint latitudes and longitudes, measurement altitudes, and instrument configuration parameters.

b. Lidar Level 1B Profile Data

Each lidar L1B data file contains approximately one-half orbit (either all daytime or all nighttime) of pseudo-single shot profiles of 532 nm total attenuated backscatter coefficients, 532 nm perpendicular channel attenuated backscatter coefficients, and 1064 nm total attenuated backscatter. Data are all nominal science mode measurements that have been altitude-registered, geolocated, and calibrated (Hostetler et al., 2006; Powell et al., 2009; Kar et al., 2018; Getzewich et al., 2018; Vaughan et al., 2019). The CALIOP L1B data product also contains additional parameters such as ancillary meteorological data, post processed ephemeris data, celestial data, and converted payload status data. Figure 2 shows an example of the 532 nm total attenuated backscatter coefficients from the L1B file for the nighttime data segment beginning at 22:40:33 UTC on 31 March 2016. Profiles in this image have been averaged to a uniform 5 km horizontal resolution. All data below 20.2 km has been averaged to 60 m vertically.

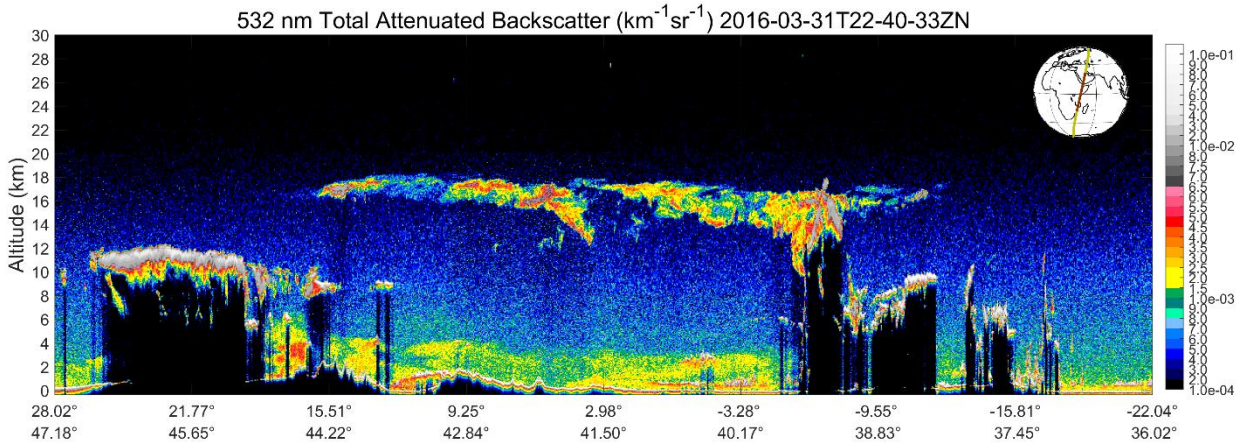

Figure 2: 532 nm total attenuated backscatter coefficients measured beginning in the Arabian Peninsula and extended along the east coast of Africa on 31 March 2016.

c. Lidar Level 2 Layer Data

The level 2 (L2) analyses of the CALIOP lidar backscatter data begins with an attempt to locate all coherent "features" - i.e., clouds and aerosol layers - in each granule of the L1B data. This search is conducted using a nested, multi-resolution averaging scheme that detects features at horizontal averaging resolutions of 333 m (i.e., single shots), 1 km (3 shots averaged), 5 km (15 shots averaged),

20 km (60 shots averaged), and 80 km (240 shots averaged). The strongest scattering features – e.g., opaque water clouds – are readily detected at single shot resolution while the faintest features – e.g., diffuse, absorbing aerosol layers – can require averaging to 80 km resolution before being detected (Vaughan et al., 2005; Vaughan et al., 2009). Irrespective of averaging required for detection, all features are subsequently classified as either clouds or aerosols (Liu et al., 2019). Aerosols are further segregated according to type (Kim et al., 2018) while clouds are partitioned according to thermodynamic phase (Avery et al., 2020). For layers detected at 5 km, 20 km, and 80 km, the final step in the process is to retrieve profiles of particulate backscatter and extinction coefficients, along with derived products such as particulate depolarization ratios, and, for ice clouds, estimates of ice-water content (Young et al., 2018). Altitude-resolved optical properties retrievals are restricted to coarser averaging intervals to ensure confident classification of feature type and to obtain signal-to-noise ratios (SNR) in the level 1B data that are high enough to minimize the propagation of errors in the retrieval process (Young et al., 2013). A high-level overview of the L2 retrieval architecture is given in Winker et al., 2009.

The combined results of the multi-resolution analyses are distributed in five separate CALIOP level 2 layer products that are partitioned according to layer detection resolution. The 333 m merged layer product (333mMLay) reports the retrieved spatial properties (e.g., feature top and base altitudes) and measured optical properties (e.g., layer integrated attenuated backscatter at 532 nm and 1064 nm) of all clouds and aerosols detected in the CALIOP single shot, 30 m vertical resolution data acquired between ~8.2 km and –0.5 km. Similar parameters are reported in the 1 km cloud layer product for clouds detected at 1 km (01kmCLay). Reporting of these data is restricted to altitudes between ~20.2 km and –0.5-km, where the horizontal resolution of the downlinked profiles is 1 km or higher. Because the 01kmCLay product was originally designed as a companion to the IIR level 2 track product, aerosol detections are not reported at 1 km resolution. Finally, there are three variants of the 5 km layer products: the 5 km aerosol layer product (05kmALay), which reports only aerosol detections; the 5 km cloud product (05kmCLay), which reports only cloud detections; and the 5 km merged layer product (05kmMLay), which reports both cloud and aerosol detections. In addition to the spatial properties and measured optical properties included in the 333mMLay and 01kmCLay products, the 5 km products also report the integrals of the retrieved optical properties (e.g., layer optical depths and layer-integrated particulate depolarization ratios). Furthermore, the 5 km layer products also report the spatial and optical properties of all layers detected at the 20 km and 80 km averaging resolutions. Irrespective of the averaging required for detection, the data for all layers are reported at a uniform 5 km horizontal resolution, with the properties of the layers detected at 20 km and 80 km being replicated as appropriate to span the full averaging interval required for feature detection. More detail on the structure of the 5 km layer products is given in the CALIOP Layer Detection and Cloud Clearing section of this document. For a complete listing and in-depth description of all parameters contained in the layer products, consult the Data Description Document for the CALIOP layer products.

d. Lidar Level 2 Vertical Feature Mask

The vertical feature mask (VFM) data product describes the vertical and horizontal distribution of all cloud and aerosol layers detected by CALIOP at any averaging resolution. The VFM Feature_Classification_Flags SDS characterizes each range bin in CALIOP's downlinked data stream using a single 16-bit integer, with the various bits in the integer representing flags that describe some aspect of the data measured within the bin. Instructions on how to decode these integer data are given in CALIPSO's VFM Data Description Document. VFM data are recorded in increments of 15 consecutive laser pulses, which is nominally equivalent to 5-km along the laser ground-track. Figure 3 shows an example VFM image that illustrates the feature type locations and classifications for all

native resolution range bins between 20 km and –0.4 km in the L1B backscatter data shown in Figure 2. The VFM Data Description Document lists all parameters contained in the VFM product and provides an in-depth description of each.

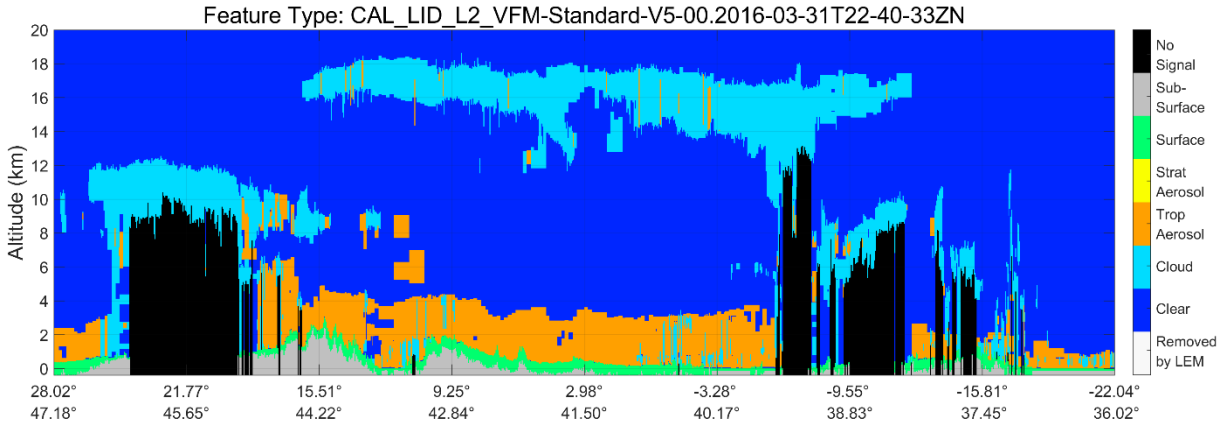

Figure 3: VFM image showing the feature types for all range bins between 20 km and –0.4 km in the level 1B backscatter data shown in Figure 2. While not present in this scene, regions shown in white would indicate places where L1B data was excluded from the L2 processing by the low energy mitigation (LEM) filter implements for the V5.00 data release (Tackett et al., 2025).

e. Lidar Level 2 Profile Data

Profiles of altitude resolved optical properties are retrieved for all features detected at 5 km, 20 km, and 80 km averaging intervals (Young et al., 2018). These profiles, which extend over a nominal altitude range of 30 km to –0.5 km, are reported separately for clouds and aerosols. Cloud data are reported in the 5 km cloud profile product (05kmCPro); aerosol data are reported in the 5 km aerosol profile product (05kmAPro). Like the 5 km layer products, the 5 km profile products are reported at a uniform 5 km horizontal resolution, with the retrieved profiles being replicated as appropriate to span the full horizontal extent required for feature detection. Also included in the profile products are the MERRA-2 meteorological data obtained from NASA's Global Modeling and Assimilation Office and used in the CALIOP retrieval process. Figure 4 shows the extinction coefficients for all clouds detected at 5 km, 20 km, and 80 km averaging intervals in the L1B data shown in Figure 2. A complete listing and in-depth description of all parameters contained in the profile products is given in the Data Description Document for the CALIOP profile products.

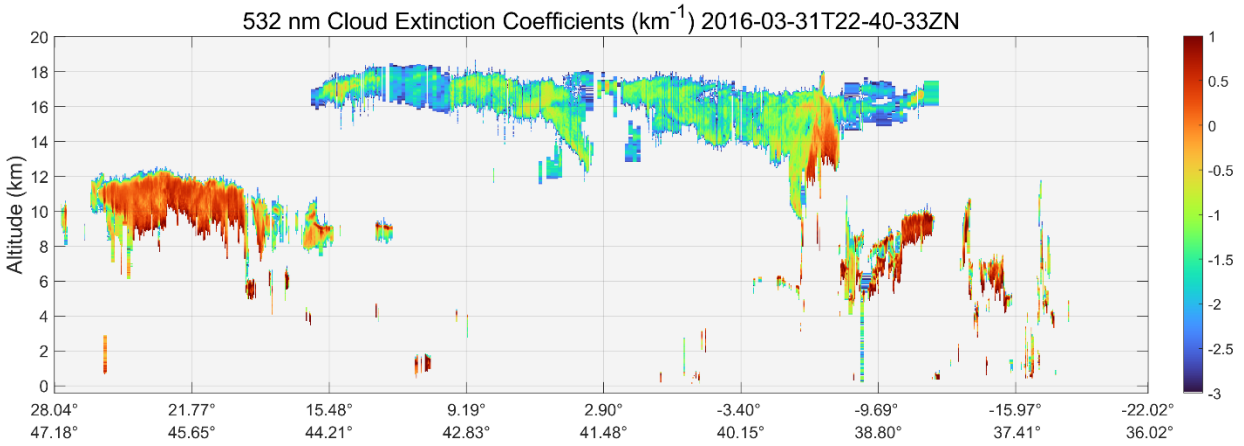

Figure 4: Altitude-resolved 532 nm extinction coefficients, $\sigma_c(z)$, for all clouds detected in the L1B data shown in Figure 2. Colors represent $\log_{10}(\sigma_c(z))$.

f. Lidar Level 2 Polar Stratospheric Cloud Mask

The polar stratospheric cloud mask (PSCMask) data product describes the spatial distribution, optical properties, and composition of polar stratospheric clouds (PSCs) detected during polar winters over the Arctic and Antarctic. The PSCMask product contains profiles of PSC presence, composition, and optical properties, along with ancillary meteorological information reported at 5-km horizontal and 180 m vertical resolutions along the CALIOP orbital track (Pitts et al., 2018). Aura Microwave Limb Sounder (MLS) measurements of the primary PSC condensable vapors of $HN0_3$ and H_20 and several parameters from the Aura MLS V2 Derived Meteorological Products are also included in the PSC data product. PSC detection is limited to nighttime CALIOP observations because higher levels of background light during daytime significantly reduce the signal-to-noise and, hence, the PSC detection sensitivity. Figure 5 shows the total PSC areal coverage over the Antarctic region as a function of altitude for the 2006 austral PSC season. As described in Pitts et al., 2018, "areal coverage is estimated as the sum of the occurrence frequencies (number of PSC detections divided by the total number of observations) in 10 equal-area latitude bands spanning latitudes from 50°S to 90°S, multiplied by the area of each band". The CALIOP L2 PSC Data Description Document provides a comprehensive listing and in-depth descriptions for all parameters reported in the PSCMask product.

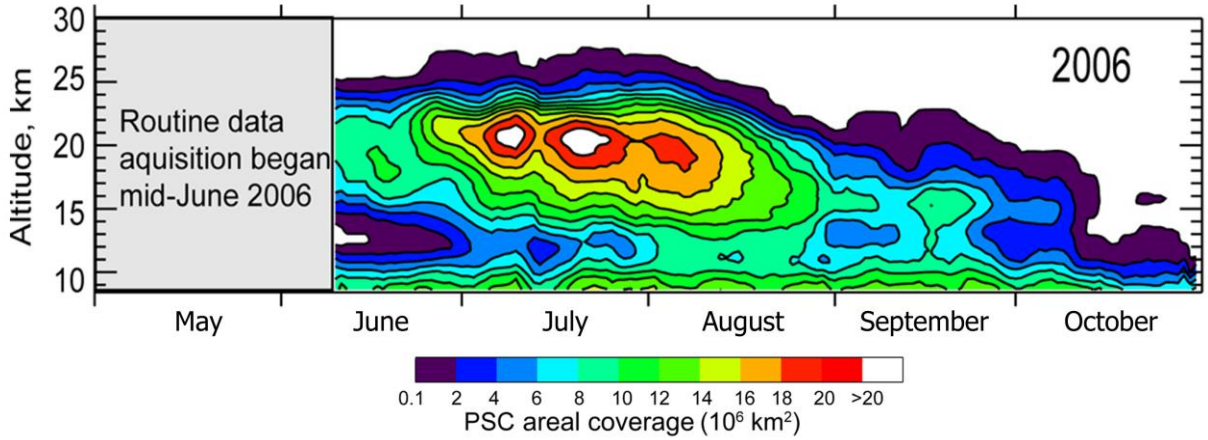

Figure 5: PSC areal coverage over the Antarctic region as a function of altitude for the 2006 austral PSC season (Figure adapted from Pitts et al., 2018 @ Authors 2018, CC BY 4.0).

g. Lidar Level 2 Blowing Snow

CALIOP's blowing snow product reports profiles of 532 nm total attenuated backscatter, 532 nm volume depolarization ratios, and total attenuated backscatter color ratios (1064 nm / 532 nm), together with geolocation fields and ancillary data (e.g., surface wind speeds and directions) for blowing snow events detected in the CALIOP L1B atmospheric attenuated backscatter measurements (Palm et al., 2017). Geographical coverage is restricted to blowing snow events occurring only over Antarctica and Greenland. Figure 6 shows an example of a typical blowing snow layer measured over Antarctica on 28 May 2015.

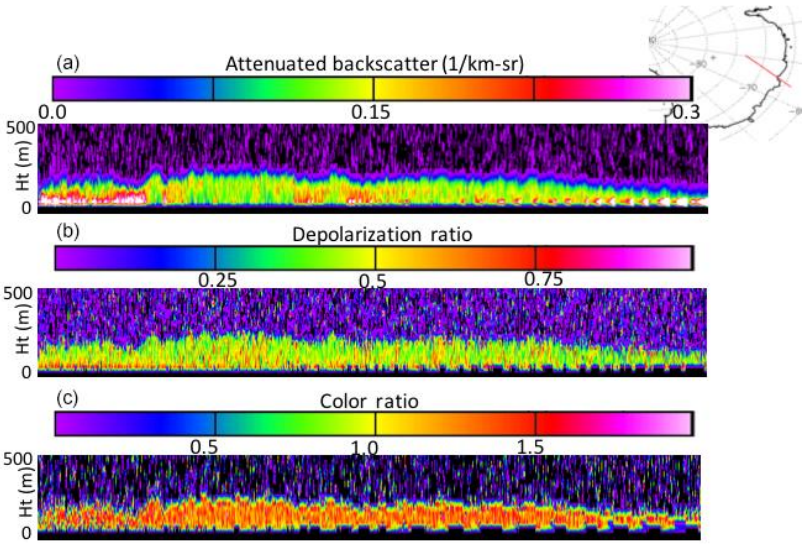

Figure 6: Measured optical properties of blowing snow measured over Antarctica on 28 May 2015 between 17:08:41 and 17:11:33 UTC; the upper panel shows 532 nm total attenuated backscatter coefficients; the middle panel shows 532 nm volume depolarization ratios; and the lower panel shows total attenuated backscatter color ratios (1064 nm / 532 nm) (Palm et al., 2017, CC BY 4.0).

h. Lidar Level 1.5 Profile Data

The CALIOP level 1.5 data are continuous segments of calibrated, geo-located, cloud-cleared, and spatially averaged profiles of lidar attenuated backscatter. Level 1.5 profiles are derived by using a cloud mask derived from the L2 vertical feature mask product to cloud-clear the L1B profiles at pseudo-single shot resolution, then averaging these cloud-cleared L1B profiles to a uniform resolution of 20 km horizontally and 60 m vertically (Vaughan et al., 2011). Figure 7 compares the L1B profile data (upper panel) to the cloud-cleared level 1.5 data (lower panel) for a daytime orbit segment extending from the subtropical Pacific Ocean up along the southern coast of California. Aerosol layers that are largely obscured by noise in the L1B data (e.g., between 28°S and 22°S) appear prominently in the level 1.5 image.

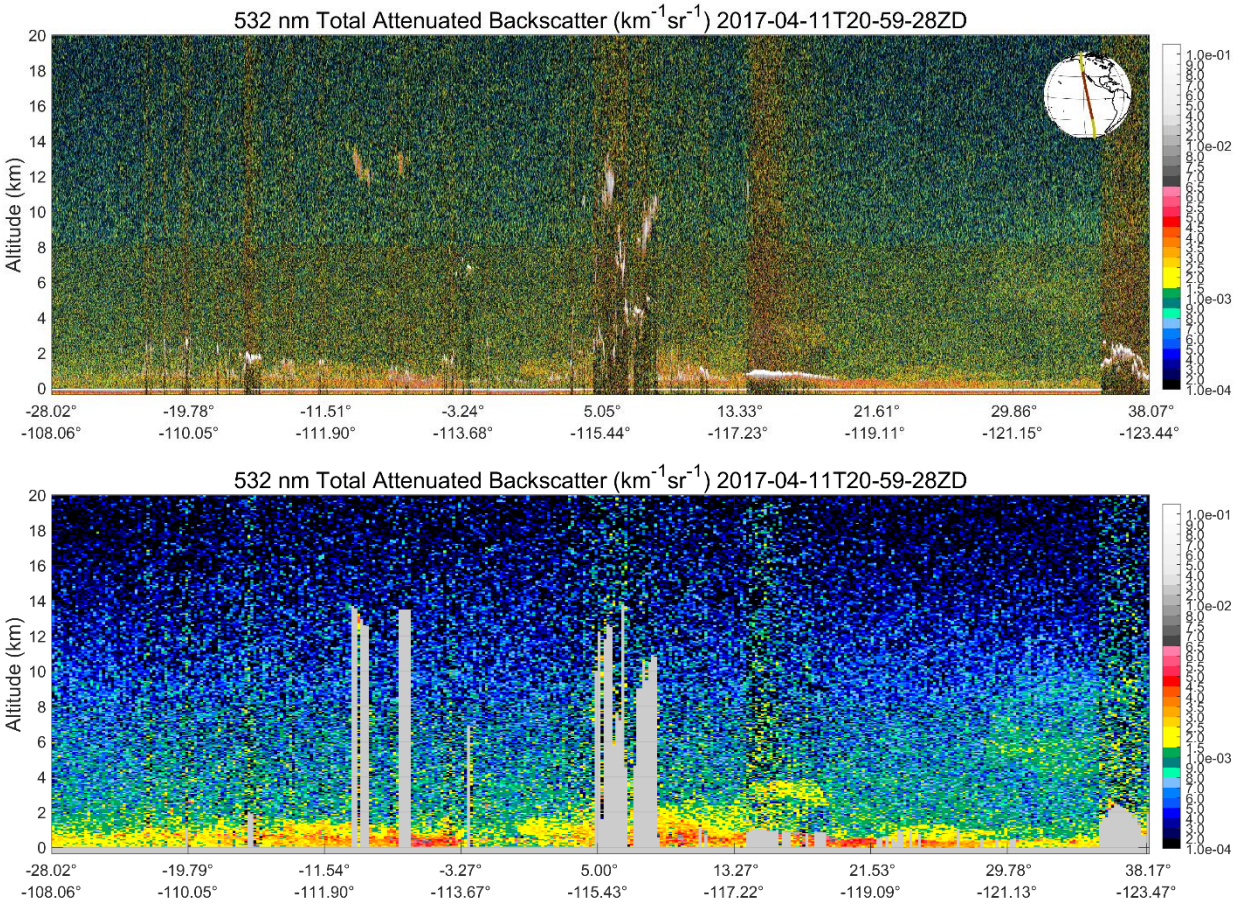

Figure 7: Upper panel shows L1B 532 nm total attenuated backscatter coefficients averaged to 1 km horizontal resolution; lower panel shows the level 1.5 data generated from the upper panel. Cloud-cleared regions in the level 1.5 image (e.g., below ~13.5 km at ~6.7°S and below ~2.5 km at ~36.4°N) are rendered in grey.

i. Lidar Level 3 Tropospheric Aerosol Data

The CALIOP level 3 (L3) tropospheric aerosol product (L3TAP) reports monthly mean profiles of aerosol optical properties on a uniform 2° latitude × 5° longitude × 60 m altitude spatial grid (Tackett et al., 2018). Since the L3TAP is intended to be a tropospheric product only, profile data are only reported up to a maximum altitude of 12 km. The primary quantities reported are vertical profiles of aerosol extinction coefficients at 532 nm and their vertical integrals, the aerosol optical depths (AODs). Aerosol type and spatial distribution information are also included. Averaged profile data are reported for all aerosols, regardless of type, and also separately for each of CALIOP's seven defined aerosol types. The methods used to distinguish between the different aerosol types are explained in detail in Kim et al., 2018.

The L3TAP is distributed in four different aggregations (Tackett et al., 2018). The "cloud-free" version is constructed using only those L2 profiles in which no clouds were detected at 5 km, 20 km, or 80 km averaging intervals. The "cloudy skies transparent" version uses all (and only) those 5 km L2 profiles in which the Earth's surface was detected, whereas the "cloudy skies opaque" version reports monthly mean aerosol properties harvested exclusively from those 5 km L2 profiles in which an opaque cloud was detected. Finally, the "all sky" L3TAP includes aerosols detected in all sky conditions; i.e., both cloud-free profiles and cloudy profiles, irrespective of cloud opacity. Figure 8 shows monthly mean

tropospheric nighttime AODs retrieved from the all sky L3TAP for September 2016. As with the L1B and L2 data products, daytime and nighttime measurements are reported separately in the L3TAP.

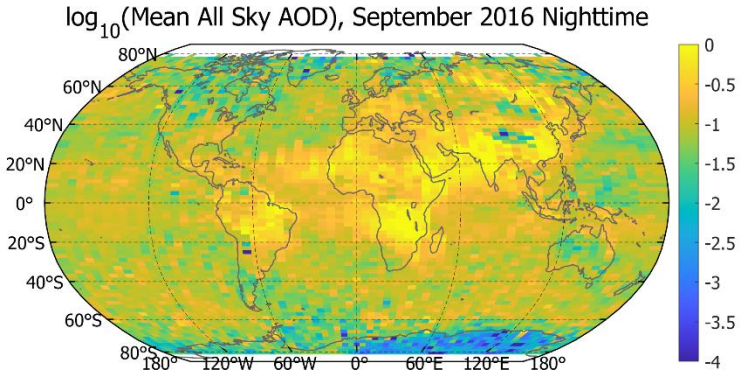

Figure 8: Global mean all sky tropospheric AOD for nighttime measurements acquired during September 2016. Colors show $\log_{10}$(AOD). Colors saturate at both extrema, so there are grid cells with AOD > 1 and other grid cells with AOD < 0.001.

j. Lidar Level 3 Stratospheric Aerosol Data

The CALIOP level 3 stratospheric aerosol product (L3SAP) monthly data product reports global distributions of altitude-resolved 532 nm total attenuated backscatter coefficients, attenuated scattering ratios, aerosol extinction coefficients, and integrated stratospheric aerosol extinction coefficients (AOD) on a uniform three-dimensional spatial grid spanning 5° latitude x 20° longitude x 360 m vertically. As described in Kar et al., 2019, the L3SAP attenuated backscatter coefficient profiles are harvested from the nighttime L1B data, then cloud-cleared using the L2 layer products. Data harvesting is limited to nighttime data only, as daytime solar background signals degrade the stratospheric signal-to-noise ratios to unacceptably low levels. Two versions are generated: a "background only" product, in which profile data from all layers detected in the L2 analyses are removed, and an "all aerosol" product, which retains profile data from aerosols while still excluding cloud data. Figure 9 shows an example of the "all aerosol" L3SAP for September 2016.

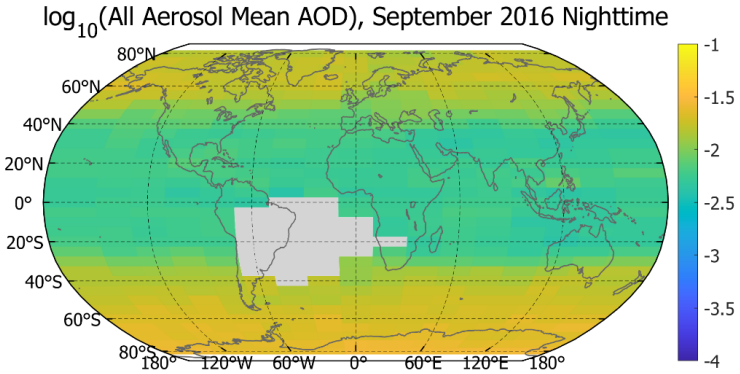

Figure 9: Global mean all aerosol stratospheric AOD for nighttime measurements acquired during September 2016. Colors show $\log_{10}$(AOD). Unlike the tropospheric AOD map shown in Figure 8, colors here do not saturate. Due to pervasive radiation-induced noise, data from the South Atlantic Anomaly (SAA; Noel et al., 2014), shown in grey, is excluded from all realizations of the L3SAP.

k. Lidar Level 3 Cloud Occurrence Data

The CALIOP level 3 cloud occurrence product (L3COP) reports global, altitude-resolved distributions of cloud occurrence at monthly intervals on a uniform three-dimensional spatial grid (2° latitude × 2.5°

longitude × 60 m altitude). The parameters reported in the L3COP are derived exclusively from the CALIPSO version 5.00 L2 5 km merged layer products and 5 km cloud profile products. Figure 10 illustrates day-night differences in detected cloud occurrence frequencies for all clouds, ice clouds only, and water clouds only during the month of June 2008.

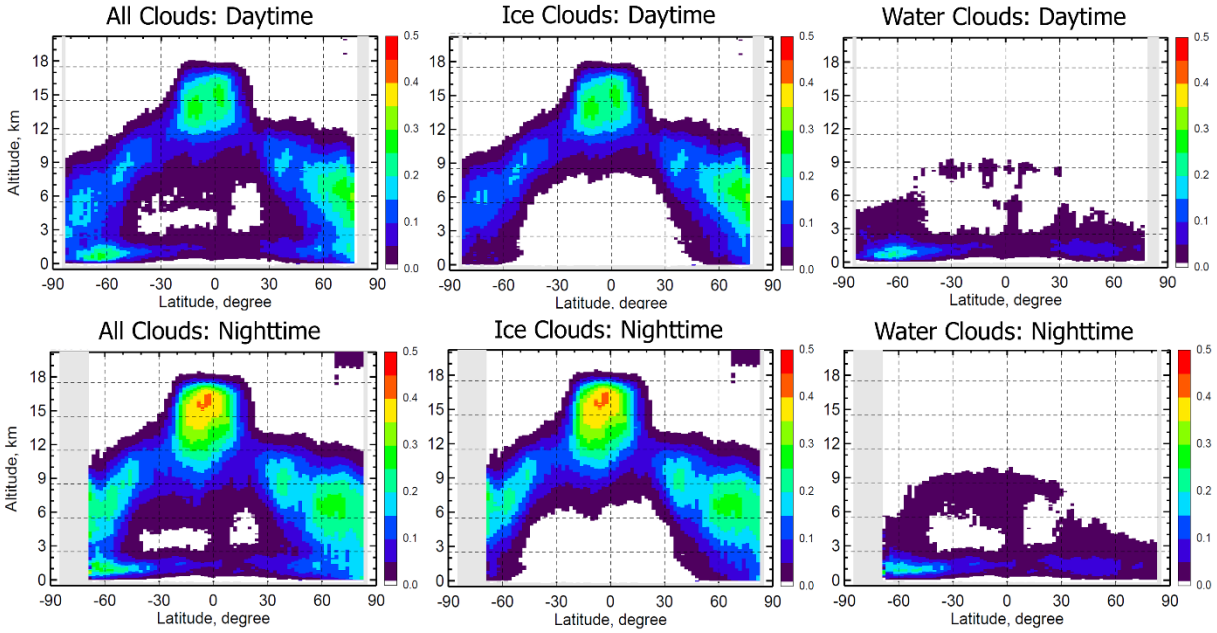

Figure 10: Image adapted from Cai et al., 2018 showing level 3 cloud occurrence distributions for daytime (top row) and nighttime (bottom row) during June 2008. The left column shows all clouds detected, the center column shows only ice clouds, and the right column shows only water clouds. The day-night differences in occurrence frequencies are at least partially, perhaps predominantly, driven by day-night differences in SNR, which in turn lead to day-night differences in detection sensitivity.

L3COP users should note that CALIOP's 3D volume cloud occurrence fractions do not convey the same information typically reported by the 2D cloud fractions derived from passive sensors measurements. Passive sensor cloud fractions report 2D gridded scalar values that quantify the monthly occurrence frequencies of clouds occurring anywhere within the vertical column defined by the latitude and longitude coordinates of each grid cell. By contrast, where passive sensor products report column-averaged scalars, CALIOP's 3D volume cloud occurrence product reports altitude-resolved vectors that quantify cloud occurrence frequencies at each of 344 altitude bins. Accounting for the vertical dimension, especially in multi-layer clouds scenes, precludes the possibility of using of L3COP parameters to replicate passive-sensor-like 2D cloud occurrence statistics, because the vertical overlap information required to reconstruct passive-sensor-like gridding is lost during the L3COP data aggregation process (Cai et al., 2018). For example, consider a L3COP altitude vector that contains zeros everywhere except for the bins centered at 1 km and 10 km, which both report monthly cloud fractions of 0.5. The corresponding passive sensor cloud fraction for this grid cell would lie between 0.5 (i.e., when only two-layer scenes were detected by CALIOP) and 1.0 (when only single-layer scenes were detected by CALIOP).

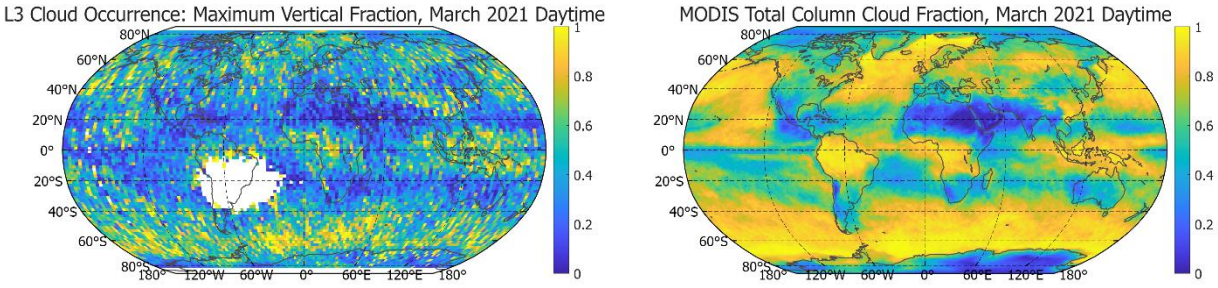

Figure 11: The left panel shows the maximum vertical cloud fraction reported for each latitude-longitude grid cell in the L3COP March 2021 daytime data. The right panel shows cloud fractions derived from the 'Cloud_Mask_Fraction' SDS in the MODIS-Aqua MCD06COSP data products for March 2021.

l. Lidar Level 3 Ice Cloud Data

The CALIOP level 3 ice cloud product reports global distributions of ice cloud extinction coefficients and ice water content at monthly intervals on a uniform three-dimensional spatial grid (2.5° longitude × 2.0° latitude × 120 m altitude). Samples are limited to stable extinction retrievals (extinction QC flags = 0, 1, 2, 16, or 18) within layers classified with high confidence as being composed of randomly oriented ice crystals. To further ensure retrieval reliability, only those range bins with overlying optical depths of 2 or less are included (Winker et al., 2024). Figure 12 shows extinction coefficient and ice water content examples extracted from the level 3 ice cloud product for March 2021.

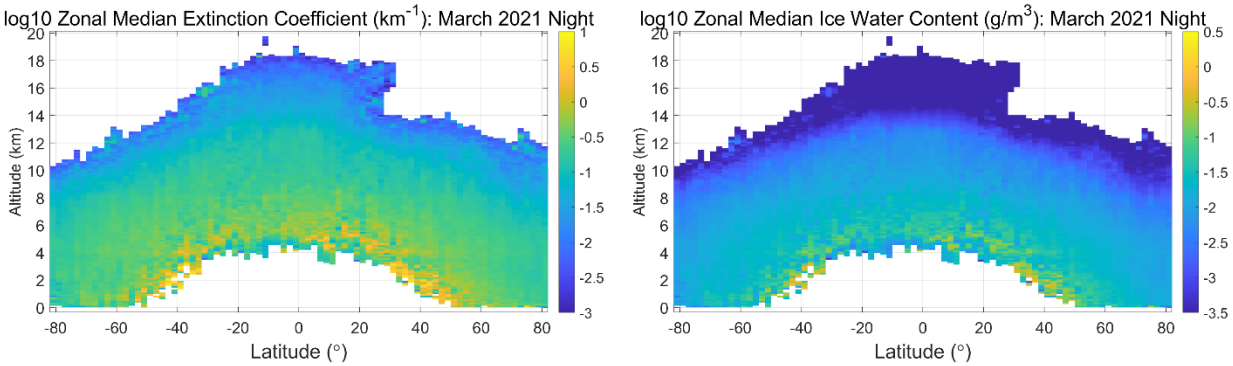

Figure 12: Example data from the March 2021 level 3 ice cloud product. The left panel shows log10 of the zonal median 532 nm extinction coefficients retrieved for all qualifying ice clouds. The right panel shows log10 of the zonal median ice water content for the same data set. Ice water content is estimated based on the retrieved extinction coefficients and the corresponding temperatures interpolated from MERRA-2 reanalysis data (Heymsfield et al., 2014).

m. Lidar Level 3 GEWEX Cloud Data

The CALIOP level 3 Global Energy and Water cycle Experiment (GEWEX) Cloud product (GEWEX_Cloud) is a reformatted version of CALIPSO's contribution to the GEWEX cloud assessment of global cloud datasets from satellites. These data products report global distributions of cloud amount and top as averages and histograms on a uniform grid as defined and formatted by GEWEX.

8. Why are there intermittent gaps in the data record?

Gaps in the CALIPSO data record are expected due to both scheduled events and unscheduled events. Scheduled events typically occur for routine spacecraft and instrument maintenance and/or calibration activities, including drag make-up maneuvers, boresight alignments (every 6-8 weeks), etalon adjustments, and polarization gain ratio calibrations. Unscheduled events are frequently caused by solar

flux increases, in which the incident energies were high enough to require turning off the instrument or, in extreme cases, the entire payload. Other unscheduled events include data loss due to unanticipated hardware failure(s) and/or to various ground station data capture anomalies.

9. Why can't I find CALIOP data over a specific location?

If you are unable to find CALIOP data over a specific location, the most likely cause is that the CALIPSO satellite does not pass over that location. CALIOP is a nadir-viewing sensor with a footprint diameter at the Earth's surface of ~90 m (Hunt et al., 2009). Unlike passive sensors which can have extensive cross-track swaths, CALIOP data is only collected directly along the ground track of the satellite.

The CALIPSO satellite was launched into a sun-synchronous orbit with an ascending node equator crossing time of 13:30 local solar time, with orbit tracks that repeat every 16 days. Figure 13 shows the daytime (left panel, ascending node) and nighttime (right panel, descending node) orbit tracks for September 16th, 2010. CALIPSO maintained this orbit configuration, flying in formation with the other A-Train satellites, until September 2018.

In June 2017, CloudSat suffered a reaction wheel failure, necessitating its exit from the A-Train in early 2018 (Braun et al., 2019). After considerable debate, the CALIPSO project decided that science yield would be maximized by continuing to fly in tandem with CloudSat. On 13 September 2018, CALIPSO halted science operations and began lowering its orbit from 705 km to 688 km to resume formation flying with CloudSat in the C-Train. Lidar data acquisition resumed on 25 September 2018.

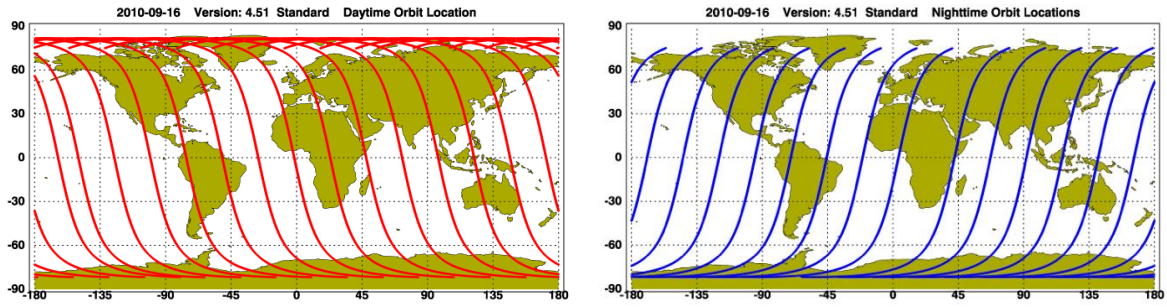

Figure 13: CALIPSO orbit tracks for 16 September 2010; the left panel shows daytime (ascending node) tracks while the right panel shows nighttime (descending node) tracks

10. Can you provide the code used to generate browse images that are posted at NASA's ASDC?

The CALIPSO browse image code is not publicly distributed. However, ccplot, an open source CloudSat and CALIPSO plotting tool written in python can be used to create browse images similar to those displayed on the CALIPSO web pages. Code to achieve similar results using Matlab is available here.

11. Why did you change the CALIOP color bars after so many years?

For CALIOP's final data release, the color maps used for the web-based browse images have been changed for several key observables. These changes were made specifically to improve the clarity of the data content in these images for individuals with color vision deficiencies (CVD). For some parameters, (e.g., depolarization ratios and total attenuated backscatter color ratios), these new CVD-friendly color maps universally replace the color maps used in previous versions. For other parameters (e.g., VFM maps of feature type and averaging required for detection), the original color maps have been retained in the final release. For the 532 nm and 1064 nm total attenuated backscatter coefficients and the 532 nm perpendicular channel attenuated backscatter coefficients, two sets of images are provided: the original legacy version and the new CVD-friendly version. An in-depth discussion of the CALIOP color maps is given

in Vaillant de Guélis et al., 2025. Section D of the Supplementary Materials for this paper lists the hexadecimal and RGB color values for all discrete colormaps. CSV files containing RGB colors values of the discrete and continuous colormaps are available via GitHub. An appendix in the CALIPSO Browse Image Tutorial document also lists the RGB triplets for both legacy and CVD versions of all CALIOP final release imagery.

12. Can you give a summary of the major changes between version 4 and version 5 that users really, really should know about?

Yes. The Data Description Documents for the individual products (e.g., L1B profile products and L2 layer, VFM, and profile products) all contain comprehensive data quality summaries that describe all of the changes made between the final data release and the previous version. The Data Description Documents include copies of the quality summaries for each CALIOP data release, allowing interested readers to track CALIOP data product development over the course of the entire mission.

13. How should I pronounce "CALIOP"?

CALIOP (i.e., **C**loud-**A**erosol **LI**dar with **O**rthogonal **P**olarization) is the name of the lidar onboard the CALIPSO satellite. CALIOP the space lidar is pronounced exactly like calliope, the musical instrument; phonetically, cal-eye-o-pee (/kəˈlaɪ.ə.pi/), not cal-ee-op (/ka.ljɔp/). See the Merriam-Webster Dictionary for audio (use the left-hand speaker button for the correct pronunciation).

CALIOP DATA QUALITY

14. What should I know about CALIOP data quality flags?

For users of the lidar level 1B profile data, there are two sets of data quality flags: QC_Flag and QC_Flag2. Both are arrays of bit-mapped integers, with one value recorded for each laser pulse, in which the individual bits signal various errors and/or warnings. Bit locations are specified using zero-based indexing. For example, if a profile cannot be successfully geolocated, bit #3 in the QC_Flag will be toggled. Similarly, bit #14 in the QC_Flag will be toggled if the pulse energy for any laser shot is below a predetermined data quality threshold (10 mJ). Complete lists of the bit interpretations for the QC_Flag and QC_Flag2 parameters are provided in the L1B Data Description Document.

For users of CALIOP L2 data, the list below provides brief descriptions of some of the most important data quality parameters.

a. Feature Classification Flags (layer products) and Atmospheric Volume Descriptions (profile products)

The feature classification flags (FCF) and atmospheric volume descriptions (AVD) are bit-mapped 16-bit integers that report (a) feature type (e.g., cloud vs. aerosol); (b) feature subtype; (c) layer ice-water phase (clouds only); and (d) the amount of horizontal averaging required for layer detection. Coarse quality assessments (e.g., high, medium, low, none) are also provided for each classification. The Data Description Documents for the CALIOP L2 VFM products, layer products and profile products provide detailed maps for the interpretation for all bits in the FCF and AVD.

b. CAD_Score

CAD scores provide a numerical classification confidence level for all layers examined by the CALIOP cloud-aerosol discrimination (CAD) algorithm. The standard CAD algorithm uses five-dimensional probability distribution functions (PDFs) to calculate standard CAD scores ranging between –100 and 100. Negative values denote aerosols and non-negative values denote clouds. In both cases, larger

magnitudes indicate higher classification confidence levels. Liu et al., 2019 gives a complete review of the CAD algorithm, along with descriptions of several special CAD scores that lie outside the –100 to 100 range.

c. Extinction_QC_532 and Extinction_QC_1064

The extinction QC flags are 16-bit integers in which each bit conveys specific information about the status of the extinction retrieval when the algorithm terminates. For transparent layers, fully successful solutions will have extinction QC values of 0, 1, and 2. For opaque layers, fully successful solutions will have extinction QC values of 16 and 18. Complete listings of extinction QC values are given in Young et al., 2018 and in the Data Descriptions Documents for the CALIOP L2 layer products and L2 profile products.

d. Overlying_Integrated_Attenuated_Backscatter_532

The overlying integrated attenuated backscatter, γ'_{above}, is the integral with respect to altitude of the 532 nm total attenuated backscatter coefficients between the top of the atmosphere (TOA; i.e., the first range bin in any L1B profile) down to the range bin immediately above the layer top altitude. γ'_{above} provides a qualitative assessment of the layer boundary detection confidence that users can apply to each layer reported. In general, detection confidence diminishes as γ'_{above} increases. γ'_{above} is obtained directly from the calibrated backscatter signal, and hence can also provide a crude proxy for the optical depth above each layer, irrespective of the averaging required for feature detection.

e. Layer_IAB_QA_Factor

The layer IAB QA factor is defined as 1 - $F(\gamma'_{above})$, where $F(\gamma'_{above})$ is the cumulative probability of measuring a total column (i.e., TOA to the DEM surface) integrated attenuated backscatter equal to γ'_{above}. Values range between 0 and 1, with lower values indicating more turbid skies above and hence reduced confidence in layer detection boundaries and optical property retrievals.

f. Overlying_Particulate_Optical_Depth_532

The overlying particulate optical depth at 532 nm reports the optical depth from clouds and aerosols (i.e., particulates) measured from TOA down to the top of each feature. This value provides a measure of the signal attenuation incurred before any layer is detected. For example, the attenuation of the backscatter signal incurred passing through an overlying particulate optical depth of 1.5 is $\exp(-2 \times 1.5) \approx 0.05$; i.e., the signal strength within the layer is ~5% of what it would have been had there been only clear skies above. CALIOP retrievals of optical properties in layers with large overlying optical depths (e.g., 3 or more) should only be used with considerable caution.

g. *Uncertainty_532 and *Uncertainty_1064

Quantitative uncertainty estimates are provided for a substantial fraction of the measured, retrieved, and assumed parameters in the CALIOP L2 analyses. Examples include integrated attenuated backscatter uncertainties (Vaughan et al., 2005), layer optical depth uncertainties (Young et al., 2018), and lidar ratio uncertainties (Kim et al., 2018).

15. How can I identify potentially unreliable atmospheric features?

The CALIOP data products offer several parameters that can be used to identify potentially unreliable atmospheric features. Perhaps the most immediately and broadly useful of these is the CAD_Score, described in FAQ #14.b. CAD scores are reported in all L2 layer products on a per layer basis and in the L2 cloud and aerosol profile products on a per range bin basis. Standard CAD scores range between –100 and 100, with negative values denoting aerosols and non-negative values denoting clouds. Larger magnitudes

indicate higher classification confidence. As shown in Table 7, the Feature Classification Flags (layer products) and Atmospheric Volume Descriptions (profile products) partition CAD scores into four general classification confidence groups. Features with CAD score magnitudes less than 20 should be considered suspicious/unreliable.

Table 7: Feature classification confidence as a function of CAD score magnitude, as reported in the FCF and AVD parameters

Classification Confidence	CAD Score Range
high	50 ≤ |CAD| ≤ 100
medium	50 ≤ |CAD| < 70
low	20 ≤ |CAD| < 50
none	0 ≤ |CAD| < 20

Figure 14 shows the distribution of CAD scores for all layers detected at 5 km, 20 km, and 80 km resolutions for the entire mission. For a host of reasons, CAD scores are seen to vary as a function of the amount of horizontal averaging required for detection. The fraction of no confidence layers (0 ≤ |CAD| < 20) is 22% for 20 km detections and 17% for 80 km detections. For features detected at 5 km resolution, the fraction of no confidence layers falls to 4%. When considering all unique layer detections, the no confidence fraction is 7.5%. 84% of all aerosols are classified as high confidence (-100 ≤ CAD ≤ -70) as are 87% of all clouds (70 ≤ CAD ≤ 100).

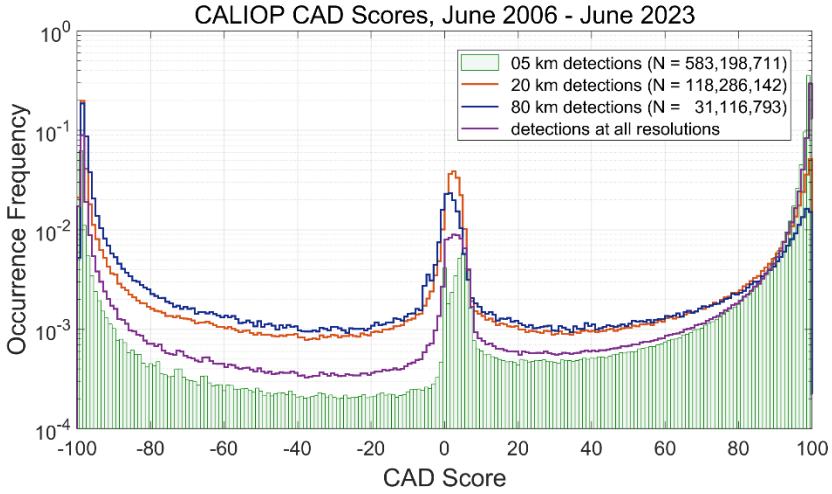

Figure 14: Distributions of CAD scores according to feature detection resolution. The pale green bars show the distribution of features detected at 5 km. The orange and blue lines show, respectively, the distributions of features detected at 20 km and 80 km resolutions. The purple line shows the distribution of CAD scores composited for all unique layers.

Relative uncertainties (i.e., ΔX/X) offer another useful metric for evaluating layer reliability. Data users are warned, however, that CALIOP SNR is notably lower than that of most other space-based sensors, and hence the relative uncertainties in both measured and retrieved quantities are considerably larger.

Because CALIOP SNR increases with increasing signal levels, fainter features (e.g., PBL aerosols) will typically have higher relative errors than more robust targets (e.g., water clouds). Similarly, as seen in Figure 15, relative uncertainties measured during daylight are, almost without exception, higher than those measured during nighttime operations. Finally, and not surprisingly, the relative uncertainties for individual range bins reported in the profile products will be higher than the relative uncertainties for the full layer reported in the layer products.

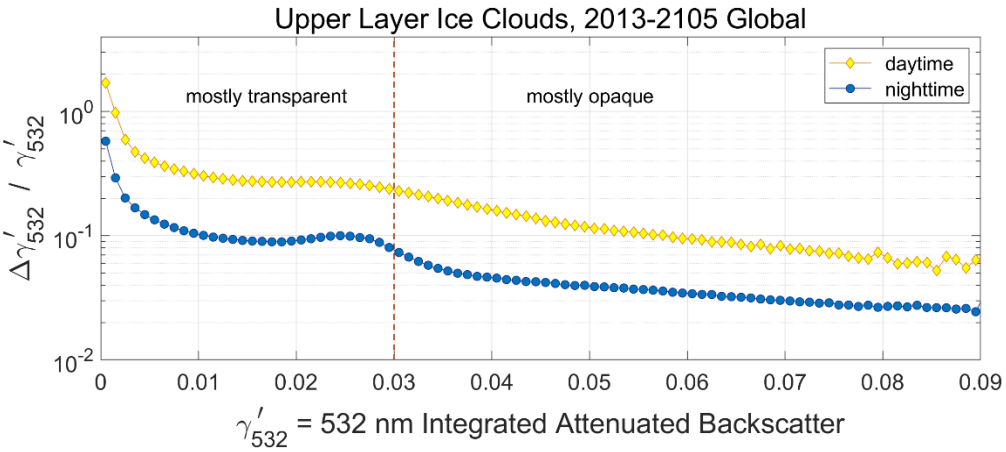

Figure 15: Relative uncertainty, $\Delta\gamma'_{532}$ / γ'_{532}, in CALIOP's 532 nm integrated attenuated backscatter for ice clouds detected at 5 km resolution that were the uppermost layer in each column. Data are restricted to layers classified as randomly oriented ice (ROI) clouds with high confidence and having 532 nm extinction QC flags of 0, 1, 2, 16, or 18. Daytime relative uncertainty is uniformly higher than nighttime uncertainty due to the large solar background signals present during daytime. For both daytime and nighttime, relative uncertainties generally decrease with increasing γ'_{532}.

For users of CALIOP layer optical properties, the Extinction_QC_532 and Extinction_QC_1064 flags provide essential guidance. For most applications, fully successful solutions will have extinction QC values of 0, 1, 2, 16, or 18 only. In certain relatively rare situations – e.g., strongly scattering, optically thick dust layers – QC values of 6 may also be assigned to a valid solution. This topic is explored in some detail in the Reevaluating Extinction QC = 6 section of this document.

Finally, for any analyses of layer geometric and optical depths, understanding the meaning of the Opacity_Flag in the layer products is essential. CALIOP cannot measure the true base of totally attenuating (i.e. opaque) features. Instead, the base altitudes reported in the CALIOP data products for these layers must be interpreted as *apparent bases* that do not indicate the full vertical extent of the feature, but instead mark the altitude at which the laser backscatter signal could no longer be distinguished from the ambient noise. Similarly, the optical depths reported for opaque layers are apparent optical depths that represent the feature optical depth penetrated when the beam was finally extinguished. The Opacity_Flag for opaque features is set to 1. Otherwise, the Opacity_Flag is set to 0. A layer is classified as opaque when it is the lowest atmospheric feature in a column and the Earth's surface cannot be detected beneath it. In the layer products there will be at most one opaque layer in each column.

16. Is CALIOP data processing uniform over the entire Earth?

Yes, the same suite of retrieval algorithms is applied to all CALIOP data uniformly around the entire globe for the entire mission. However, the quality of these retrievals varies, both spatially and temporally. The single most important cause of data quality variability within any fixed latitude-longitude region is the magnitude of the incident sunlight at the overpass time. The high solar background signal present during the sunlit portions of the orbit (i.e., daytime data) generates substantially more background noise than is seen in measurements acquired when the satellite is in full darkness (i.e., nighttime data). Data quality will therefore vary according to the local diurnal cycle, with SNR being significantly lower during the day than at night. Furthermore, as seen in Figure 16, the daytime noise enhancements also depend strongly on the albedo of the scene being observed. The noise magnitudes in signals measured above daytime stratus clouds are significantly larger than those measured in cloud-free skies over the ocean; e.g., see the noise envelop discontinuity just north of 25.04°S in Figure 16. Daytime retrievals of spatial and optical

properties from layers lying above these clouds are typically much more uncertain than retrievals for layers lying above a dark ocean.

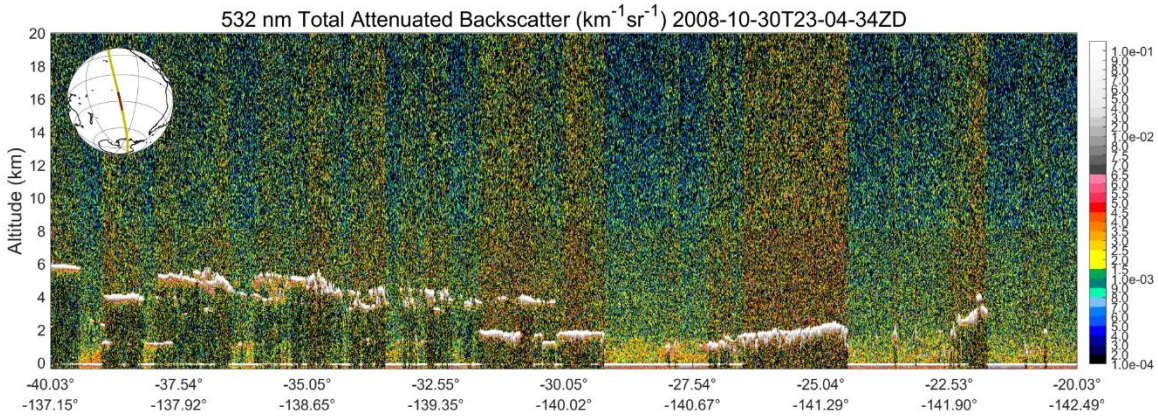

Figure 16: Daytime measurements acquired over the south-central Pacific on 2008-10-30. Note the significant change in noise magnitudes as the lidar transitions from measuring dense water clouds to clear skies over the ocean (e.g., just north of 25.04° S).

Calibration accuracies and uncertainties can also vary as a function of geophysical location and/or season. Within the SAA, increased radiation in the Van Allen Belts introduces additional noise everywhere in the profile measurements. The additional noise at the highest altitudes leads to increased uncertainty in the 532 nm nighttime calibration (because fewer valid calibration samples are found), which in turn propagates into the uncertainties of all subsequently derived parameters within the SAA latitude belt, both daytime and nighttime (Noel et al., 2014; Kar et al., 2018; Getzewich et al., 2018). Outside the SAA, noise levels in the 532 nm calibration region are relatively stable except at the poles, which show some increase in radiation-induced noise (Hunt et al., 2009). Moreover, molecular densities can vary significantly, and are especially low in the wintertime polar vortices, which, when combined with the increased radiation noise, can cause intermittent increases in nighttime calibration uncertainties (Kar et al., 2018).

Another fundamental limitation on CALIOP data quality uniformity is the vertically varying SNR of the measurements. For the uppermost layer in any profile, the SNR for nighttime data is largely a function of the lidar instrument state and feature scattering intensity and generally does not vary as a function of orbit location. However, for both nighttime and daytime measurements, the backscatter signal is increasingly attenuated as it penetrates further into the Earth's atmosphere. In particular, the SNR is reduced after the laser light passes through layers of atmospheric particulates, so that measurements of an otherwise identical aerosol layer will have higher SNR in cloud-free conditions than (for example) on those occasions when there are cirrus clouds overhead.

17. What are 'constrained retrievals' and why are they important?

Constrained extinction retrievals are attempted whenever suitable regions of "clear sky" can be found immediately above and immediately below a feature (Young et al., 2009). The mean attenuated scattering ratio in the lower clear-sky region divided by the mean attenuated scattering ratio in the upper clear-sky region provides a direct measurement of the feature two-way transmittance. This value is used to constrain the solution of the lidar equation and retrieve optimized estimates of feature lidar ratios. Constrained retrievals deliver the highest quality backscatter coefficients, extinction coefficients, and lidar ratios reported in the CALIOP data products.

The requirement for clear sky immediately above and below a layer limits the applicability of the constrained retrieval method. By definition, surface attached aerosol layers will never be candidates for

constrained retrievals. On the other hand, the optical properties of cirrus clouds are frequently obtained via constrained retrievals.

Constrained retrievals can be readily identified in the CALIOP data products by examining the least significant bit in the Extinction_QC_Flag_532. If this bit is toggled on, a constrained retrieval has been attempted. Other bits in the QC flag will provide further information on algorithm success. Extinction_QC_Flag_532 = 1 indicates a fully successful constrained retrieval. Because the 1064 nm molecular backscatter signal is so weak and the APD dark noise is so high, constrained solutions are not viable at 1064 nm.

CALIOP's Vertical and Horizontal Data Product Resolutions

To meet data downlink volume restrictions, CALIOP is averaged onboard the satellite prior to being telemetered to ground stations on Earth. This height-varying onboard averaging scheme is explained in detail in FAQ #6: What are CALIOP's sampling resolutions?

Largely as a result of the onboard averaging, the publicly distributed CALIOP data products may contain a mix of different averaging resolutions, depending on data processing level. The L0 data and L1B data are distributed at pseudo-single shot resolution, with data that are averaged horizontally onboard (see Table 6) being replicated as necessary to mimic true single shot data. The vertical resolutions in the L0 and L1B products vary with altitude and are identical to the vertical resolutions in the downlinked data. For the L3 profile products, which are aggregated over large spatial and temporal extents, the concept of "horizontal resolution" vanishes, and is instead replaced by a 2D areal resolution. Although not identical across all products, these areal resolutions are all congruent with one another. So too are the vertical resolutions: 360 m for the stratospheric aerosol product, 120 m for the cloud ice product, and 60 m for the tropospheric aerosol and cloud occurrence products.

CALIOP's onboard averaging scheme imposes its most stringent challenges on the level 2 retrievals. The peak backscatter intensities of the features measured by space-borne lidar range over several orders of magnitude. Strongly scattering features such as stratus and fair-weather cumulus clouds are easily detected within a single laser pulse. For more tenuous features – e.g., thin cirrus clouds – the average of several laser pulses may be required to obtain the SNR necessary to differentiate feature boundaries from the ambient scattering environment. The unambiguous detection of the very weakest features, such as faint aerosol layers and subvisible cirrus, may require averaging over a substantial number of pulses. And although the onboard averaging scheme is structured to generally match averaging intervals with the expected backscatter intensities within each discrete averaging region, there are times when nature refuses to cooperate. For example, many orographically forced PSCs over Antarctic could conceivably be detected at single shot resolution, and most certainly be detected at 1 km resolution. However, at these altitudes CALIOP data is averaged to 5/3 km (5 shots) along track. Similarly, while the robust scattering from dense ice clouds found in mesoscale convective systems would surely be detected at single shot resolution, these clouds typically form above 8.2 km where CALIOP data is averaged to 1 km along track.

To reliably identify all features within a given scene at the highest possible spatial resolution, CALIOP employs a Selective Iterated Boundary Location (SIBYL) scheme. The SIBYL algorithm makes multiple passes through the L1B data, eventually searching for features at 5 different horizontal resolutions: single shot, 1 km (3 shots averaged), 5 km (15 shots averaged), 20 km (60 shots averaged) and 80 km (240 shots averaged). Figure 17 shows a schematic of the SIBYL processing engine. As explained in the CALIOP Layer Detection and Cloud Clearing section of this document, bookkeeping of SIBYL's native output can be somewhat convoluted, which in turn can lead to some confusion about the spatial resolutions reported in the 5 km layer and profile products.

CALIOP LAYER DETECTION AND CLOUD CLEARING

18. Why do layer boundaries in the 5 km layer products appear to overlap one another?

The apparent overlap of layer boundaries sometimes seen in the 5 km layer products is a data reporting oddity spawned by CALIOP's Selective Iterated Boundary Location (SIBYL) algorithm. This situation occurs because the 5 km layer products report the final outputs of the SIBYL's nested multi-grid layer detection scheme, without attempting any additional spatial reorganization. Overlap sources and interpretations are explained in the condensed, step-by-step review of the SIBYL architecture given below. Full details are found in Vaughan et al., 2005 and Vaughan et al., 2009.

The SIBYL algorithm examines the L1B data in "chunks" of 240 consecutive laser pulses, representing a nominal horizontal distance of 80-km. Each chunk of data will ultimately be searched for the presence of cloud and aerosol layers at 5 along-track averaging resolutions: 333 m (single shot), 1 km (3 shots averaged), 5 km (15 shots averaged), 20 km (60 shots averaged), and 80 km (240 shots averaged). Figure 17 (adapted from Vaughan et al., 2009) illustrates the procedures with critical steps enumerated below.

1. To initiate the search for features, chunk data are first averaged to a nominal horizontal resolution of 5-km, creating 16 profiles each averaged over 15 consecutive laser pulses. Each of these 5-km profiles are then searched independently for the presence of cloud and/or aerosol layers.

2. If atmospheric layers are detected anywhere below 20.2 km, SIBYL executes the upper 'high resolution cloud clearing' loop in Figure 17. In this loop, regions identified as layers in the 5 km profile scan are reaveraged to finer spatial resolutions and searched again for the presence of strongly scattering layer segments that can be detected at the lower SNRs that characterize higher spatial resolution profiles. First, profiles in which features were detected at 5 km are reaveraged and searched at 1 km resolution. Those regions in which features are detected at 1 km are subsequently searched at single shot resolution. The spatial, temporal, and optical properties for all layers detected in the 1 km and single shot scans are recorded and reported in, respectively, the 01kmCLay and 333mMLay data products. All features detected at these higher resolutions are immediately classifies as either clouds or aerosols.

   Additional analyses are conducted whenever clouds are detected in the planetary boundary layer (PBL), defined as extending upward by 4 km from the Earth's surface (see FAQ #22). In these cases, the attenuated backscatter coefficients are REMOVED (i.e., set to fill values) in each profile in which clouds were detected at single-shot resolution, beginning from the top of the highest cloud found downward to the end of the profile at ~ −2 km AMSL (see FAQs #19, #20, and #21). All data remaining in the original 15 single-shot profiles are then reaveraged and searched a second time to determine whether the feature boundaries detected in the original 5 km average can still be detected in the cloud cleared and reaveraged profile. Note that this cloud clearing operation is only applied at single shot resolution. Features detected at 1 km resolution are not cleared before reaveraging the data to a nominal 5 km resolution. Because the high intensity cloud backscatter has been removed, this second search at 5 km frequently fails to detect features in (for example) scenes containing fair weather cumulus embedded in a moderate boundary layer aerosol. Tackett et al., 2022 provides additional details on the complexities involved in the cloud clearing operation.

3. After completing passage through the high-resolution cloud clearing loop, the cloud-cleared back-scatter data and associated features detected at 5 km resolution enter the "intensity clearing" loop shown in the bottom portion of Figure 17. After recording the spatial and temporal properties and initial estimates of optical properties for each layer detected in the sixteen 5 km averaged profiles,

   a. an initial two-way transmittance estimate is made for each layer;

b. the attenuated backscatter coefficients between layer base and top are REMOVED (i.e., set to fill values); and

c. the 5 km averaged attenuated backscatter data beneath each layer are corrected for the estimated signal attenuation (i.e., the two-way transmittance) of the layer.

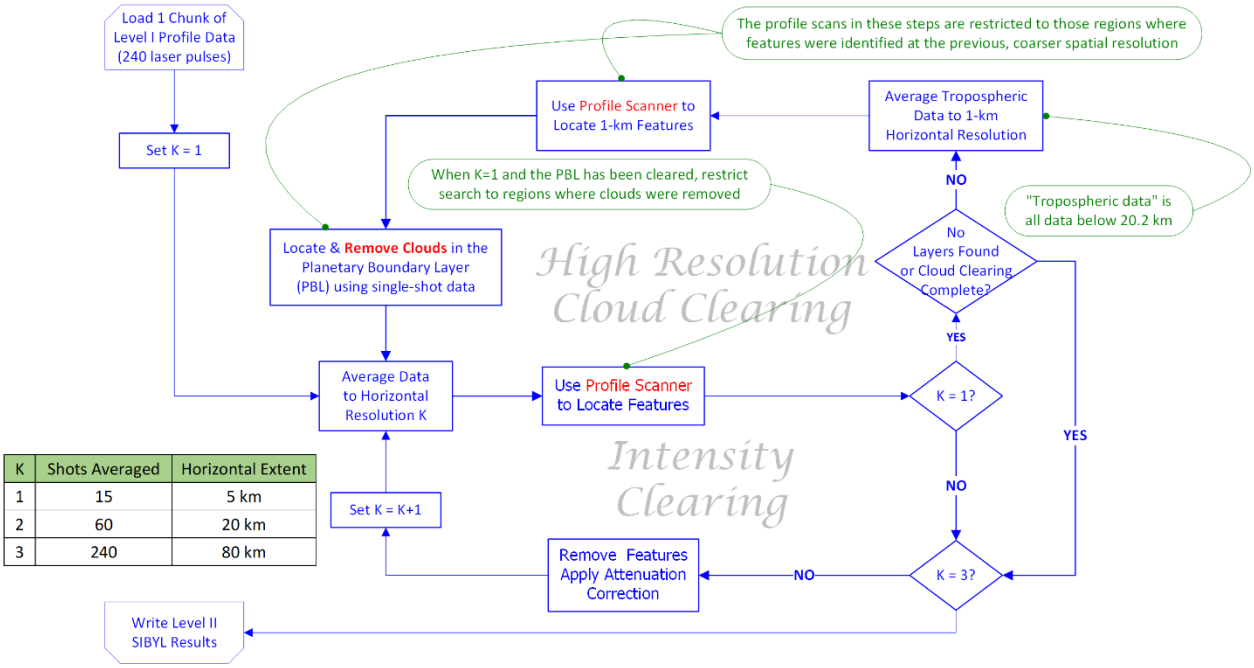

Figure 17: Flowchart illustrating the workings of the CALIOP feature finder. Profiles averaged to the 5 km along-track resolution will go through the upper "high resolution cloud clearing" loop prior to entering the "intensity clearing" loop. Subsequent averages to 20 km and 80 km resolutions are only processed by the intensity clearing loop.

4. Having located and removed all features detected at 5 km resolution, the attenuation corrected 5 km profiles are reaveraged to 20 km resolution. Note that all of the backscatter data within all of the layers detected at 5 km resolution have been REMOVED from this second round of averaging. Consequently, segments of the nominal 20 km averaged profile will be constructed using fewer than 60 profiles in those altitude regions where features were detected at 5 km resolution. The CALIOP profile scanner (Vaughan et al., 2005) is then independently applied to each of these "intensity cleared" 20-km profiles, searching for those features that were too faint to be distinguished from the ambient background noise at the 5-km averaging interval.

5. Finally, after completing the search for features at 20 km resolutions, steps 3 and 4 are repeated, using the intensity cleared 20 km profiles to create a single intensity cleared 80 km profile. Once again, all of the backscatter data within all of the layers detected at both the 5 km and 20 km resolution have been REMOVED from this third and last round of averaging, so that segments of the nominal 80 km averaged profile can be constructed using substantially fewer than 240 profiles in those altitude regions where features were previously detected at 5 km and 20 km.

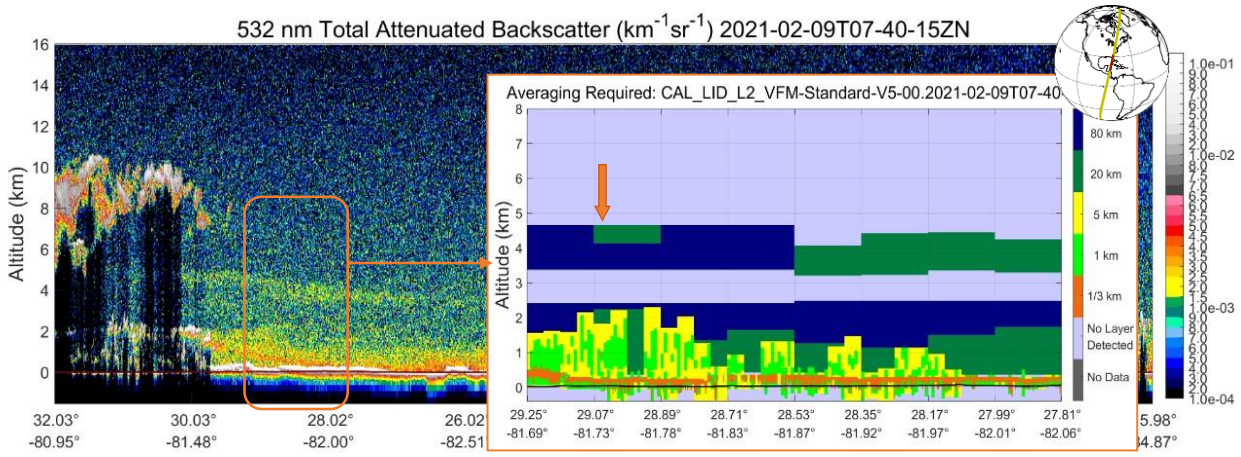

Figure 18: CALIOP measurements over the western Gulf of America acquired 9 February 2021. The 532 nm total attenuated backscatter profiles are averaged to a 1 km (3 laser pulses) along-track resolution. The vertical feature mask inset shows the averaging required for feature detection within a 160 km subset of the level 1B data enclosed by the orange rectangle centered at approximately 24° N and 82° W. In both panels, the DEM ocean surface is shown by a dark horizontal line at 0 km.

Figure 18 shows several examples of (apparently) overlapping layers in a 160 km segment of nighttime data acquired over the Gulf of America on 9 February 2021. Two vertically and horizontally contiguous layers are detected. The lower layer, with segments detected at multiple averaging resolutions, extends from ~2.5 km down to the base of the surface-attached cloud (see the bright white regions above the 0 km line in the larger image). The fainter upper layer, lying between ~4.6 km and ~3.3 km, is only detected after averaging to either 20 km or 80 km. Table 8 lists the layer boundaries of all atmospheric features detected at 5 km, 20 km, and 80 km in the 5 km data segment indicated by the orange arrow in Figure 18. Taken at face value, the base and top altitudes reported for the two uppermost layers suggest that the layer detected at 20 km, between 4.663 km and 4.154 km, fully overlaps the layer detected at 80 km, between 4.663 km and 3.406 km. However, recall step 5 in the above description of the SIBYL architecture: all backscatter data within the layer detected at 20 km resolution have been REMOVED before creating the nominal 80 km averaged profile. There is no overlap of the two layers because the data used to construct the 20 km average and the (nominal) 80 km average are disjoint sets.

Table 8: Top and base altitudes and horizontal averaging required for layer detection reported in the V5.00 05kmMay product for the 5 km data segment measured at 29.0661° N and 81.7342° W on 2021-02-09 beginning at 07:58:29.288 UTC. Only layers detected at 5 km, 20 km, and 80 km are shown.

top altitude (km)	base altitude (km)	averaging required (km)
4.663	4.154	20
4.663	3.406	80
2.418	1.370	80
2.238	0.382	20
1.819	0.322	5

A similar situation is seen in the lower layer. In the profile scan conducted at the 5 km averaging resolution, a feature was detected between 1.819 km and 0.322 km. The intensity clearing operation subsequently removes all backscatter coefficients between these boundaries and those between the boundaries of all other features detected at 5 km resolution within this chunk. A (nominal) 20 km averaged profile was then created by averaging four consecutive intensity cleared 5 km profiles. The backscatter coefficients from all features previously detected at the 5 km resolution were excluded when creating this (nominal) 20 km

averaged profile. Conducting a profile scan on this profile yields a 20 km resolution feature detected between 2.238 km and 0.382 km. Based on an examination of the numbers in Table 8 (which are obtained directly from the 05kmMLay product for this granule), one might conclude that the 5 km feature overlaps the bottom 1.437 km of the 20 km feature. However, examining the 'averaging required' panel in Figure 18 tells a different, much more accurate story. Within the 80 km chunk, the regions painted in yellow and bright green contain backscatter coefficients that contribute only to the 5 km layer detections. Similarly, only those data in the dark green regions contribute to the 20 km layer detections and only those data in the dark blue regions contribute to the 80 km layer detections. The different colors in the averaging required for detection images can thus be interpreted as a coarse contour plot of backscatter intensity.

19. What is 'single shot cloud clearing' and why is it done?

The function of CALIOP's single shot cloud clearing procedure is to separate the very large attenuated backscatter coefficients characteristic of dense water clouds from the surrounding, much smaller backscatter coefficients of the aerosols in the planetary boundary layer. The goal of the procedure is to eliminate cloud contamination in the retrievals of extinction and optical depth in the PBL aerosols in which these clouds are embedded. Figure 19 illustrates the desired behavior. As seen in the larger image, a persistent aerosol layer extends along the full orbit track. However, retrieving aerosol optical properties is challenging because the layer is capped with dense broken water clouds in which the optical properties are drastically different from the surrounding aerosols. Furthermore, the data are so noisy that substantial along-track averaging is required to accurately detect aerosol layer boundaries and retrieve reliable estimates of aerosol extinction. The effectiveness of the cloud clearing procedures is demonstrated by the smaller image inset at the top right of Figure 19, which shows the level 1.5 data extracted from the level 1 data shown in the larger panel. To create the level 1.5 profiles, the backscatter coefficients from clouds detected at single shot resolution are removed prior to averaging the remaining data to an along-track resolution of 20 km. In this scene the cloud clearing procedure performs exactly as intended, resulting in a homogeneous, easily detected aerosol layer.

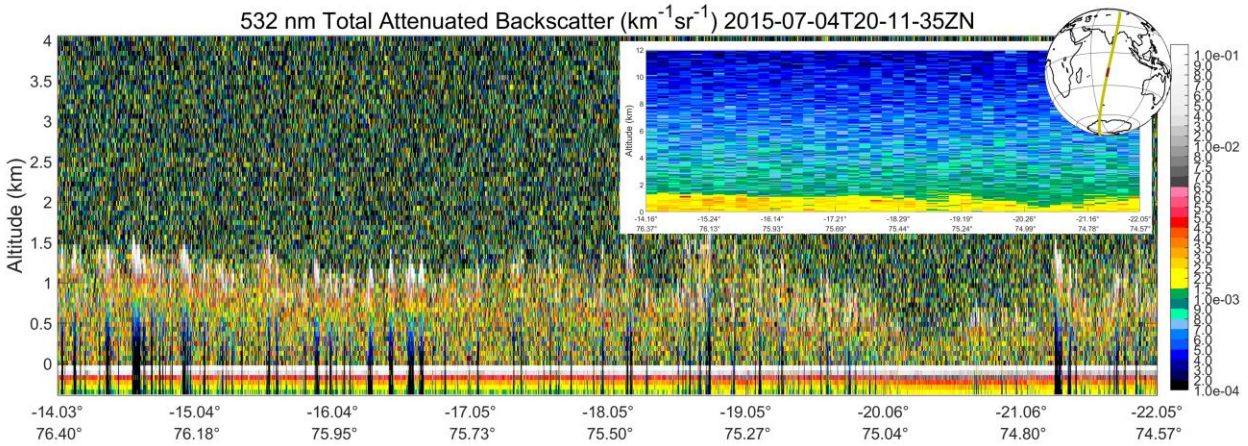

Figure 19: The larger outer image shows single shot L1B profile measurements of PBL aerosols (maximum height ~2 km) interspersed with intermittent boundary layer water clouds, acquired on 4 July 2015. Even though these are nighttime measurements, the data are very noisy, making it difficult to visually distinguish the smaller, isolated clouds from the ambient aerosol. On those occasions when the clouds are opaque, their presence can be confirmed by the thin black vertical lines seen in the surface and subsurface signals. These lines, which appear frequently (e.g., between 18.05° S and 20.06° S), indicate profiles in which the backscatter signals have been totally attenuated by atmospheric layers. After cloud clearing the L1B profiles at single shot resolution, the L1.5 data are generated by averaging the remaining L1B profile data to an along-track resolution of 20 km. The smaller image inset at the top right shows the cloud cleared level 1.5 data for the same scene.

20. Why does 'cloud clearing' also remove backscatter data below the clouds?

Single shot cloud clearing starts by identifying those features detected at single shot resolution that were subsequently classified as clouds. Once this is done, all attenuated backscatter coefficients from cloud top downward to the end of the single shot profile are flagged as *cloud-cleared data*. Cloud-cleared data in any single shot profile are then excluded when the profiles are composited into the coarser spatial resolution profiles that are subsequently searched in an attempt to detect faintly scattering aerosol layers.

The cloud clearing operation was specifically designed to separate small scale water clouds from the surrounding aerosols in the planetary boundary layer. Ideally, cloud clearing would remove only those backscatter coefficients identified as belonging to clouds and retain all useable data beneath the clouds. However, in practice this approach faces some currently unsurmountable difficulties, as obtaining accurate extinction profiles requires that the attenuated backscatter coefficients below the clouds be renormalized to account for the signal attenuation that occurs within the clouds (Young and Vaughan, 2009). But because characterizing range-resolved multiple scattering in water clouds remains highly uncertain, extinction retrievals in these clouds are likewise highly unreliable and hence cannot be used to derive the unbiased attenuation corrections required for accurate extinction retrievals in below-cloud aerosols. Consequently, as described above, cloud clearing in any single shot profile proceeds from the top of the uppermost cloud detected within the boundary layer and extends downward throughout the remainder of the profile, irrespective of the feature type classification assigned to any underlying range bin.

21. Why is cloud clearing only done in the boundary layer?

At higher altitudes, the occurrence frequency of small horizontal scale water clouds embedded in significant aerosol layers (i.e., aerosols that CALIOP can detect) is substantially reduced. Instead, mid-level water clouds (e.g., altostratus) typically extend unbroken over relatively large horizontal extents. Moreover, because the aerosol loading in the free troposphere is typically much lower than in the PBL, transparent mid-level water clouds are often suitable candidates for constrained retrievals (see FAQ #17). Because constrained retrievals deliver more accurate optical depth estimates than unconstrained retrievals, the attenuation corrections made in underlying PBL features are also more reliable, leading to reduced uncertainties in PBL aerosol extinction coefficients.

22. Why is the top of the boundary layer fixed globally at 4 km?

This definition can be traced directly to our lack of knowledge about the seasonal and geographic variability of global boundary top heights at the start of the mission. Consequently, the 4 km number is a one size fits all guesstimate for a single value that would provide a reasonable upper bound for the top of the boundary layer everywhere on Earth. To date, we have not updated this guesstimate with a more robust approximation, either derived from external sources (e.g., GMAO or ECMWF) or via analysis of our own data (e.g., see McGrath-Spangler and Denning, 2013 and/or the global data set available from the University of Wisconsin).

23. Where do you report boundary layer heights?

Boundary layer heights are not reported in the CALIPSO data products. Kim et al., 2021 discuss some of the many difficulties impeding fully automated retrievals of PBL heights from CALIOP profile measurements.

CALIOP LEVEL 1B PRODUCT

24. Why are there negative attenuated backscatter values in the lidar level 1B data?

The negative attenuated backscatter values arise from statistical variations in the CALIOP receiver photodetectors, as explained in section 2.3 (page 11) of the CALIPSO Lidar Level 1 ATBD.

> The solar background signal can be significant - as large as the clear-sky atmospheric signal. The instrument measures the DC background of each profile [i.e., the time invariant component] from the signal acquired between 112 km and 97 km, where the laser backscatter signals are negligible. This DC signal is electronically subtracted from the analog profile before digitization to allow the dynamic range of the digitizer to be used most effectively. This subtraction will result in negative-going noise excursions if the laser backscatter signal is small.

The consequences of excluding negative values are illustrated in Figure 20, which shows a 15 shot averaged profile both with the negative backscatter values included (green) and excluded (blue). For reference, the modeled molecular backscatter is shown in orange. Excluding the negative values when averaging clearly leads to a high bias in the resulting profile. Negative values occur in both daytime and nighttime measurements but are significantly more common during daytime.

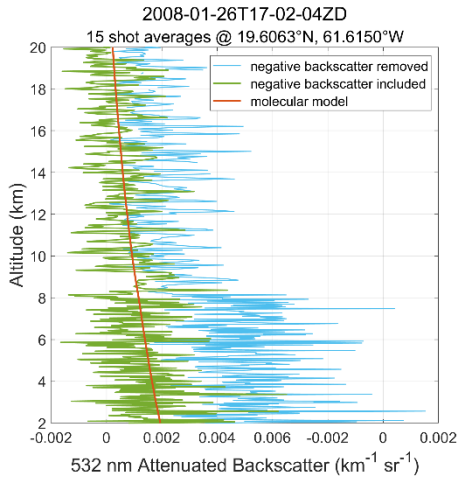

Figure 20: 15 shot averaged profile acquired during daytime over the west central Atlantic Ocean. The negative values are included when creating the green curve but excluded when creating the blue curve. Relative to the molecular model derived from MERRA-2 data, the blue curve shows a pronounced high bias. The magnitude of this bias increases sharply at ~8.2 km, where CALIOP's onboard averaging scheme changes from 3 shots horizontally × 60 m vertically to single shot resolution @ 30 m vertically. This step function change in the attenuated backscatter profiles is absent in the green curve.

25. Are these negative values removed before calculating the Level 2 optical properties?

No, negative values are not removed when computing L2 optical properties. In particular, negative attenuated backscatter coefficients are retained in the retrieval of the extinction coefficient profiles from which CALIOP's estimates of optical depths are derived. Removing the negative values would introduce a bias into the retrievals, as the lowest components of the random noise in the signal would be systematically removed, while the highest components would be retained.

26. Why are there discontinuities at ~8.2 km and ~20.2 km in plots of Level 1B data?

As described in FAQ #4 (What are CALIOP's sampling resolutions?), CALIOP profile data are collected on board the satellite at a nominal vertical resolution of 15 m with a profile spacing of ~333 m in the

horizontal (along track) dimension. However, due to bandwidth limitations, these data are averaged on board prior to downlink using the altitude-dependent scheme shown in Table 6. The apparent signal discontinuities at ~8.2 km and ~20.2 km correspond to the altitudes at which the spatial resolutions of the downlinked data change.

CALIOP LEVEL 2 LAYER PRODUCTS

27. In the layer products the data set Number_Layers_Found indicates that there are N (e.g. 3) layers in a column, does this imply that there are N (e.g. 3) unique atmospheric layers in the column?

Interpretation of the number of layers found parameter is straightforward for the 1 km and 333 m layer products, in which layer boundaries never overlap in the vertical dimension. However, this straightforward interpretation does not always apply to the layers reported into the 5 km cloud, aerosol, and merged layer products. CALIPSO uses a nested multi-grid feature finding algorithm, and thus the search for layer boundaries is conducted at multiple horizontal averaging resolutions. While the 1 km and 333 m layer products report only those features detected at, respectively, averaging resolutions of 1 km and 333 m, the 5 km products report layers detected at multiple averaging resolutions (5 km, 20 km, and 80 km). Because the reporting resolution (5 km) is not always identical to the detection resolution, layers may appear to overlap in the vertical dimension. This paradox is discussed in detail in FAQ #18.

28. The file names of CALIOP 5 km layer and profile products imply that the detection resolution for all feature data reported therein is 5 km. However, those files also report the properties of features detected at 20 km and 80 km detection resolutions. How should I interpret the information contained in these files?

In CALIOP's 5 km layer and profile products, a uniform 5 km horizontal grid is used to report the spatial and optical properties of features detected at averaging resolutions of 5 km and coarser. The 5 km data reporting resolution was chosen because CALIOP's coarser averaging resolutions are always multiples of 5 km. Properties from these coarser resolutions are replicated as appropriate over the horizontal extent spanned by the 20 km and 80 km features. Within the 5 km profile products this reporting strategy generally causes little, if any, confusion, as feature characteristics such as detection resolution, feature type, and CAD score are reported separately for each range bin. However, grappling with the 5 km layer products can be considerably more challenging. Interested readers are referred to FAQ #18 (Why do layer boundaries in the 5 km layer products appear to overlap one another?) for an in-depth explanation of the structure of these products.

29. Why are the 5 km merged diagnostic files assigned a "Beta" maturity level?

The 5 km merged diagnostic products are designated as 'Beta' products because several of the optical properties reported at 1064 nm have not yet been validated. These properties include 1064 nm cloud optical depths and 1064 nm ocean-derived column optical depths (ODCOD; see Ryan et al., 2024). While 1064 nm ODCOD is a wholly new product, 1064 nm cloud optical depths have been calculated since the beginning of the mission and are essential for renormalizing feature attenuated backscatter coefficients lying beneath transparent clouds. Accurate renormalization is required at both wavelengths to ensure the correctness of the total attenuated backscatter color ratios used in the CAD algorithm.

30. How should the CALIOP data products be used to compile comprehensive global or regional climatologies of cloud optical depths? Why are optical depths retrieved only for features detected at horizontal averaging resolutions of 5 km, 20 km, and 80 km and not for clouds

detected and cleared at single shot resolution in the PBL? What are the scientific ramifications of excluding single shot optical depth estimates from the CALIOP dataset?

CALIPSO delivered a near-global, 17-year survey of the spatial and optical properties of aerosols and clouds throughout the Earth's atmosphere. Nevertheless, constructing accurate optical depth climatologies using CALIPSO retrievals requires careful attention to feature type, vertical and geographic location, and backscatter intensity. For example, while CALIOP is well-suited for characterizing occurrence frequencies and optical depth distributions of subvisible cirrus and transparent ice clouds (e.g., Winker et al., 2024), it cannot provide reliable insights into the optical depth distributions of other cloud types, such as convective cores and the extensive stratus decks that are ubiquitous off the west coasts of Africa and North and South America. Unrestricted use of the CALIOP optical depth data is constrained by two primary factors. First, there is a distinct low bias in CALIOP optical depths reported for opaque layers. CALIOP optical depths are retrieved by integrating CALIOP's vertically resolved profiles of particulate extinction coefficients between the detected top of each feature and its reported base. However, as illustrated in Figure 21, whenever the CALIOP signal fails to penetrate the full vertical extent of an optically thick layer, the reported base must be considered as an *apparent* base that only identifies the altitude at which the CALIOP backscatter signal becomes completely attenuated. The CALIOP optical depths associated with these cases must likewise be considered *apparent* optical depths because the extinction integration terminates at the geometric signal penetration depth and thus necessarily omits any potential contributions from the undetected lower levels of the features. Given that ~31% of the Earth is blanketed by clouds that are opaque to CALIOP (Guzman et al., 2017), comprehensive cloud optical depth climatologies constructed from CALIOP retrievals alone would significantly underestimate the true optical depths over most, perhaps all, of the planet.

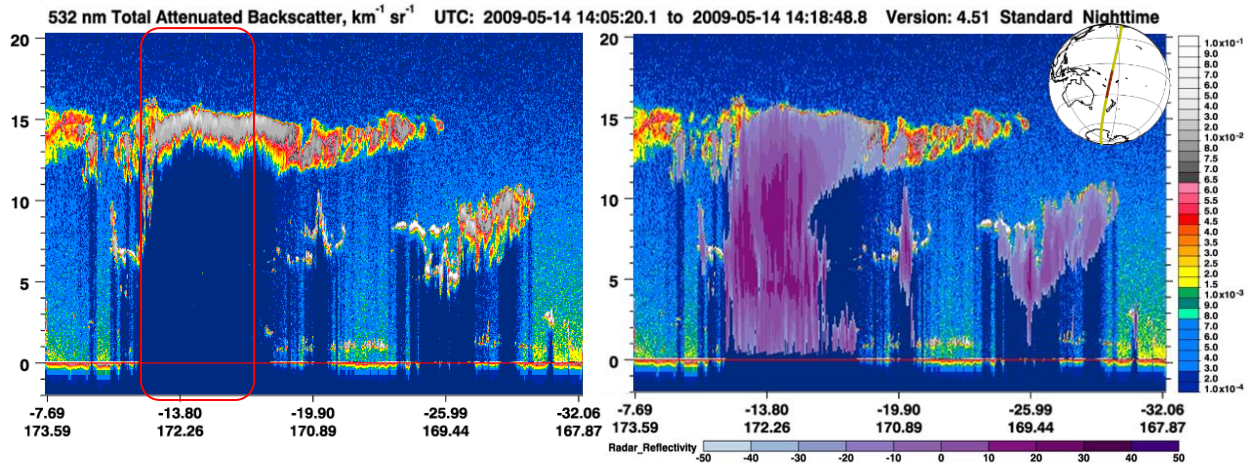

Figure 21: The left panel shows CALIOP total attenuated backscatter measurements for a mesoscale convective system off the east coast of New Caledonia on 14 May 2009. The right panel shows the same scene overlaid with radar reflectivities in regions where clouds are detected in the collocated CloudSat measurements. In the vicinity of 13.8° S, the CALIOP signals are totally attenuated at ~13 km, whereas the CloudSat signals extend down to the Earth's surface. CALIOP provides only *apparent* optical depth estimates that excluded the totally attenuated regions of this cloud (e.g., in the regions enclosed by the red rectangle in the left panel).

The second primary reason for not using CALIOP for constructing comprehensive cloud optical depth climatologies is a by-product of the cloud-clearing procedure used to retrieve the optical properties of boundary layer aerosols. Among space-based Earth-observing sensors, CALIOP is unique in providing estimates of AOD in heterogeneous scenes that have intermittent small-scale clouds embedded within the surrounding boundary layer aerosol. To accomplish this task, the CALIPSO lidar science working group (LSWG) developed a robust cloud-clearing procedure that, within each 15-shot frame of level 1 data,

separates the backscatter coefficients from clouds detected at single-shot resolution from the surrounding "not cloud" data (Vaughan et al., 2009; Vaughan et al., 2010; Tackett et al., 2022). The cloud-cleared 5 km profiles generated by this operation are immediately rescanned to detect any residual aerosols. If none are found, these profiles are subsequently averaged to increasing coarse horizontal resolutions (i.e., 20 km and 80 km) in the search for increasingly faint PBL aerosols (e.g., as shown in Figure 19). A full set of optical properties is retrieved for all aerosols detected using this approach.

The goal of the CALIOP layer detection algorithm is to identify features "at the highest possible spatial resolution while simultaneously ensuring that the SNR within each feature is sufficient to meet the requirements of the extinction retrieval algorithm" (Vaughan et al., 2009). Because the SNR in features detected at 5 km, 20 km, and 80 km horizonal resolutions is assumed to always satisfy these requirements, extinction coefficients and optical depths are always calculated for these layers. On the other hand, the cloud-clearing procedure partitions 5 km frames into three classes: cloud-free frames, in which no clouds were detected in any of the 15 single shot profiles; overcast frames, in which spatially contiguous clouds were detected at single shot resolution in every profile; and partly cloudy frames, in which one or more clouds were detected in one or more (but not all) single shot profiles (Tackett et al., 2022). Within these partly cloudy frames, no attempt is made to extract optical properties for the clouds detected and cleared at single shot resolution. The reasons for this decision are both historical and data driven. CALIOP excels at characterizing the vertical structure of the atmosphere and can reliably measure the *spatial properties* of multiple layers and layer types within a single atmospheric column. But from its conception, CALIOP's retrievals of *optical properties* focused almost exclusively on aerosols and transparent ice clouds (Winker et al., 2010). In prelaunch algorithm development, dense PBL clouds were regarded as nuisances to be removed to prevent contamination of subsequent aerosol retrievals. The approach was motivated predominately by our incomplete knowledge of signal saturation frequencies and range-resolved multiple scattering at the start of the mission. On-orbit studies have since shown that multiple scattering effects are generally insignificant in all but the densest aerosols (Liu et al., 2011) and can be well-parameterized using a temperature-dependent constant in ice clouds (Garnier et al., 2015). But in the dense water clouds typically found in the PBL, multiple scattering accumulates rapidly as a function of signal penetration depth, droplet size distribution, and extinction coefficient in ways that are very difficult to predict for an arbitrary measurement. The uncertainties in estimating range-dependent multiple scattering profiles on a single shot basis are so pervasive that retrievals of optical properties in these features are wholly unreliable and thus excluded from the CALIOP data products. However, consistent with all other features detected at 5 km resolution, the optical properties of clouds in overcast frames are estimated after averaging the contiguous cloud data over all 15 profiles in the frame. For boundary layer ice clouds, the uncertainties reported for the retrieved quantities can provide a useful metric for evaluating retrieval quality and useability. But the same is not true for dense water clouds. Because characterizing the range-resolved multiple scattering occurring within dense boundary layer water clouds remains highly uncertain, even after averaging (Winker, 2003; Sato and Okamoto, 2020; Shcherbakov et al., 2022), the reliability of optical property estimates in these features degrades very rapidly with increasing signal penetration depth. This near complete lack of trust is reflected in the CALIOP data products, where the uncertainties for the backscatter and extinction coefficients reported for opaque water clouds are set uniformly to a flag value of -29, indicating essentially zero confidence in the retrieved values.

For visual context, Figure 22 shows representative examples of a partly cloudy scene (left panel) and an overcast scene (right panel). An analysis of all CALIOP measurements acquired during 2010, 2011, and 2012 shows that 20.2% of PBL clouds detected at single shot resolution were found in partly cloudy frames, while the remaining 79.8% were found in overcast frames. As expected based on daytime solar background noise levels, the detection fractions are different for daytime and nighttime measurements. During daytime, 16.3% of all single shot detections occurred in partly cloudy frames whereas at night this

fraction rises to 24.4%. The scientific ramifications of omitting optical property statistics for the sizeable fraction of clouds detected at (only) single shot resolution have not been rigorously explored.

Figure 22: Left panel: example of the small-scale scattered clouds that would be detected intermittently along the CALIOP orbit track. The backscatter coefficients from these clouds are removed from each profile at single shot resolution and the resulting cloud-cleared profiles are composited into increasing coarse horizontal averages in the search for increasingly tenuous boundary layer aerosols. For this scene, retrieval of cloud optical properties would not be attempted. (Photo credit: Evgueni Kassianov, Pacific Northwest National Laboratory.) Right panel: overcast low clouds above NASA Langley Research Center. The cloud deck in this scene would be detected continuously at single shot resolution over multiple frames. Cloud optical properties estimates would be retrieved from data segments averaged to 5 km (15-shot) resolution. (Photo credit: authors, NASA LaRC.)

Paradoxically, while the altitude-resolved backscatter and extinction coefficients retrieved in dense water clouds are extremely uncertain, layer-effective multiple scattering factors and lidar ratios (i.e., backscatter-to-extinction ratios) can be retrieved with high confidence using Hu's method (Hu et al., 2007), even at single shot resolution. This is possible because Hu's method does not attempt altitude-resolved retrievals, but instead deals only with the bulk properties of a cloud.

31. How should I interpret features that are detected at 5 km resolution and classified as clouds for which the 'Single Shot Cloud Cleared Fraction' parameter is greater than 0?

As discussed earlier (see FAQ #19 and FAQ #20), the goal of the single shot cloud clearing procedure is to identify and remove backscatter from clouds detected at single shot resolution so that the remaining data can be reaveraged and searched for the presence of aerosols. This technique enables high quality aerosol optical property retrievals in heterogenous scenes having small-scale, strongly scattering clouds embedded in a much larger and fainter aerosol layers (e.g., as in the left panel of Figure 22). For all features in the 5 km layer products, the 'Single Shot Cloud Cleared Fraction' parameter reports the areal fraction (i.e., the along-track averaging distance times the vertical extent) of a feature that was removed by the cloud clearing procedure within any 5 km along-track distance. However, not all features that have been "cloud cleared" are guaranteed to be aerosols. Layers detected at single shot resolution and classified as clouds retain their classification throughout the remainder of the level 2 processing. Layers detected at 5 km, 20 km, and 80 km resolutions are assigned an initial classification once the cloud clearing procedure has executed. However, the typing of these layers is subsequently reevaluated immediately prior to executing the optical properties retrieval. By doing this, feature data used in the CAD algorithm can be properly corrected for attenuation by overlying features. This correction has direct impacts on two of the most important CAD parameters: the layer-mean attenuated backscatter at 532 nm and the layer-mean total attenuated backscatter color ratio. One notable side effect of this correction is that layers originally

classified as aerosol can potentially be reclassified as clouds and these reclassified clouds have single shot cloud cleared fractions greater than 0. The optical depths of *clouds* that have cloud cleared fractions greater than 0 are biased low, because all cloud data detected at single shot resolution is excluded from the horizontal averaging done in order to reconstruct profiles used to retrieve optical properties (Vaughan et al., 2009; Young and Vaughan, 2009). This bias does not affect *aerosols* with cloud cleared fractions greater than 0, because the reconstructed profiles are aerosol measurements from which single shot cloud data is correctly excluded. Because CALIOP boundary layer retrievals prioritize aerosols above clouds, and because CALIOP's optical property retrievals in dense boundary layer clouds are highly uncertain in the best of cases, this data processing choice was deemed an acceptable and expedient trade-off in the prelaunch algorithm and code development phase.

To separately quantify the relative cloud cleared frequencies of aerosols and clouds, Table 9 partitions the along-track distance spanned by cloud cleared features according to feature type for all data acquired in 2010 and 2019. Both of these are data-rich years with very few data gaps caused by instrument anomalies. While the 2019 data is perturbed by a large number of low energy laser pulses, the 2010 data is pristine in this regard. Nevertheless, the yearly cloud clearing statistics are essentially identical, with aerosol layers being cloud cleared twice as often as cloud layers.

Table 9: Cloud cleared frequencies of aerosols and clouds globally for all data acquired during 2010 and 2019. Cloud frequencies are further partitioned by cloud thermodynamic phase (ice, water, and unknown). The size of the data sets is essentially identical. In 2010, the along-track distance spanned by cloud cleared features was 54,345,635 km at night and 58,381,510 km during the day. For 2019, the nighttime distance is 52,545,395 and the daytime distance is 58,990,450. The partitioning according to type is also essentially identical for both nighttime and daytime data set.

	2010 Global		2019 Global	
	day	night	day	night
all aerosols	0.6951	0.6397	0.6907	0.6303
all clouds	0.3049	0.3603	0.3093	0.3697
ice clouds	0.0734	0.0826	0.0742	0.0893
water clouds	0.0600	0.1108	0.0593	0.1124
unknown clouds	0.1715	0.1669	0.1758	0.1680

CALIOP LEVEL 2 PROFILE PRODUCTS

32. What is the difference between 'attenuated backscatter' and 'particulate backscatter'?

Profiles of "attenuated backscatter coefficients", $\beta'_\lambda(r)$, are the primary quantities reported in the lidar L1B product. $\beta'_\lambda(r)$ is derived from the raw profile measurements, $P_\lambda(r)$, as follows:

$$\beta'_\lambda(r) = \frac{r^2 \times \left(P_\lambda(r) - P_{bkg,\lambda}\right)}{E_\lambda \times G_\lambda \times C_\lambda} = \left(\beta_{m,\lambda}(r) + \beta_{p,\lambda}(r)\right) \times T_m^2(0,r) \times T_{O_3}^2(0,r) \times T_p^2(0,r).$$

Table 10 provides a key to the notation used. Translated into words, this equation says that the attenuated backscatter coefficients are the background subtracted, range squared corrected raw signals after being gain and energy normalized and calibrated. The attenuated backscatter coefficient within any scattering volume is the product of the sum of the backscatter from molecular (m) and particulate (p) components and the signal attenuation between the lidar and the scattering volume due to molecules, particulates, and ozone (O_3).

Table 10: Notation used in the attenuated backscatter coefficient equation

symbol	interpretation
λ	measurement wavelength
r	range from the lidar to the sample volume
β′(r)	attenuated backscatter coefficient at range r
E	laser pulse energy
G	receiver electronic gain
C	calibration coefficient
P(r)	backscattered laser power at range r
P_{bkg}	background signal (e.g., from sunlight and or dark noise)
m	molecular component of backscatter and signal attenuation
p	particulate component of backscatter and signal attenuation
O_3	ozone component of signal attenuation
T_x^2	signal attenuation between the lidar and range r due to light extinction by component x

The "particulate backscatter coefficient" is the $\beta_{p,\lambda}(r)$ component of the attenuated backscatter coefficient. $\beta_{p,\lambda}(r)$ quantifies the magnitude of the *unattenuated* backscatter from all particulates with any measurement volume (i.e., range bin). Deriving particulate backscatter coefficients from attenuated backscatter coefficients requires a solution to the lidar equation, which, for elastic backscatter lidars like CALIOP, most often also requires an assumption of the relationship between particulate extinction and particulate backscatter (Young and Vaughan, 2009; Young et al., 2018). The extinction-to-backscatter ratio, commonly known as the lidar ratio, is assumed to be constant throughout any homogeneous layer, and is known to vary according to particulate type by a factor of 5 or more (Kim et al., 2018). Lidar ratio uncertainties are a primary source of uncertainties in $\beta_{p,\lambda}(r)$ (Young et al., 2013).

33. What's the difference between volume and particulate depolarization ratios?

The volume depolarization ratio, $\delta_v(z)$, refers to the perpendicular-to-parallel ratio of the 532 nm attenuated backscatter coefficients reported in the L1B data product. The parallel component of the signal is obtained by subtracting the perpendicular attenuated backscatter coefficients from the total attenuated backscatter coefficient. Because signal attenuation is independent of polarization state,

$$\delta_v(z) = \frac{\beta_{\perp,m}(z) + \beta_{\perp,p}(z)}{\beta_{\parallel,m}(z) + \beta_{\parallel,p}(z)}$$

where the subscripts m and p represent, respectively, molecular and particulate contributions to the total backscatter, ⊥ and ∥ represent the perpendicular (⊥) and parallel components (∥), and $\beta_{w,v}(z)$ is the backscatter coefficient measured at altitude z for polarization state w and scattering species v.

The particulate depolarization ratio, $\delta_p(z)$, refers to the perpendicular-to-parallel ratio of the particulate backscatter coefficients, and can be calculated only after an extinction profile is retrieved:

$$\delta_p(z) = \frac{\beta_{\perp,p}(z)}{\beta_{\parallel,p}(z)}$$

$\delta_p(z)$ is an intrinsic property that depends on particulate type but is independent of particulate concentration. $\delta_v(z)$ is an extrinsic property that depends jointly on $\delta_p(z)$ and the magnitude of the particulate concentration relative to the molecular density within the measurement volume. The higher the relative particulate concentration, the more closely $\delta_v(z)$ will approximate $\delta_p(z)$.

34. If I am only interested in aerosols, what is the best way to filter profile data to exclude clouds?

For the CALIOP L2 and L3 data products this question has a very straightforward answer. The Lidar Level 2 Layer Data and the Lidar Level 2 Profile Data both offer "aerosol only" and "cloud only" versions of the L2 data, with the discrimination between clouds and aerosols accomplished by the CALIOP CAD algorithm (Liu et al., 2019). A similar situation exists for the L3 data products, which are also partitioned into cloud-only offerings (e.g., the Lidar Level 3 Ice Cloud Data) and aerosol-only offerings (e.g., the Lidar Level 3 Tropospheric Aerosol Data).

For users who prefer to do their own aerosol retrievals, the hybrid Lidar Level 1.5 Profile Data contains cloud-cleared L1B attenuated backscatter averaged to a uniform resolution of 20 km horizontally and 60 m vertically. Cloud clearing is done using feature type information reported in the Lidar Level 2 Vertical Feature Mask product. Those users who want spatial resolutions different from what is provided (or can be derived) from the L1.5 product, or who want more control over the cloud clearing process, can use matched L1B and VFM files to create aerosol-only profiles. Depending on the application, there are no doubt a myriad of methods that could be devised to handle this chore.

35. The Level 3 stratospheric aerosol profile products report extinction coefficients over their entire altitude range. Why then are there (sometimes substantial) gaps in the extinction coefficient profiles reported in the Level 2 aerosol profile products?

In the L2 aerosol profile products, stratospheric aerosol extinction is only reported when aerosols are detected in L1B profiles that have been averaged to 5 km, 20 km, or 80 km horizontal resolutions within a single granule. To create the L3 stratospheric aerosol product, L1B profiles are first averaged over a one-month time period and a spatial grid of 5° latitude × 20° longitude. Two versions of these averaged data are created. The "background only" version excludes all attenuated backscatter coefficients within cloud and aerosol layers detected in the L2 analyses, whereas the "all aerosol" version retains the attenuated backscatter coefficients from within aerosol layers but continues to exclude those from within clouds (Kar et al., 2019). In both cases, the SNR in these heavily averaged L3 profiles is substantially higher than the SNR in their L2 counterparts, and this much higher SNR enables reliable aerosol extinction throughout the full vertical extent of the profiles. However, the backscatter coefficients in these profiles are almost always well below the minimum detectable backscatter estimates for the L1B data averaged to 5 km, 20 km, or 80 km horizontal resolutions (Vaughan et al., 2005; McGill et al., 2007). The exceptions occur in very strong and persistent layers such as fresh volcanic ash injections.

Unlike the L3 stratospheric profile product, the profiles of aerosol extinction reported in the L3 tropospheric product frequently contain large gaps. This difference can be directly traced to the different data aggregation strategies implemented by the two products. The L3SAP adopts an average-then-retrieve approach, in which the L1B profiles are heavily averaged prior to retrieving extinction estimates. The L3TAP, on the other hand, uses a retrieve-then-average procedure in which the aerosol extinction coefficients retrieved in the L2 analyses are averaged to create the L3TAP profiles. Consequently, the valid extinction coefficients reported in the L3TAP are limited to those regions in which aerosols were first detected in the L2 processing.

CALIOP Level 2 Vertical Feature Mask

36. Why does the surface occupy multiple range bins in the vertical feature mask?

The photomultipliers (PMTs) in the 532 nm receiver channels do not recover instantaneously when measuring very strong backscatter returns such as those from the Earth's surface and opaque water

clouds. Instead, they produce a non-ideal response: exponentially decaying noise tails that persist for some time after encountering the peak signal (Hunt et al., 2009). Due to this effect, spurious lidar backscatter is often seen well beneath the Earth's surface. As illustrated in the left panel of Figure 23, this effect is particularly noticeable over ice-covered surfaces, where cloud-free atmospheres and a very high surface albedo generate 532 nm surface signals which extend significantly below the true surface. As demonstrated in the right panel of Figure 23, this non-ideal detector behavior is not present in the 1064 nm measurements, where detection is done using an avalanche photodiode (APD) instead of a PMT.

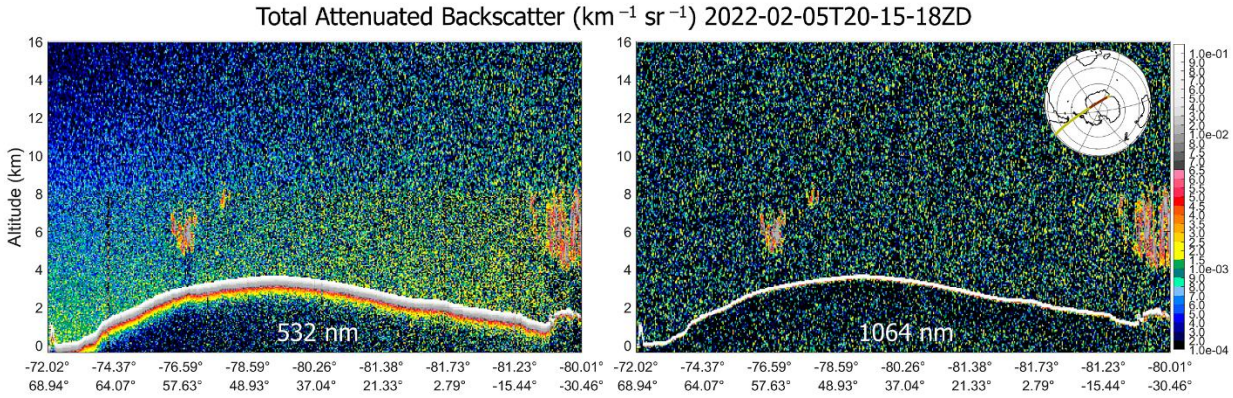

Figure 23: 532 nm (left panel) and 1064 nm (right panel) measurements over Antarctica, acquired 2022-02-05.

The CALIOP layer detection algorithm will correctly identify the top altitude in layers affected by the non-ideal transient response. However, by design it defines the base location as the first range bin in which the signal drops below an altitude-dependent detection threshold. Consequently, in strongly scattering features the anomalously enhanced signal frequently leads to large errors in which the reported vertical extent of the 532 nm surface measurements is significantly overestimated. These overestimates cause the (apparent) surface echo to span multiple range bins in the VFM images.

This non-ideal detector response can also cause misestimates of the layer boundaries of atmospheric features. In particular, the apparent bases of opaque water clouds may appear to extend further toward the surface than would otherwise be expected. However, this error is largely inconsequential, since CALIOP cannot accurately measure the true base altitudes of opaque layers. A study by Lu et al., 2020 suggests that these unwanted detector transients can be expected for any target in which the peak attenuated backscatter exceeds 0.01 km $^{-1}$ sr $^{-1}$. Below that limit, non-ideal response effects on CALIOP's layer detection scheme can largely be ignored, as they introduce vertical extent errors of less than 2%.

37. Please explain the differences between the Feature Classification Flags (in the VFM and Layer Products) and the Atmospheric Volume Descriptions (in the Profile Products)

Both the Feature Classification Flags (FCF), reported in the VFM and layer products, and the Atmospheric Volume Descriptions (AVD), reported in the profile products, are 16-bit integers, with bit 0 being the least significant bit. Interpretation of the first 13 of these bits is identical for both parameters. Bits 0–2 report feature type. Bits 3 and 4 provide discrete quality assessments for the feature type identifications. Decoding bits 5 and 6 identifies cloud ice-water phase while bits 7 and 8 provide quality assessments for the ice-water phase classifications. Note that bits 5–8 are only relevant for those features classified as clouds and contain no information about other feature types. Bits 9–11 identify the feature subtype for clouds, tropospheric aerosols, and stratospheric aerosols. Correct interpretation of these bits depends entirely on the feature type identified in bits 0–2, and the interpretations are different for clouds, aerosols, and clear air. Bit 12 provides a binary quality assessment for the classification of feature subtype. In both

the FCFs and the AVDs, bits 13–15 convey information about the amount of horizontal averaging required for feature detection. Spatial resolutions reported in the FCFs will range between 333 m and 80 km; i.e., all resolutions searched by the CALIOP feature finder. Since CALIOP extinction and backscatter profiles are only retrieved at 5 km, 20 km, and 80 km, in addition to identifying the averaging required for feature detection, bits 13–15 in the AVDs also identify those range bins in which features were detected at single shot resolution.

The reporting format for these parameters varies according to data product. Within the CALIOP level 2 analyses, FCFs are originally assigned when the layer detection and scene classification tasks are complete. Consequently, the layer products report a single set of FCFs for each unique atmospheric feature detected. In the VFM product, FCFs are 2D matrices, with each matrix element corresponding to a single range bin in CALIOP's altitude-dependent downlinked data. These matrices cover the altitude range between 30.1 km and –0.5 km and extend along the full granule ground track. The FCFs reported in each matrix element are the FCFs belonging the highest resolution feature detected in each range bin and are replicated as appropriate to cover the full vertical and horizontal extent of the feature. The FCF matrices in the VFM files will contain additional information that is not available in the FCFs reported in the layer products, including the locations of clear air regions, surface echoes, subsurface measurements, and range bins in which the signal has been totally attenuated. In the profile products, the AVDs are modified versions of the FCFs stored in the layer products. For each 5 km column in the layer products, the FCFs are converted to AVDs for each layer, then assigned to all range bins spanned by each feature within the corresponding profile product column. The "Unique Layer ID" parameter can be used to ascertain the mapping between the layer product FCFs and the profile product AVDs.

The Data Description Documents for the CALIOP L2 VFM products, layer products, and profile products all provide additional information and detailed maps for the interpretation for all bits in the FCF and AVD.

CALIOP Known Issues

This section provides brief descriptions of potential problems identified since the final release of the CALIOP data products. Where possible, potential remedies are also offered.

38. Reevaluating Extinction QC = 6

According to Young et al., 2018, an extinction QC flag of 6 occurs whenever bits 1 and 2 (zero-based indexing) are simultaneously toggled on in the solution of a transparent feature. Bit 1 in an extinction QC flag signals that the "initial lidar ratio [was] reduced to achieve successful solutions for backscatter coefficients and uncertainties throughout the full vertical extent of the layer". Bit 2 indicates a "suspicious retrieval [in which the] layer or overlying integrated attenuated backscatter [is] too high or [the] lidar ratio reduction [is] excessive". The primary purpose of the test flagged by bit 2 is to identify possibly misclassified layers. As seen in Figure 24, the integrated attenuated backscatter for opaque layers, γ'_{opaque}, is inversely proportional to the layer effective lidar ratio, $S^* = \eta \times S$, which implies that the measured integrated attenuated backscatter, γ'_m, in transparent layers is bounded above by γ'_{opaque}. To determine if/when γ'_m is too high, we estimate $\gamma'_{opaque} = (2 \times S^*)^{-1}$ using Platt's equation (Platt, 1979) for opaque layers applied to the lidar ratio (S) and multiple scattering factor (η) specified for a given feature. Bit 2 is toggled whenever γ'_m calculated for a *transparent* layer exceeds the value predicted for an opaque layer of the same feature type.

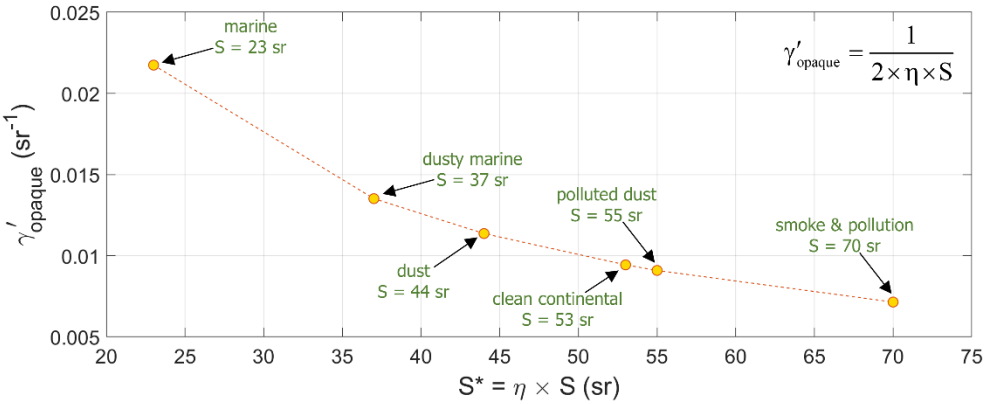

Figure 24: Integrated attenuated backscatter for opaque layers as a function of lidar ratio. The lidar ratios shown are the ones used in the V4.51 release of the CALIOP data products. η = 1 in all cases.

The problem with this initial formulation is that it does not account for variability in the lidar ratio. For example, the standard CALIOP dust lidar ratio is 44 ± 9 sr at both wavelengths and η for all aerosols is fixed at 1. Consequently, $\gamma'_{opaqueDust} = (2 \times 1 \times 44)^{-1} = 0.0114$ sr^{-1}. However, if the true lidar ratio for the layer in question is one standard deviation lower than the characteristic value and $\gamma'_{m} = 0.0120$ sr^{-1}, the bit 2 will be toggled on, even though in this case $\gamma'_{opaqueDust} = (2 \times 1 \times 35)^{-1} = 0.0143$ sr^{-1}. So, to accommodate lidar ratio variability across different feature types, the members of the CALIPSO LSWG are proposing a new test for γ'_{opaque} that can be applied retrospectively to the existing data products:

$$\gamma'_{opaque} = \frac{1}{2\left(\eta_{FT} S_{FT} - N \times \eta_{FT} \Delta S_{FT}\right)}.$$

ΔS_{FT} is the standard deviation of the lidar ratio for feature type FT and N specifies some number of standard deviations. Since we report η, S, and ΔS for all layers in the CALIOP 5 km layer products, this test can be applied after the fact to correct possibly overaggressive application of the bit 2 test. Choosing N too large will accept many more genuinely suspicious solutions than setting N = 0, as is currently done in the CALIOP level 2 analyses. On the other hand, as seen in Figure 25, choosing N = 0 can reject a sizeable fraction of valid solutions.

Note that this overly aggressive assignment of QC = 6 in the L2 products is reevaluated using a variant of the method described above when creating the L3 tropospheric aerosol products.

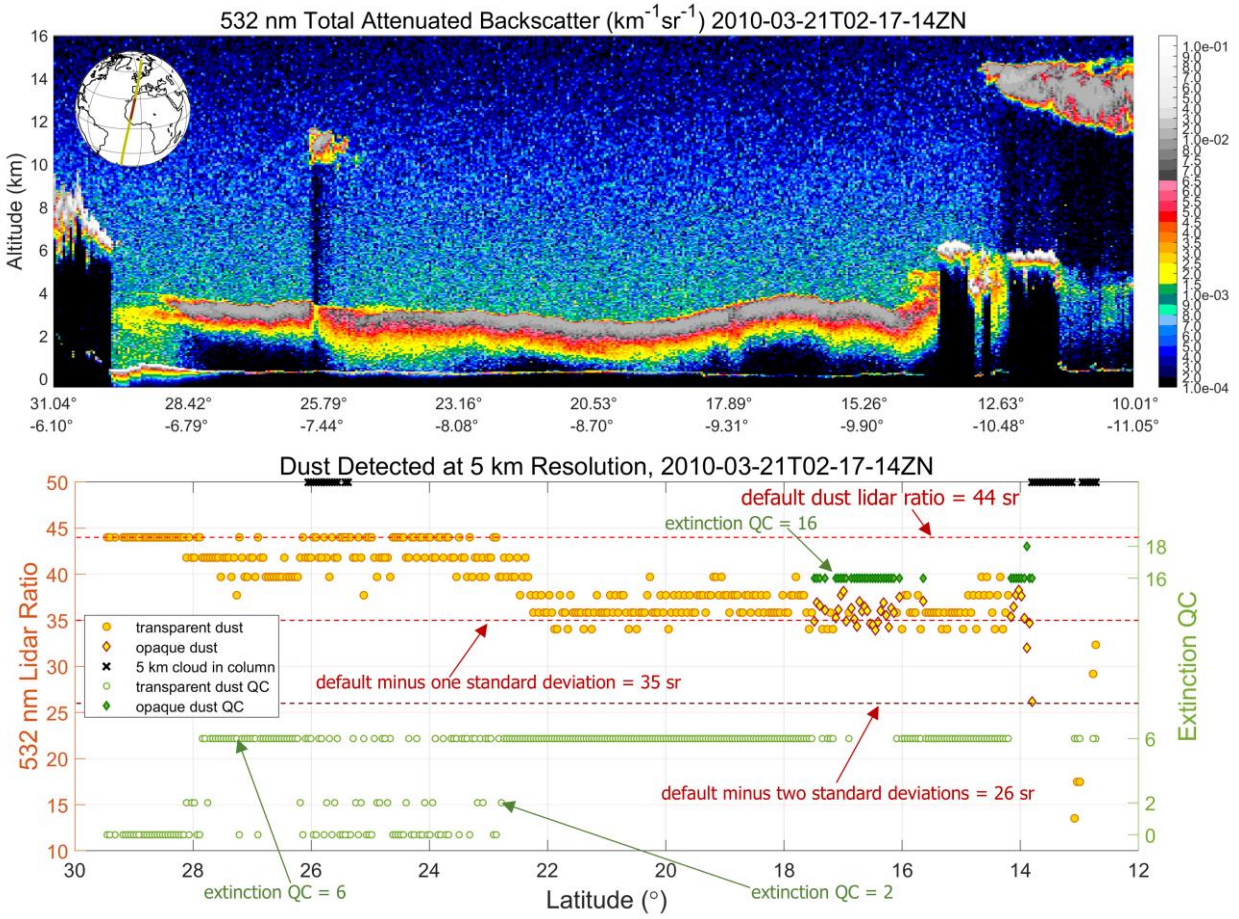

Figure 25: Very dense, sometimes opaque dust layer measured 2010-03-21 in western Africa. The upper panel shows 532 nm attenuated backscatter coefficients. The lower panel illustrates the V5.00 L2 retrievals for dust layers detected at 5 km resolution in this segment. The final lidar ratios obtained for unconstrained retrievals (QC = 0,2,6) are shown in orange circles. Descending from the top of the plot down, the dashed red horizontal lines show CALIOP's default dust lidar ratio (44 ± 9 sr), the default value minus one standard deviation (35 sr), and the default value minus two standard deviations (26 sr). The red diamonds with yellow centers show optimized lidar ratios obtained by constraining the lidar equation with the integrated attenuated backscatter for opaque layers (Young et al., 2018). These constrained solutions provide the most reliable estimates of lidar ratio available in the CALIOP data set. The 37 instances in this data set have a mean value of 35.7 ± 2.1 sr, which is very slightly above the "default value minus one standard deviation" line. The extinction QC flags for these constrained solutions are shown using dark green diamonds. Extinction QC flags for unconstrained solutions are shown in open light green circles. In this scene there are 13 times more QC = 6 cases than QC = 2. However, the mean of the 227 QC = 6 lidar ratios is 37.9 ± 2.5 sr, which is slightly *larger* than the mean of the constrained solutions. Clearly, then, designating these cases as suspicious retrievals is incorrect. Choosing N = 1.2 would rectify this situation.

39. Why does the L1B "Number of Bins Shifted" parameter sometimes oscillate from profile to profile?

In the early stages of the CALIOP level 1 analyses, each laser pulse is geolocated to the CALIPSO DEM used in the level 1 analyses. Altitudes for the downlinked L1B profiles are then computed relative to this level 1 DEM altitude based on photon time of flight as a function of the spacecraft off-nadir angle, which is derived from the high-resolution postprocessed ephemeris data generated by CNES and delivered to LaRC on a daily basis. Because the altitudes produced by this high-resolution calculation can vary slightly from those calculated using the (lower resolution) onboard DEM and commanded off-nadir angle, adjustments

are sometimes required to ensure that the downlinked data is properly registered to CALIOP's fixed altitude grid. This process first computes the altitude difference, in kilometers, between mean sea level according to the CALIPSO DEM, which occurs at range bin 563 in CALIOP's fixed altitude grid, and the altitude calculated for bin 563 when using the high-resolution off-nadir angle. These differences are reported in the 'Surface_Altitude_Shift' SDS reported in the CALIOP L1B files. Figure 26(a) shows an example of the calculated 'Surface_Altitude_Shift' for a short segment of data measured over the Gulf of America on 24 March 2016.

When the 'Surface_Altitude_Shift' is large (i.e., greater than 30 m), the corresponding profile data will need to be vertically shifted by one or more range bins to ensure the most accurate registration of the measurements to the fixed altitude grid. To do this, the continuous 'Surface_Altitude_Shift' data are converted to an integer number of 30 m range bins that defines both the magnitude and direction of the shift. For measured off-nadir angles close to the commanded CALIOP off-nadir angle, the number of bins shifted is approximately equal to round(Surface Altitude Shift / (0.029979 × cos(off-nadir angle))). The L1B 'Number_Bins_Shifted' parameter reports the number of 30-m altitude bins shifted by the altitude registration algorithm to achieve the best match between apparent MSL in the measured profile and MSL in CALIOP's fixed altitude array.

While differences in the magnitudes of horizontally adjacent 'Surface Altitude Shift' within the same DEM grid cell are typically 4 m or less, the rounding operation used to calculate the 'Number of Bins Shifted' can cause (apparent) 30 m shifts (i.e., one range bin) between 'Surface Altitude Shifts' that differ by less than 4 m. This phenomenon is illustrated in Figure 26(b), which plots 'Surface Altitude Shift' in green and 'Number of Bins Shifted' in blue. Regrettably, as seen in panels (c) and (d) in Figure 26, this bin shift oscillation reverberates into the lidar surface detections reported in the level 2 products. Most often, the surface detection algorithm correctly identifies the onset of the surface signal. However, because the range bins in these profiles have been erroneously shifted by one extra bin, the lidar-retrieved surface altitudes are in error by 30 m. Panel (d) in Figure 26 shows the surface signals for two adjacent profiles. According to the 'Surface Altitude Shift' parameter, the vertical distance between these two profiles is ~3.4 m. The actual distances from MSL in the DEM are -47.46 m and -44.09 m. Dividing by 30 yields -1.582, which rounds to 2 bins shifted, and -1.470, which rounds to only 1 bin shifted.

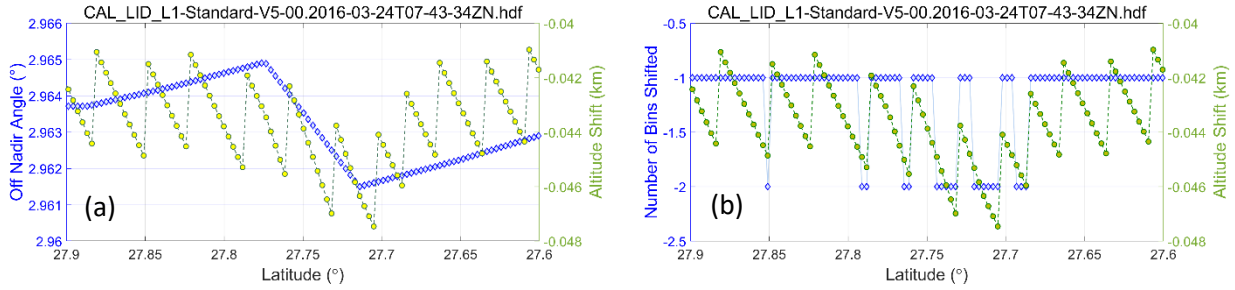

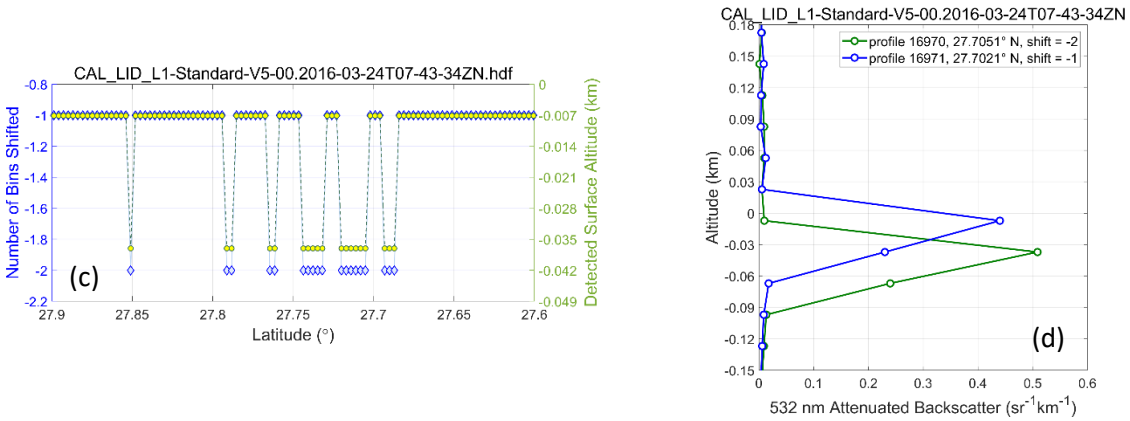

Figure 26: (a) the off-nadir angle retrieved from the postprocessed ephemeris data (blue) and the corresponding 'Surface_Altitude_Shift' (green) for a short segment of data measured over the Gulf of America on 24 March 2016. The sawtooth pattern in the surface altitude shift occurs because the onboard data acquisition start time is constantly adjusted to compensate for changes in the distance from the satellite to MSL. These changes caused by CALIPSO's elliptical orbit and required to keep MSL registered to altitude bin #563. (b) 'Number_Bins_Shift' (blue) and the corresponding surface altitude shift. (c) 'Number of Bins Shifted' (blue) and the altitude of the lidar-detected surface (green) for the same data segment. (d) Attenuated backscatter profiles near the Earth's surface for two consecutive laser pulses having different 'Number of Bins Shifted'. A shift of one bin (in blue) aligns the surface echo with the ocean surface altitude, whereas a shift of two bins (in green) places the maximum surface signal ~37 m below the true ocean surface.

As expected, the bin shift errors cause a number of additional complications elsewhere within the level 2 products. Chief among these, layer altitudes will be biased high or low depending on the magnitude and direction of the bin shift error. Because the measurement profiles will be offset by one or more range bins from the molecular model profiles required in the retrievals, there will be small (though perhaps insignificant) errors in the optical properties retrievals. ODCOD retrievals at 1 km and 5 km resolutions are also degraded by erroneous bin shifts. Whenever the 'Number of Bins Shift' parameter is not constant everywhere within an ODCOD retrieval interval, bit 7 (1-based indexing) in the ODCOD_QC_Flag_532 will be toggled on, indicating a lack of confidence in the retrieved values due to insufficient confidence in the quality of the inputs provided to the ODCOD algorithm.

40. False positives when flagging 1064 nm calibration biases using Bit 27 in the Lidar Level 1B QC_Flag_2 parameter

Bit 27 (1-based indexing) in the QC_Flag_2 parameter reported in the lidar level 1B product is intended to flag profiles that might have biased 1064 nm calibration coefficients due to the low temperatures following an earlier shutdown of the lidar receiver electronics (LRE). Following any extended shutdown, the 1064 nm APD takes substantially longer to reach thermal stability at its optimum operating temperature than do the 532 nm PMTs. The measurement disparities introduced by this anomaly

are illustrated in Figure 27, where the mean attenuated backscatter color ratios, χ', of calibration-quality cirrus clouds are seen to be biased low following an extended instrument outage in April 2014. Per the discussion in Vaughan et al., 2019 for details, this low bias in χ' can be traced to corresponding low biases in the 1064 nm backscatter measurements.

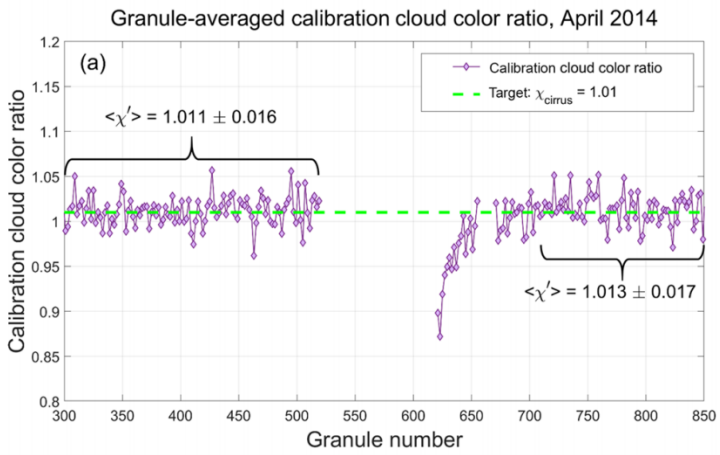

Figure 27: The text that follows quotes the caption for that figure. "Time series of granule mean χ′ measured for calibration quality clouds detected during nighttime orbit segments beginning on 11 April 2014 (granule 301) and extending through 30 April 2014 (granule 849). Due to adverse space weather, CALIOP was placed in safe mode, and thus data are missing for over 3 days, from 19 April 2014 at 08:29:42 UTC to 22 April 2014 at 16:26:07 UTC, spanning granules 521–619. A smaller data gap of just over 8 h (from 01:09:36 until 09:38:09 UTC on 24 April 2014, spanning granules 657–669) occurs during a satellite drag make-up maneuver. A distinct drop in the magnitude of χ′ occurs when the lidar is restarted on 22 April. Because there were two instrument shutdowns in relatively rapid succession, full recovery to the pre-outage values takes place over ~ 72 h." (Vaughan et al., 2019 © Authors 2019, CC BY 4.0).

To automatically identify occurrences of these anomalies in an asynchronous data stream, bit 27 is toggled on whenever the mean χ′ for all calibration-quality cirrus clouds within a granule exceed ±5% of the expected value of 1.01. This rudimentary algorithm is highly effective at identifying genuine 1064 nm calibration coefficient anomalies. However, because it does not also check the time elapsed from the most recent instrument shutdown, it also generates a large number of false positives; i.e., alleged anomalies that occur days or even weeks after the most recent shutdown. Most likely these false positives occur because the threshold values are too tight. Nevertheless, the net effect is small: ~1.2% of all granules have bit 27 toggled on in the QC_Flag_2 parameter.

41. PSCs are not included in the cloud subtyping algorithm

The CALIOP cloud subtyping algorithm recognizes eight cloud types: low, overcast, and optically thin (e.g., transparent stratus); low, overcast, and optically thick (e.g., opaque stratus); transition stratocumulus; low, broken clouds (e.g., trade wind cumulus); transparent altocumulus; opaque altostratus; transparent cirrus; and deep convective (e.g., cumulonimbus and nimbostratus). Polar stratospheric clouds are not called out separately but are instead most often reported as transparent cirrus. Atypical cases may also be flagged as deep convective clouds. This occurs because the three bits allocated to feature subtyping in the feature classification flags were fully subscribed by the original eight cloud types. Were there ever to be a future release of the CALIPSO data products, the feature classification flags would be implemented as 32-bit integers rather than 16-bit integers.

42. Inconsistencies in different L2 cloud classifications

CALIOP's cloud subtyping and ice-water phase classification algorithms were developed independently. As a result, there can be inconsistencies between the reported cloud type and the ice-water phase classifications that would not typically be expected for each type. Table 11 compares cloud types assigned by the CALIOP cloud typing algorithm (rows) with the ice water phase determined by the phase classification algorithm (columns). While some fuzziness should probably be expected in these comparisons, the

question arises: how much disparity is too much disparity? For example, the phase algorithm claims that ~6% of the clouds identified as "cirrus (transparent)" are water clouds. Similarly, the phase algorithm identifies ~17% of "deep convective (opaque)" clouds as being water clouds and ~18% of "low broken cumulus" as being ice clouds.

Further study would be needed to resolve this paradox. In particular, assessing the seasonal and geographic distributions of layers with apparently contradictory classifications (e.g., do the low broken cumulus identified as ice clouds occur predominantly in polar regions?) could resolve a large number of conflicting cases and help determine the more reliable of the two algorithms. Examining the distributions of phase confidences assigned to the suspicious cases (e.g., cirrus clouds classified as water) might also yield some helpful insights.

Table 11: Fraction of ice-water phase classifications (columns) determined within each cloud subtype (rows); data harvested globally for all 5 km detections in the V5.00 release

subtype / cloud phases	unknown	ROI	water	HOI	samples
low overcast (transparent)	0.0727	0.0246	0.8982	0.0046	98822
low overcast (opaque)	0.0201	0.0192	0.9578	0.0029	238930
transition stratocumulus	0.1600	0.0761	0.7579	0.0060	417078
low broken cumulus	0.3600	0.1810	0.4493	0.097	101730
altocumulus (transparent)	0.1271	0.4701	0.3981	0.0047	335098
altostratus (opaque)	0.1200	0.1444	0.7224	0.0132	238851
cirrus (transparent)	0.0264	0.9149	0.0578	0.0008	836842
deep convective (opaque)	0.0256	0.7965	0.1719	0.0060	302102

IIR DATA PRODUCTS

43. What information is provided by the IIR data products?

a. IIR Level 1 Calibration data and Level 1 Calibration Correction data

The IIR acquisition is organized around cycles composed of 5 sequences with 1 sequence every 8.184 seconds. A sequence is a collection of 6 images composed of 64 x 64 = 4096 pixels: 1 Earth view and 1 calibration view for each of the three IIR channels at 8.65, 10.6, and 12.05 µm (see Figure 28). IIR includes three filters arranged on a filter wheel for sequential acquisition in the three channels. In each cycle, the calibration views are blackbody (BB) images in the first sequence and space view (SV) images in the four following sequences.

The IIR acquisition timing and calibration procedures are presented in Garnier et al. (2018). Each IIR Level 1 Calibration data file contains a full orbit of the SV and BB images, and the gains derived in each of the three channels at 8.65, 10.6, and 12.05 µm. This file is complemented by the IIR Level 1 Calibration Correction data file which contains semi-empirical corrections of the initial gains. These corrections were defined to reduce a "Tartan" striping effect and biases with respect to MODIS/Aqua observations.

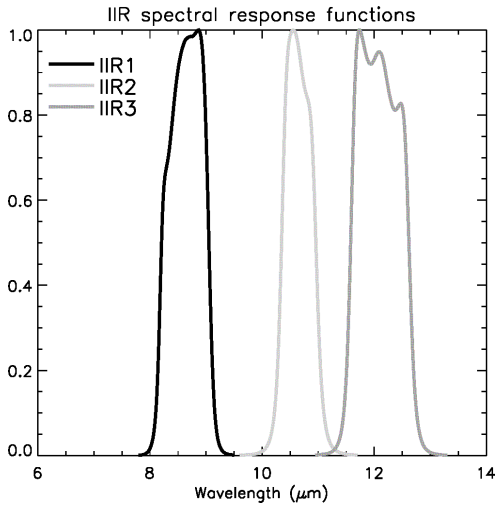

Figure 28: IIR spectral response functions

b. IIR Level 1B Data

Each IIR Level 1B data file contains approximately a half orbit of calibrated radiances in IIR channels at 8.65 um, 10.6, and 12.05 µm. The files match the CALIOP definition of all daytime or all nighttime data. The initial 64 km x 64 km calibrated Earth view images in each channel are re-sampled and geo-located on a unique 1 km grid centered on the CALIOP track, with a resulting 69 km swath. Along the track, each IIR 1 km pixel has its center co-located with a CALIOP lidar shot (whose time is provided), and two successive IIR pixels are separated by exactly 3 lidar shots. The elapsed time between two successive Earth views in a given channel is 8.184 s, during which the satellite has moved forward by about 55 km, so that two successive Earth view images always overlap. Image acquisition time and sequence number are provided. An example of co-located CALIOP and IIR observations is shown in Figure 29. The IIR Level 1B calibrated radiances are converted to the radiative temperatures available in the IIR Level 2 swath data product using Equation 3 and the coefficients given in Table 2 in Sect. 2.4 of Garnier et al. (2018).

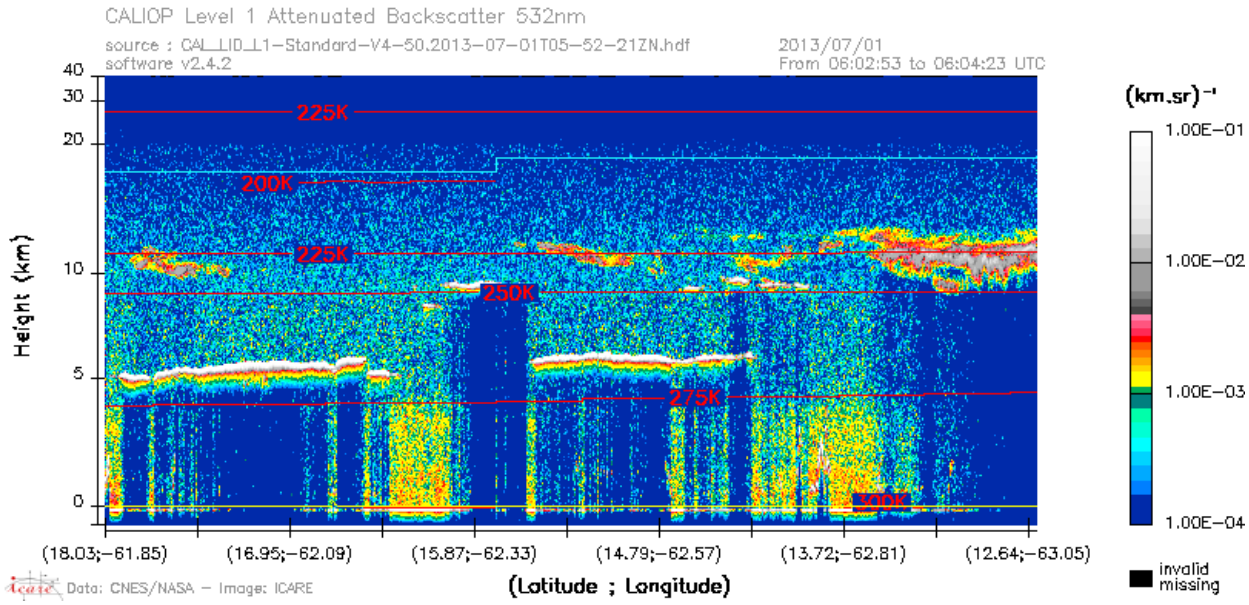

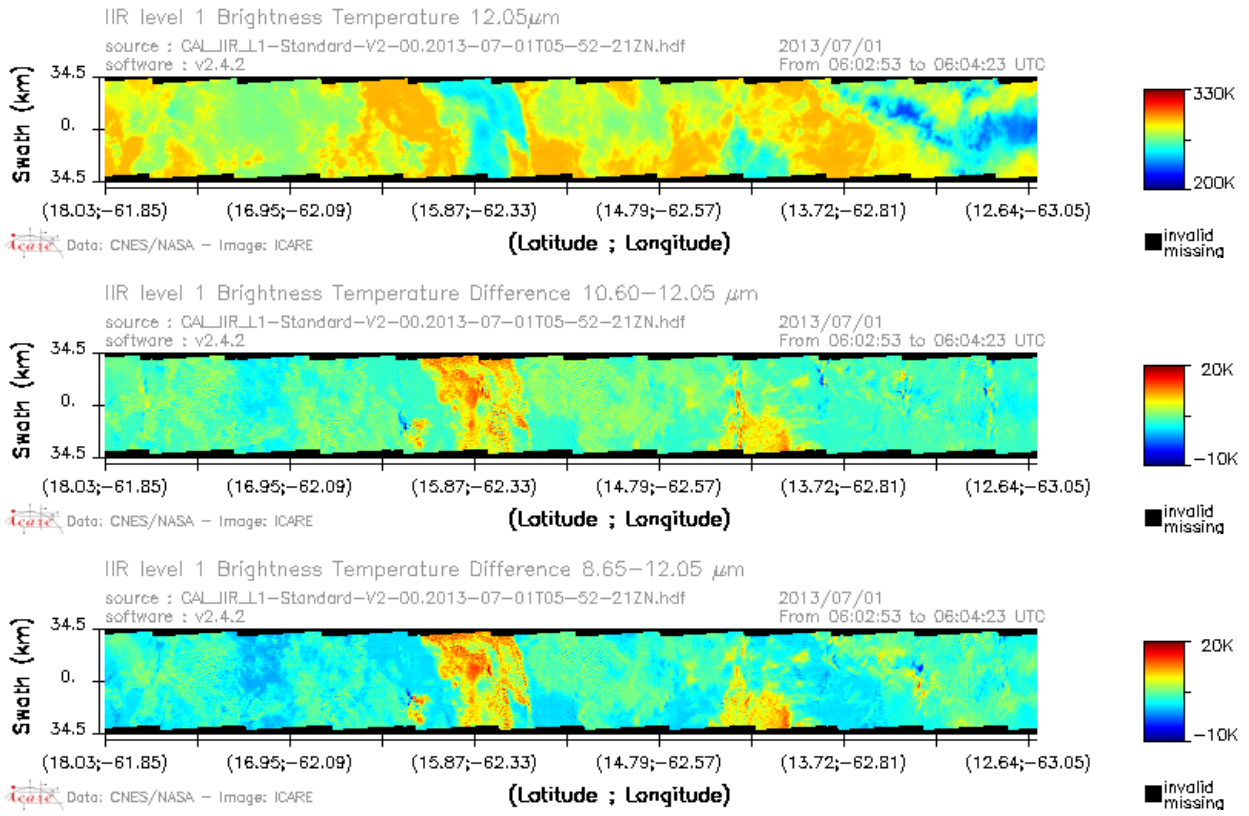

Figure 29: IIR Level 1B measured radiances converted to brightness temperatures (BTs). The center of the ±34.5 km swath is co-located with the CALIOP observations shown in the top panel. The following panels are from top to bottom BTs at 12.05 μm, BT difference (BTD) between channels 10.6 μm and 12.05 μm, and BTD between channels 8.65 μm and 12.05 μm. Granule 2013-07-01T05-52-21ZN.

c. IIR Level 2 Track Data

The primary geophysical variables reported in the IIR Level 2 track data product at 1-km pixel resolution are the measured brightness temperatures under the lidar track in the three IIR channels (8.65, 10.60, and 12.05 μm), a scene classification derived from the Lidar level 2 5-km cloud and aerosol layer products, and for suitable scenes: effective emissivity in each IIR channel, cloud optical depth and cloud microphysical properties. Standard microphysical properties (Garnier et al., 2021a, 2021b) include effective diameter and ice or liquid water path. A new series of so-called "Cirrus" retrievals is added with the V5.00 release, which includes in particular layer ice number concentration, ice water content, extinction, and effective diameter in semi-transparent ice clouds (Mitchell et al., 2025).

Emissivity retrievals require a correction for the contribution from the "background". When the lowermost of at least two layers in the column is opaque to CALIOP, the background reference is from this opaque layer, which is called *lower level*, and the retrievals characterize the *upper level* defined as the ensemble of layers located above the *lower level*. Otherwise, the reference for the emissivity retrievals is from the Earth surface and the *upper level* corresponds to all the layers in the atmospheric column. Thus, the *upper level* includes one or several semi-transparent layer(s) or one opaque layer.

Several *upper level and lower level* properties inferred from CALIOP are provided in addition to the IIR scene classification and a multi-layer flag. Because IIR retrievals are typically more accurate over water than over land surfaces, several parameters characterizing the surface are provided.

Figure 28 gives an example of IIR track retrievals for one granule on 10 January 2008 between 60° S and 60° N. The layer retrievals are for *upper levels* composed of ice clouds only or of liquid water clouds only. The top panel shows all effective emissivity values at 12.05 µm. The vertical lines are between the bottom and top altitudes of the *upper level,* and the black crosses indicate its radiative altitude. The large vertical extents seen for instance for ice clouds between 8° S and 5° S are multi-layer cases. Standard effective diameter (middle panel) and ice or liquid water path (bottom panel) are shown when the particle shape index confidence parameter indicates a good or medium agreement between the retrievals based on the 12.05/10.6 and 12.05/8.65 pairs of channels.

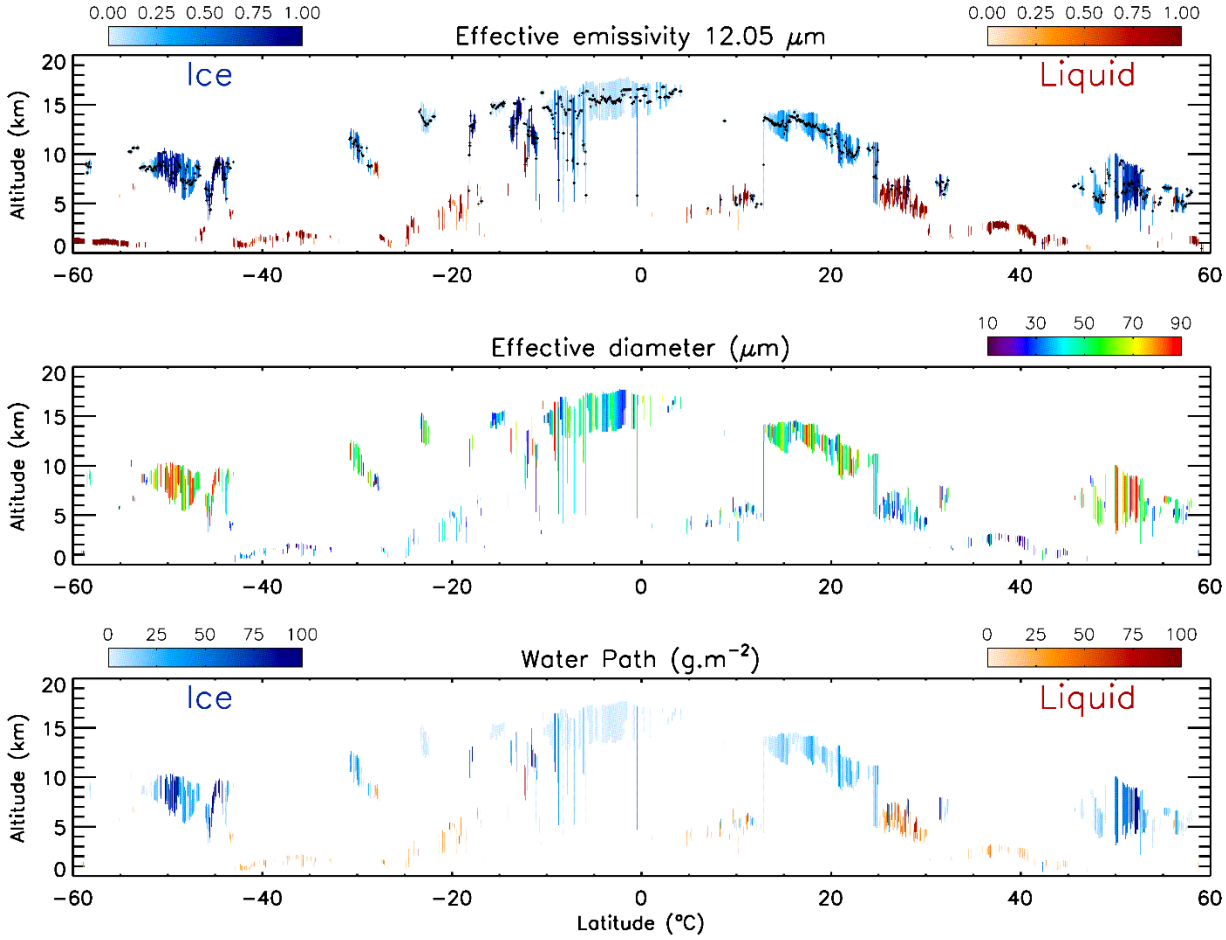

Figure 30: Example of IIR level 2 track retrievals for granule 2008-01-10T10-25-23ZD between 60° S and 60° N. The layer retrievals characterize *upper levels* composed of ice clouds only (blue hues in the top and bottom panels showing effective emissivity and water path, respectively) or of liquid water clouds only (red hues in the top and bottom panels). The same colormap is used for the ice and liquid water effective diameters shown in the middle panel. The vertical lines are between the bottom and top altitudes of the *upper level,* and the black crosses in the top panel indicate its radiative altitude.

d. IIR Level 2 Swath Data

The IIR Level 2 swath data product contains data assigned to 1-km IIR pixels on a 69-km wide grid centered on the CALIOP track. This product includes the brightness temperatures in the three IIR channels (8.65, 10.60, and 12.05 µm) corresponding to the calibrated radiances reported in the IIR Level 1B data product.

One key parameter is IIR_Track_Pixel_ID, which is the identification number of the neighboring track pixel within 100 km in the IIR Level 2 track product that is the most "similar" to the current swath pixel. This "similarity" is based on radiative homogeneity criteria (Garnier et al., 2012) and is quantified using the homogeneity index in each channel. Several parameters such as scene classification, effective emissivity, and standard microphysical retrievals are propagated from the track to the swath by assigning to a swath pixel the track retrievals of the similar track pixel. IIR_Track_Pixel_ID can be used to extract any track parameter not already reported in the swath product.

e. IIR Level 3 GEWEX Cloud Data

The IIR L3 GEWEX Cloud data product reports global distributions of IIR cloud effective radius and water path averages and histograms on a uniform 2-dimensional 1° latitude by 1° longitude spatial grid with a temporal averaging of one month. For the final V2.00 release, the level 3 parameters are derived from the IIR level 2 Version 5.00 track data products.

The product is designed to follow the general guidance of the GEWEX Cloud Assessment (Stubenrauch et al., 2024). Cloud amount, radiative temperature, effective emissivity, and optical depth characterize the cloud samples for which IIR microphysical retrievals are successful. Cloud properties are reported for pseudo mono-layer ice clouds composed of randomly oriented ice, liquid water clouds, and high ice clouds of layer pressure lower than 440 hPa, all having high confidence in the phase assignment by the CALIOP algorithms. The retrievals must apply to all the clouds included in the atmospheric column, i.e. the background reference used for emissivity retrievals is the surface. As an illustration, Figure 29 shows maps of ice clouds mean effective radius (left) as reported in the product for all the months of July from 2006 through 2016. In the dark blue areas in the tropics seen in the corresponding mean optical depth map (right), the effective radius retrievals are in thin cirrus clouds of mean optical depth smaller than 0.3.

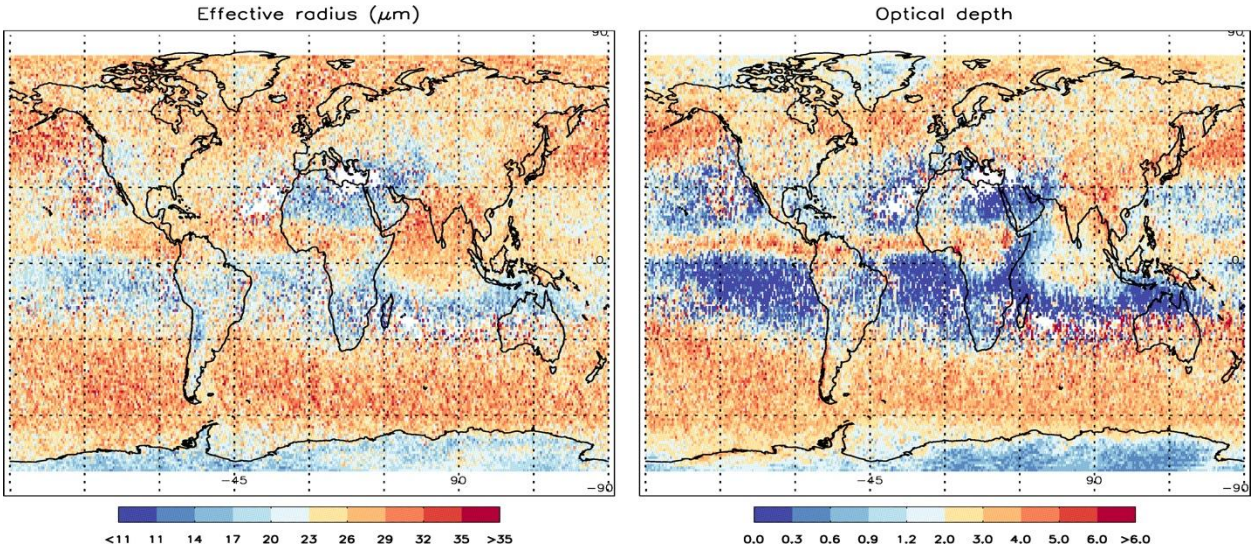

Figure 31: Mean effective radius (left) and corresponding optical depth (right) for all randomly oriented ice clouds observed during the month of July in the years from 2006 through 2016.

44. IIR Data Quality

What should I know about the quality of IIR effective emissivity retrievals?

a. Surface vs opaque reference

Emissivity retrievals require a correction for the contribution from the "background" reference. When the reference is an opaque layer, this layer is called *lower level*, and its characteristics are reported in parameters with names ending with "Lower_Level". When the background reference is the Earth surface, the "Lower_Level" parameters are fill values. Retrievals over opaque layers assume that the opaque layer behaves as a blackbody source, which is deemed justified when the lower level is a liquid water cloud. However, this assumption is questionable if this layer is opaque to CALIOP because the overlying optical depth is large, preventing the CALIOP algorithm from detecting the surface.

b. For surface: Land vs. Ocean

The type of surface is reported in the TGeotype parameter. When the background reference is the Earth surface, uncertainties are smaller over water surface than over land due to larger uncertainties in the surface parameters over land. TGeotype = 1700 indicates high confidence in the presence of non-frozen water surface.

c. Was_Cleared_Flag_1km

The IIR scene classification is based on the Lidar level 2 5-km cloud and aerosol layer products, from which clouds detected at single shot resolution might have been cleared. This piece of information is available in the Was_Cleared_Flag_1km parameter. For effective emissivity retrievals, the background radiance is computed regardless of Was_Cleared_Flag_1km. Unless the bias in the background radiance due to the cleared clouds can be estimated a posteriori and can be deemed acceptable, it is recommended to ensure that Was_Cleared_Flag_1km = 0 for detailed analyses of optically thin clouds over Earth surface as a reference.

d. Multi-layer vs. monolayer retrievals

The Type_of_Scene parameter provides a qualitative description of the *upper level* and of the *lower level,* if any. We recall that layers detected with 80-km horizontal averaging are ignored from the IIR scene classification, except for CLEAR SKY and AEROSOLS ONLY Type_of_Scene 51 to 56 which do not contain clouds at any resolution. The Multi_Layer_Flag parameter provides the number of layers included in the *upper level*, and the distance between the lowermost and the uppermost layers. Because IIR is a passive instrument, the scientific interpretation of IIR retrievals is more straightforward for single-layer *upper levels* or, given the sensitivity of the CALIOP multi-averaging layer detection scheme, for *upper levels* composed of overlapping layers or layers separated by small distances. The user can use Multi_Layer_Flag to select the configuration adapted to his/her application.

e. CALIOP cloud feature type and phase assignment

The phase assignment of cloudy *upper levels* is reported in the Ice_Water_Flag_Upper_Level parameter, and Ice_Water_Flag_QA_Upper_Level represents the mean confidence in the cloud-aerosol discrimination and in the phase assignment. For instance, a user interested in retrievals in *upper levels* composed exclusively of randomly oriented ice should select Ice_Water_Flag_Upper_Level =1. Scenes with high confidence in both cloud feature type and phase assignment for all the layers of the *upper level* have Ice_Water_Flag_QA_Upper_Level = 100.1.

f. Absorbing aerosols in the column

When the *upper level* is composed of cloud layers, the semi-transparent aerosol layers, if any, are ignored when computing the cloud effective emissivity. The presence of potentially absorbing aerosol

layers (i.e. tropospheric dusty aerosols or stratospheric aerosols) is reported in the Dust_Stratospheric_Aerosol_Flag parameter.

g. Confidence in microphysics retrievals

Retrievals of standard effective diameter and sub-sequent ice or liquid water path are deemed "confident" when the $\beta_{eff}12/10$ and $\beta_{eff}12/08$ microphysical indices are both within the range of expected values according to the look-up tables, that is when the particle shape index confidence parameter equals 1 or 2. The confidence in the particle shape index is good (1) when the diameters derived from $\beta_{eff}12/10$ and $\beta_{eff}12/08$ agree within 30% and medium (2) otherwise. Random uncertainties in the microphysical indices can trigger non-confident retrievals even if D_e is truly smaller than the sensitivity limit set at 120 µm. This is more likely to occur when D_e is close to this limit and in optically thinner clouds.

The new "Cirrus" retrievals added with the V5.00 release use three look-up tables based on in situ observations relating D_e to $\beta_{eff}12/10$ only. Pixels with $\beta_{eff}12/10$ smaller than the sensitivity limits are assigned maximum retrieved D_e = 77.7, 136.2 and 129.8 µm for the SPARTICUS, TC4 and ATTREX-POSIDON formulations, respectively.

45. How can I co-locate IIR and CALIOP Data?

a. IIR Level 1 Product

The IIR level 1 product reports parameters in 1-km pixels over a 69-km swath centered on the CALIOP track.

Counting the cross-track swath pixels from 1 to 69, the lidar track is in swath pixel #35.

Along the track, each IIR 1-km pixel has its center co-located with a CALIOP lidar shot, and two successive IIR pixels are separated by exactly 3 lidar shots.

The lidar shots are identified using their International Atomic Time reported in the Lidar_Shot_Time SDS as well as their UTC time reported in the Lidar_Shot_UTC_Time SDS. They are typically in CALIOP files having the same timestamp as the IIR file.

b. IIR Level 2 Track Product

This product reports IIR retrievals at 1-km resolution derived from co-located CALIOP and IIR observations, which are at the center of the IIR swath. IIR brightness temperatures are also reported. A given IIR track granule is produced using as input the 5-km aerosol and cloud granules having the same version (i.e. V5.00 for the latest release) and same timestamp.

The center of each IIR 1-km track pixel is co-located with a CALIOP lidar shot, which is identified using its International Atomic Time reported in the LIDAR_Shot_Time SDS and its profile ID reported in the LIDAR_Profile_ID SDS. Two successive IIR pixels are separated by exactly 3 lidar shots.

Each 5-km segment (or 15 lidar shots) in the CALIOP products reported at 5-km resolution is co-located with five consecutive IIR track pixels. The "Profile_ID" parameter in the CALIOP file contains start and end profile IDs, hereafter named startID and endID. The five consecutive IIR track pixels corresponding to a 5-km CALIOP segment have LIDAR_Profile_ID equal to startID+1, startID+4, startID+7, startID+10, and startID+13. They are the five pixels having startID < LIDAR_Profile_ID < endID. Note that the center of the third of these five consecutive IIR pixels, that is the pixel having LIDAR_Profile_ID equal to startID+7, is at the 5-km segment midpoint and can also be identified using the time at the temporal midpoint reported in the CALIOP products. Likewise, the center of this third IIR pixel has latitude and longitude equal to latitude and longitude at temporal midpoint reported in the CALIOP products.

For the user's convenience, some CALIOP parameters reported at 5-km resolution are reported in the IIR product by repeating the same CALIOP value in the 5 successive IIR pixels. The procedure described above can be used if more CALIOP information is needed.

c. IIR Level 2 Swath Product

The IIR level 2 swath product reports brightness temperatures and retrievals in 1-km IIR pixels over a 69-km swath centered on the CALIOP track. The grid is the same as in the level 1 product, the lidar track is at the center of the swath, and each IIR 1-km pixel along the track has its center co-located with a CALIOP lidar shot, which can be identified using the Lidar_Shot_Time SDS. The retrievals at the center of the swath are copied from the level 2 track product.

46. Why are IIR and CALIOP Ice Water Paths different?

IIR and CALIOP Ice Water Path (IWP) are derived using two independent approaches. On one hand, IIR IWP is derived as IWP = $(1/3)\cdot\rho_i\cdot D_e\cdot\tau_{vis}$, where ρ_i is the ice bulk density, D_e is the layer effective diameter, and τ_{vis} is the visible optical depth retrieved by IIR. On the other hand, CALIOP IWP is obtained by vertically integrating the ice water content (IWC) profile. As stated in Winker et al. (2024), "profiles of IWC are derived from ice cloud extinction coefficients using a temperature-dependent parameterization based on in situ measurements acquired during a number of aircraft field campaigns conducted between 1991 and 2007 (Heymsfield et al., 2014)".

While CALIOP and IIR visible optical depths are in good agreement for semi-transparent ice clouds (Figure 30, left), the discrepancies between CALIOP and IIR IWP seen in Figure 30 (right) originate mostly from the fact that D_e implicitly included in the CALIOP parameterization is notably larger than IIR D_e at temperatures warmer than 210 K. This discrepancy could be explained by the lack of sensitivity of the IIR analysis to large (typically > 100 µm) particle sizes, which could introduce a bias in the statistical analysis. It is noted that combined lidar-radar retrievals of D_e also yield smaller values than the CALIOP parameterization (Dolinar et al., 2022). Because all the retrievals include instrumental or microphysical assumptions, solving the discrepancies between ice water path from various in situ and remote sensing sensors is still an open question.

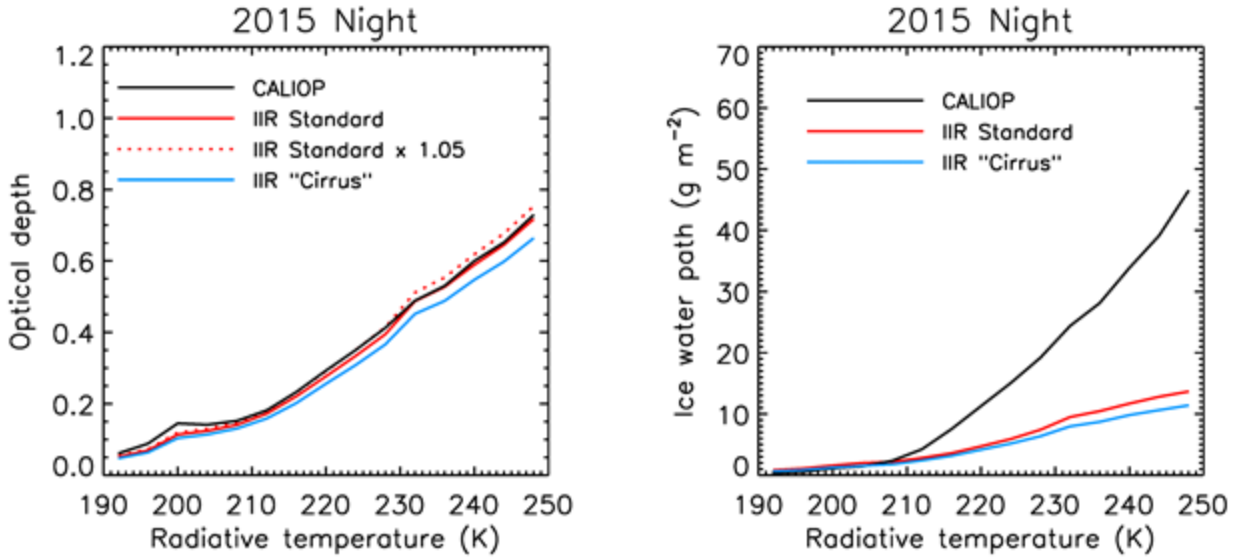

Figure 30: Comparison of nighttime CALIOP and IIR-derived median optical depth (left) and median ice water path (right) in semi-transparent single-layer ice clouds over oceans during 2015. CALIOP retrievals are in black and shown in blue are the new IIR "Cirrus" retrievals reported in the V5.00 release. IIR standard

retrievals are based on β_{eff}12/10 only and use D_e derived using the "severely rough 8-element column aggregate crystal model reported in the Microphysics parameter. The X-axis is the IIR layer radiative temperature. The dotted red line in the left-hand side panel is optical depth estimated as 1.05 x standard IIR optical depth to establish the temperature-dependent CALIOP multiple scattering correction factor (Young et al., 2018).

IIR Known Issues

This section provides brief descriptions of potential problems identified since the final release of the CALIPSO data products. Where possible, potential remedies are also offered.

47. Some radiative heights and pressures are not reported

In rare occasions (less than 0.1 % of the cases), the radiative height of an icy upper level is not reported, while a radiative temperature is provided, because this height is not found between the top and base altitudes. The same applies for the radiative pressure. This is explained by the fact that the temperature profile used to retrieve the radiative temperature is from the CALIOP Cloud profile product at 5-km resolution and might slightly differ from the profile used to infer radiative height and pressure. The code could be revised to avoid this mismatch. The rare instances are prevailingly over land at high latitude and at low altitude.

WFC Known Issues

There are no known residual issues with any of the WFC data products.

References

Avery, M. A., R. A. Ryan, B. J. Getzewich, M. A. Vaughan, D. M. Winker, Y. Hu, A. Garnier, J. Pelon, and C. A. Verhappen, 2020: CALIOP V4 Cloud Thermodynamic Phase Assignment and the Impact of Near-Nadir Viewing Angles, *Atmos. Meas. Tech.*, **13**, 4539–4563, https://doi.org/10.5194/amt-13-4539-2020.

Braun, B. M., T. H. Sweetser, C. Graham and J. Bartsch, 2019: CloudSat's A-Train Exit and the Formation of the C-Train: An Orbital Dynamics Perspective, 2019 IEEE Aerospace Conference, Big Sky, MT, USA, pp. 1-10, https://doi.org/10.1109/AERO.2019.8741958.

Cai, X. D. M. Winker, M. Vaughan, B. Magill, B. J. Getzewich, C. R. Trepte, and P. Lucker, 2018: Introduction of the CALIOP Level 3 3-dimensional Cloud Occurrence Product, American Geophysical Union, Fall Meeting 2018, abstract #A11I-2353, https://agu.confex.com/agu/fm18/mediafile/Handout/Paper345072/2018AGU_poster_xcai_final.pdf.

Dolinar E. K., J. R. Campbell, J. W. Marquis, A. E. Garnier, and M. Karpowicz, 2022: Novel Parameterization of Ice Cloud Effective Diameter from Collocated CALIOP-IIR and CloudSat Retrievals, *J. Appl. Meteor. Clim.*, **61**, 891-905, https://doi.org/10.1175/JAMC-D-21-0163.1.

Garnier, A., J. Pelon, P. Dubuisson, M. Faivre, O. Chomette, N. Pascal and D. P. Kratz, 2012: Retrieval of cloud properties using CALIPSO Imaging Infrared Radiometer. Part I: effective emissivity and optical depth, *J. Appl. Meteor. Climatol.*, **51**, 1407–1425, https://doi.org/10.1175/JAMC-D-11-0220.1.

Garnier, A., T. Trémas, J. Pelon, K.-P. Lee, D. Nobileau, L. Gross-Colzy, N. Pascal, P. Ferrage and N. A. Scott, 2018: CALIPSO IIR Version 2 Level 1b calibrated radiances: analysis and reduction of residual biases in the Northern Hemisphere, *Atmos. Meas. Tech.*, **11**, 2485–2500, https://doi.org/10.5194/amt-11-2485-2018.

Garnier, A., J. Pelon, N. Pascal, M. A. Vaughan, P. Dubuisson, P. Yang and D. L. Mitchell, 2021a: Version 4 CALIPSO IIR ice and liquid water cloud microphysical properties, Part I: the retrieval algorithms, *Atmos. Meas. Tech.*, **14**, 3253–3276, https://doi.org/10.5194/amt-14-3253-2021.

Garnier, A., J. Pelon, N. Pascal, M. A. Vaughan, P. Dubuisson, P. Yang and D. L. Mitchell, 2021b: Version 4 CALIPSO IIR ice and liquid water cloud microphysical properties, Part II: results over oceans, *Atmos. Meas. Tech.*, **14**, 3277–3299, https://doi.org/10.5194/amt-14-3277-2021.

Getzewich, B. J., M. A. Vaughan, W. H. Hunt, M. A. Avery, K. A. Powell, J. L. Tackett, D. M. Winker, J. Kar, K.-P. Lee, and T. Toth, 2018: CALIPSO Lidar Calibration at 532-nm: Version 4 Daytime Algorithm, *Atmos. Meas. Tech.*, **11**, 6309–6326, https://doi.org/10.5194/amt-11-6309-2018.

Guzman, R., H. Chepfer, V. Noel, T. Vaillant de Guélis, J. E. Kay, P. Raberanto, G. Cesana, M. A. Vaughan, and D. M. Winker, 2017: Direct atmosphere opacity observations from CALIPSO provide new constraints on cloud-radiation interactions, *J. Geophys. Res. Atmos.*, **122**, 1066–1085, https://doi.org/10.1002/2016JD025946.

Heymsfield, A., D. Winker, M. Avery, M. Vaughan, G. Diskin, M. Deng, V. Mitev, and R. Matthey, 2014: Relationships between Ice Water Content and Volume Extinction Coefficient from In Situ Observations for Temperatures from 0° to -86°C: Implications for Spaceborne Lidar Retrievals, *J. Appl. Meteor. Climatol.*, **53**, 479–505, https://doi.org/10.1175/JAMC-D-13-087.1.

Hostetler, C., Z. Liu, J. Reagan, M. Vaughan, D. Winker, M. Osborn, W. H. Hunt, K. A. Powell, and C. Trepte, 2006: CALIOP Algorithm Theoretical Basis Document: Calibration and Level 1 Data Products, PC-SCI-201, 66 pp., https://ntrs.nasa.gov/citations/20250006623.

Hu, Y., M. Vaughan, Z. Liu, K. Powell, and S. Rodier, 2007: Retrieving Optical Depths and Lidar Ratios for Transparent Layers Above Opaque Water Clouds From CALIPSO Lidar Measurements, *IEEE Geosci. Remote Sens. Lett.*, **4**, 523–526, https://doi.org/10.1109/LGRS.2007.901085.

Hunt, W. H, D. M. Winker, M. A. Vaughan, K. A. Powell, P. L. Lucker, and C. Weimer, 2009: CALIPSO Lidar Description and Performance Assessment, *J. Atmos. Oceanic Technol.*, **26**, 1214–1228, https://doi.org/10.1175/2009JTECHA1223.1.

Kar, J., M. A. Vaughan, K. P. Lee, J. Tackett, M. Avery, A. Garnier, B. Getzewich, W. Hunt, D. Josset, Z. Liu, P. Lucker, B. Magill, A. Omar, J. Pelon, R. Rogers, T. D. Toth, C. Trepte, J-P. Vernier, D. Winker, and S. Young, 2018: CALIPSO Lidar Calibration at 532 nm: Version 4 Nighttime Algorithm, *Atmos. Meas. Tech.*, **11**, 1459–1479, https://doi.org/10.5194/amt-11-1459-2018.

Kar, J., K.-P. Lee, M. A. Vaughan, J. L. Tackett, C. R. Trepte, D. M. Winker, P. L. Lucker, and B. J. Getzewich, 2019: CALIPSO Level 3 Stratospheric Aerosol Product: Version 1.00 Algorithm Description and Initial Assessment, *Atmos. Meas. Tech.*, **12**, 6173–6191, https://doi.org/10.5194/amt-12-6173-2019.

Kim, M.-H., A. H. Omar, J. L. Tackett, M. A. Vaughan, D. M. Winker, C. R. Trepte, Y. Hu, Z. Liu, L. R. Poole, M. C. Pitts, J. Kar, and B. E. Magill, 2018: The CALIPSO Version 4 Automated Aerosol Classification and Lidar Ratio Selection Algorithm, *Atmos. Meas. Tech.*, **11**, 6107-6135, https://doi.org/10.5194/amt-11-6107-2018.

Kim, M.-H.; H. Yeo, S. Park, D.-H. Park, A. Omar, T. Nishizawa, A. Shimizu, S.-W. Kim, 2021: Assessing CALIOP-Derived Planetary Boundary Layer Height Using Ground-Based Lidar, *Remote Sens.*, **13**, 1496, https://doi.org/10.3390/rs13081496.

Liu, Z., J. Kar, S. Zeng, J. Tackett, M. Vaughan, M. Avery, J. Pelon, B. Getzewich, K.-P. Lee, B. Magill, A. Omar, P. Lucker, C. Trepte, and D. Winker, 2019: Discriminating Between Clouds and Aerosols in the CALIOP

Version 4.1 Data Products, *Atmos. Meas. Tech.*, **12**, 703–734, https://doi.org/10.5194/amt-12-703-2019.

Lu, X., Y. Hu, M. Vaughan, S. Rodier, C. Trepte, P. Lucker, and A. Omar, 2020: New attenuated backscatter profile by removing the CALIOP receiver's transient response, *JQSRT*, **255**, 107244, https://doi.org/10.1016/j.jqsrt.2020.107244.

McGill, M. J., M. A. Vaughan, C. R. Trepte, W. D. Hart, D. L. Hlavka, D. M. Winker, and R. Kuehn, 2007: Airborne validation of spatial properties measured by the CALIPSO lidar, *J. Geophys. Res.*, **112**, D20201, https://doi.org/10.1029/2007JD008768.

Mitchell, D. L., A. Garnier and S. Woods, 2025: Advances in CALIPSO (IIR) cirrus cloud property retrievals – Part 1: Methods and testing, Atmos. Chem. Phys., 25, 14071–14098, https://doi.org/10.5194/acp-25-14071-2025.

Noel, V., H. Chepfer, C. Hoareau, M. Reverdy and G. Cesana, 2014: Effects of solar activity and geomagnetic field on noise in CALIOP profiles above the South Atlantic Anomaly, *Atmos. Meas. Tech.*, **7**, 1597–1603, https://doi.org/10.5194/amt-7-1597-2014.

Palm, S. P., V. Kayetha, Y. Yang and R. Pauly, 2017: Blowing snow sublimation and transport over Antarctica from 11 years of CALIPSO observations, *The Cryosphere*, **11**, 2555–2569, https://doi.org/10.5194/tc-11-2555-2017.

Pitts, M. C., L. R. Poole and R. Gonzalez, 2018: Polar stratospheric cloud climatology based on CALIPSO spaceborne lidar measurements from 2006 to 2017, *Atmos. Chem. Phys.*, **18**, 10881–10913, https://doi.org/10.5194/acp-18-10881-2018.

Platt, C. M. R., 1979: Remote Sounding of High Clouds: I. Calculation of Visible and Infrared Optical Properties from Lidar and Radiometer Measurements, *J. Appl. Meteor. Climatol.*, **18**, 1130–1143, https://doi.org/10.1175/1520-0450(1979)018<1130:RSOHCI>2.0.CO;2.

Powell, K. A., C. A. Hostetler, Z. Liu, M. A. Vaughan, R. E. Kuehn, W. H. Hunt, K. Lee, C. R. Trepte, R. R. Rogers, S. A. Young, and D. M. Winker, 2009: CALIPSO Lidar Calibration Algorithms: Part I - Nighttime 532 nm Parallel Channel and 532 nm Perpendicular Channel, *J. Atmos. Oceanic Technol.*, **26**, 2015–2033, https://doi.org/10.1175/2009JTECHA1242.1.

Ryan, R. A., M. A. Vaughan, S. D. Rodier, J. L. Tackett, J. A. Reagan, R. A. Ferrare, J. W. Hair, and B. J. Getzewich, 2024: Total Column Optical Depths Retrieved from CALIPSO Lidar Ocean Surface Backscatter, *Atmos. Meas. Tech.*, **17**, 6517–6545, https://doi.org/10.5194/amt-17-6517-2024.

Shcherbakov, V., F. Szczap, A. Alkasem, G. Mioche and C. Cornet, 2022: Empirical model of multiple-scattering effect on single-wavelength lidar data of aerosols and clouds, *Atmos. Meas. Tech.*, **15**, 1729–1754, https://doi.org/10.5194/amt-15-1729-2022.

Stubenrauch, C. J., S. Kinne, G. Mandorli, W. B. Rossow, D. M. Winker, S. A. Ackerman, H. Chepfer, L. Di Girolamo, A. Garnier, A. Heidinger, K.-G. Karlsson, K. Meyer, P. Minnis, S. Platnick, M. Stengel, S. Sun-Mack, P. Veglio, A. Walther, X. Cai, A. H. Young and G. Zhao, 2024: Lessons Learned from the Updated GEWEX Cloud Assessment Database, *Surv. Geophys.*, **45**, 1999–2048, https://doi.org/10.1007/s10712-024-09824-0.

Tackett, J. L., D. M. Winker, B. J. Getzewich, M. A. Vaughan, S. A. Young, and J. Kar, 2018: CALIPSO lidar level 3 aerosol profile product: version 3 algorithm design, *Atmos. Meas. Tech.*, **11**, 4129-4152, https://doi.org/10.5194/amt-11-4129-2018.

Tackett, J., M. Vaughan, J. Lambeth, and A. Garnier, 2022: Critical Improvements to CALIOP Boundary Layer Cloud-Clearing in Version 4.5, 2022 CALIPSO/CloudSat Science Team Meeting, 12–14 September 2022, Fort Collins, CO USA, https://ntrs.nasa.gov/citations/20220013563.

Tackett, J. L., R. A. Ryan, A. E. Garnier, J. Kar, B. Getzewich, X. Cai, M. A. Vaughan, C. R. Trepte, R. Verhappen, D. M. Winker, and K.-P. A. Lee, 2025: "Mitigating Impacts of Low Energy Laser Pulses on CALIOP Data Products", *Atmos. Meas. Tech.*, **18**, 6211–6231, https://doi.org/10.5194/amt-18-6211-2025.

Vaillant de Guélis, T., J. L. Tackett, A. Garnier, R. A. Ryan, S. P. Burton, and K. A. Powell, 2025: Color-Vision-Deficiency-Accessible Colormaps for Cloud and Aerosol Atmospheric Lidar Visualization, *Bull. Am. Met. Soc.*, https://doi.org/10.1175/BAMS-D-25-0059.1, accepted for publication [October 2025].

Vaughan, M. A., D. M. Winker, and K. A. Powell, 2005: CALIOP Algorithm Theoretical Basis Document, Part 2: Feature Detection and Layer Properties Algorithms, PC-SCI-202.01, 87 pp., https://ntrs.nasa.gov/citations/20250006627.

Vaughan, M., K. Powell, R. Kuehn, S. Young, D. Winker, C. Hostetler, W. Hunt, Z. Liu, M. McGill, and B. Getzewich, 2009: Fully Automated Detection of Cloud and Aerosol Layers in the CALIPSO Lidar Measurements, *J. Atmos. Oceanic Technol.*, **26**, 2034–2050, https://doi.org/10.1175/2009JTECHA1228.1.

Vaughan, M., C. Trepte, D. Winker, M. Avery, J. Campbell, R. Hoff, S. Young, B. Getzewich, J. Tackett and J. Kar, 2011: Adapting CALIPSO Climate Measurements for Near Real Time Analyses and Forecasting, 34th International Symposium on Remote Sensing of Environment, 10–15 April 2011, Sydney, Australia, https://ntrs.nasa.gov/citations/20110010975.

Vaughan, M., A. Garnier, D. Josset, M. Avery, K.-P. Lee, Z. Liu, W. Hunt, J. Pelon, Y. Hu, S. Burton, J. Hair, J. Tackett, B. Getzewich, J. Kar, and S. Rodier, 2019: CALIPSO Lidar Calibration at 1064 nm: Version 4 Algorithm, *Atmos. Meas. Tech.*, **12**, 51–82, https://doi.org/10.5194/amt-12-51-2019.

Winker, D., 2003: Accounting for multiple scattering in retrievals from space lidar, in 12th International Workshop on Lidar Multiple Scattering Experiments, Werner, C., U. G. Oppel and T. Rother, Eds., International Society for Optical Engineering, SPIE Proc., 5059, 128–139, https://doi.org/10.1117/12.512352.

Winker, D. M., M. A. Vaughan, A. H. Omar, Y. Hu, K. A. Powell, Z. Liu, W. H. Hunt, and S. A. Young, 2009: Overview of the CALIPSO Mission and CALIOP Data Processing Algorithms, *J. Atmos. Oceanic Technol.*, **26**, 2310–2323, https://doi.org/10.1175/2009JTECHA1281.1.

Winker, D. M., J. Pelon, J. A. Coakley, Jr., S. A. Ackerman, R. J. Charlson, P. R. Colarco, P. Flamant, Q. Fu, R. Hoff, C. Kittaka, T. L. Kubar, H. LeTreut, M. P. McCormick, G. Megie, L. Poole, K. Powell, C. Trepte, M. A. Vaughan and B. A. Wielicki, 2010: The CALIPSO Mission: A Global 3D View Of Aerosols And Clouds, *Bull. Am. Meteorol. Soc.*, **91**, 1211–1229, https://doi.org/10.1175/2010BAMS3009.1.

Winker, D., X. Cai, M. Vaughan, A. Garnier, B. McGill, M. Avery and B. Getzewich, 2024: A Level 3 monthly gridded ice cloud dataset derived from 12 years of CALIOP measurements, *Earth Syst. Sci. Data*, **16**, 2831–2855, https://doi.org/10.5194/essd-16-2831-2024.

Young, S. A. and M. A. Vaughan, 2009: The retrieval of profiles of particulate extinction from Cloud Aerosol Lidar Infrared Pathfinder Satellite Observations (CALIPSO) data: Algorithm description, *J. Atmos. Oceanic Technol.*, **26**, 1105–1119, https://doi.org/10.1175/2008JTECHA1221.1.

Young, S. A., M. A. Vaughan, R. E. Kuehn, and D. M. Winker, 2013: The Retrieval of Profiles of Particulate Extinction from Cloud-Aerosol Lidar Infrared Pathfinder Satellite Observations (CALIPSO) Data:

Uncertainty and Error Sensitivity Analyses, *J. Atmos. Oceanic Technol.*, **30**, 395–428, https://doi.org/10.1175/JTECH-D-12-00046.1.

Young, S. A., M. A. Vaughan, J. L. Tackett, A. Garnier, J. B. Lambeth, and K. A. Powell, 2018: Extinction and Optical Depth Retrievals for CALIPSO's Version 4 Data Release, *Atmos. Meas. Tech.*, **11**, 5701–5727, https://doi.org/10.5194/amt-11-5701-2018.